



*Midwest Pooled Fund Program  
Research Project Number TPF-5(430) Supplement #2  
NDOT Sponsoring Agency Code RPFP-20-AGT-1*

# **SURFACE-MOUNTED POST RETROFIT FOR APPROACH GUARDRAIL TRANSITIONS: PHASE I**

## Submitted by

Scott K Rosenbaugh, M.S.C.E.  
Research Engineer

Gnyarienn Kumar  
Former Graduate Student

Cody S. Stolle, Ph.D.  
Research Assistant Professor

Ronald K. Faller, Ph.D., P.E.  
Research Professor & MwRSF Director

## **MIDWEST ROADSIDE SAFETY FACILITY**

Nebraska Transportation Center  
University of Nebraska-Lincoln

### **Main Office**

Prem S. Paul Research Center at Whittier School  
Room 130, 2200 Vine Street  
Lincoln, Nebraska 68583-0853  
(402) 472-0965

### **Outdoor Test Site**

4630 N.W. 36<sup>th</sup> Street  
Lincoln, Nebraska 68524

## Submitted to

## **MIDWEST POOLED FUND PROGRAM**

Nebraska Department of Transportation  
1500 Nebraska Highway 2  
Lincoln, Nebraska 68502

MwRSF Research Report No. TRP-03-492-25

December 17, 2025

## TECHNICAL REPORT DOCUMENTATION PAGE

<b>1. Report No.</b> TRP-03-492-25	<b>2. Government Accession No.</b>	<b>3. Recipient's Catalog No.</b>	
<b>4. Title and Subtitle</b> Surface-Mounted Post Retrofit for Approach Guardrail Transitions: Phase I		<b>5. Report Date</b> December 17, 2025	
		<b>6. Performing Organization Code</b>	
<b>7. Author(s)</b> Rosenbaugh, S.K., Kumar, G.S., Stolle, C.S., and Faller, R.K.		<b>8. Performing Organization Report No.</b> TRP-03-492-25	
<b>9. Performing Organization Name and Address</b> Midwest Roadside Safety Facility (MwRSF) Nebraska Transportation Center University of Nebraska-Lincoln  Main Office: Prem S. Paul Research Center at Whittier School Suite 130, 2200 Vine Street Lincoln, Nebraska 68583-0853		<b>10. Work Unit No.</b>	
		<b>11. Contract</b> TPF-5(430) Supplement #2	
<b>12. Sponsoring Agency Name and Address</b> Midwest Pooled Fund Program Nebraska Department of Transportation 1500 Nebraska Parkway Lincoln, Nebraska 68502		<b>13. Type of Report and Period Covered</b> Final Report: 2020-2025	
		<b>14. Sponsoring Agency Code</b> RPFP-20-AGT-1	
<b>15. Supplementary Notes</b> Prepared in cooperation with U.S. Department of Transportation, Federal Highway Administration			
<b>16. Abstract</b> <p>The objective of this project was to develop retrofit options for approach guardrail transitions (AGTs) where obstructions prevent the proper installation of the guardrail posts. The project began with a survey of state departments of transportation to better understand the ground obstructions and site issues that were preventing posts from being properly installed. From this survey, it was determined that the best retrofit option would be a surface-mounted post. Thus, the project scope became the development and testing of a surface-mounted W6x15 AGT post.</p> <p>The surface-mounted post was required to provide similar strength to a standard W6x15 AGT post embedded in strong soil. The post was also required to prevent damage to the anchors and supporting concrete slab to avoid costly repairs when impacted. Additionally, the anchors were limited to an embedment of 6 in. to fit within an 8-in. thick concrete slab.</p> <p>Multiple post assemblies were configured with varying base plate sizes, base plate thicknesses, anchor rod diameters, post-to-plate weld specifications, weakening holes and cuts in the compression flange of the post. The configurations were evaluated through dynamic component testing. In all, nine component tests were conducted over three rounds of testing.</p> <p>Ultimately, Post Assembly M consisting of a W6x15 post with Ø1¼-in. x 3-in. slots in the compression flange and a 1-in. thick base plate was selected as the preferred surface-mounted post configuration. This configuration was recommended for further evaluation via <i>Manual for Assessing Safety Hardware</i> (MASH) crash testing, which would occur in a future Phase of this study.</p>			
<b>17. Key Words</b> Highway Safety, Approach Guardrail Transition, Retrofit, Post, Surface-Mounted, LS-DYNA, Dynamic Component Testing, Bogie Testing		<b>18. Distribution Statement</b> No restrictions. This document is available through the National Technical Information Service. 5285 Port Royal Road Springfield, VA 22161	
<b>19. Security Classification (of this report)</b> Unclassified	<b>20. Security Classification (of this page)</b> Unclassified	<b>21. No. of Pages</b> 105	<b>22. Price</b>

## **DISCLAIMER STATEMENT**

This material is based upon work supported by the Federal Highway Administration, U.S. Department of Transportation and the Midwest Pooled Fund Program under TPF-5(430) Supplement #2. The contents of this report reflect the views and opinions of the authors who are responsible for the facts and the accuracy of the data presented herein. The contents do not necessarily reflect the official views or policies of the University of Nebraska-Lincoln, state highway departments participating in the Midwest Pooled Fund Program nor the Federal Highway Administration, U.S. Department of Transportation. This report does not constitute a standard, specification, or regulation. Trade or manufacturers' names, which may appear in this report, are cited only because they are considered essential to the objectives of the report. The United States (U.S.) government and the State of Nebraska do not endorse products or manufacturers.

## **UNCERTAINTY OF MEASUREMENT STATEMENT**

The Midwest Roadside Safety Facility (MwRSF) has determined the uncertainty of measurements for several parameters involved in full-scale crash testing and non-standard testing of roadside safety features. Information regarding the uncertainty of measurements for critical parameters is available upon request by the sponsor and the Federal Highway Administration. Test nos. AGTRB-1 through AGTRB-9 were non-certified component tests used for research and development purposes only and are outside the scope of MwRSF's A2LA Accreditation.

## **ACKNOWLEDGEMENTS**

The authors wish to acknowledge several sources that made a contribution to this project: (1) the Midwest Pooled Fund Program funded by the California Department of Transportation, Florida Department of Transportation, Georgia Department of Transportation, Hawaii Department of Transportation, Illinois Department of Transportation, Indiana Department of Transportation, Iowa Department of Transportation, Kansas Department of Transportation, Kentucky Department of Transportation, Minnesota Department of Transportation, Missouri Department of Transportation, Nebraska Department of Transportation, New Jersey Department of Transportation, North Carolina Department of Transportation, Ohio Department of Transportation, South Carolina Department of Transportation, South Dakota Department of Transportation, Utah Department of Transportation, Virginia Department of Transportation, Wisconsin Department of Transportation, and Wyoming Department of Transportation for sponsoring this project; (2) MwRSF personnel for constructing the barriers and conducting the crash tests, and (3) the Holland Computing Center at the University of Nebraska, which receives support from the Nebraska Research Initiative, for providing computational resources. Acknowledgement is also given to the following individuals who contributed to the completion of this research project.

### **Midwest Roadside Safety Facility**

J.C. Holloway, M.S.C.E., Research Engineer & Assistant Director –  
Physical Testing Division  
K.A. Lechtenberg, M.S.M.E., Research Engineer  
R.W. Bielenberg, M.S.M.E., Research Engineer  
J.S. Steelman, Ph.D., P.E., Associate Professor  
B.J. Perry, M.E.M.E., Research Engineer  
A.E. Loken, Ph.D., Research Assistant Professor  
T.Y. Yosef, Ph.D., Research Assistant Professor  
Q.A. Alomari, Ph.D., Research Assistant Professor  
A.T. Russell, B.S.B.A., Testing and Maintenance Technician II

### **Midwest Roadside Safety Facility, Cont.**

E.W. Krier, B.S., Former Engineering Testing Technician II  
D.S. Charroin, Engineering Testing Technician II  
R.M. Novak, Engineering Testing Technician II  
T.C. Donahoo, Engineering Testing Technician I  
J.T. Jones, Engineering Testing Technician II  
E.L. Urbank, Research Communication Specialist  
Z.Z. Jabr, Engineering Technician  
J.J. Oliver, Solidworks Drafting Coordinator  
Undergraduate and Graduate Research Assistants

**California Department of Transportation**

David Whitesel, P.E., Transportation Engineer  
Thomas Mar, P.E., Transportation Engineer

**Florida Department of Transportation**

Derwood Sheppard, P.E., State Roadway Design Engineer  
Richard Stepp, P.E., Senior Standard Plans Engineer  
Rick Jenkins, P.E., State Standards Plans Engineer

**Georgia Department of Transportation**

Christopher Rudd, P.E., State Design Policy Engineer  
Frank Flanders IV, P.E., Assistant State Design Policy  
Engineer  
Doug Franks, P.E., Bridge Design Group Leader, Sr.

**Hawaii Department of Transportation**

Brent Ching, Structural Engineer  
Keith Kalani, Structural Engineer  
Kimberly Okamura, Engineer

**Illinois Department of Transportation**

Martha Brown, P.E., Safety Policy & Initiatives Engineer  
Edgar Galofre, P.E., Safety Design Engineer  
Kelli Erickson, Safety Design Evaluation Engineer

**Indiana Department of Transportation**

Katherine Smutzer, P.E., Standards Engineer  
Andrew Blackburn, P.E., Engineer  
Elizabeth Mouser, P.E., Standards & Policy Director

**Iowa Department of Transportation**

Daniel Harness, P.E., Transportation Engineer Specialist  
Brian Smith, P.E., Methods Engineer  
Mike Thiel, P.E., Transportation Engineer Specialist  
Stuart Nielsen, P.E., Methods Engineer

**Kansas Department of Transportation**

Scott King, P.E., Road Design Bureau Chief  
August Zuno, Engineer  
Jackie Austin, Engineer  
Jeff Sims, P.E., Road Design Leader

**Kentucky Transportation Cabinet**

Jason J. Siwula, P.E., Assistant State Highway Engineer  
Jeff Jasper, Program Leader, University of Kentucky  
Transportation Center  
Matthew Sipes, Transportation Engineer Branch Manager  
Tim Layson, Transportation Engineer Director

**Minnesota Department of Transportation**

Khamsai Yang, P.E., State Design Standards Engineer  
Michelle Moser, P.E., Assistant Design Standards Engineer  
Braden Cyr, P.E., Bridge Engineer  
Brian Tang, P.E., Assistant State Design Standards Engineer  
Arielle Ehrlich, P.E., State Bridge Design Engineer

**Missouri Department of Transportation**

Gidget Koestner, P.E., Policy & Innovations Engineer  
Kirby Woods, Jr., Roadside Design Engineer

**Nebraska Department of Transportation**

Jim Knott, P.E., Construction Engineer  
Mick Syslo, P.E., Deputy Director – Operations  
Mark Fischer, P.E., PMP, Research Program Manager  
Austin White, P.E., Plan Quality & Standards Engineer  
Brandie Neemann, P.E., Roadway Design Engineer  
Fouad Jaber, Assistant State Bridge Engineer  
Todd Hill, P.E., Assistant Roadway Design Engineer

**New Jersey Department of Transportation**

Hung Tang, P.E., Principal Engineer, Transportation  
Joseph Warren, Assistant Engineer, Transportation  
Xiaohua "Hannah" Cheng, P.E., Ph.D., Supervising Engineer,  
Structures  
Binyamin Abu Haltam, Engineer  
Sowatta Seng Eap, Engineer  
Madhavi Andey, Principal Engineer  
Vipul J. Shah, Engineer  
Manar Alsharaa, Supervising Engineer

**North Carolina Department of Transportation**

Jordan Woodard, P.E., Design Development & Support Group  
Lead  
Nicole Hackler, P.E., State Plans and Standards Engineer  
Shawn Troy, P.E., State Traffic Safety Engineer

**Ohio Department of Transportation**

Don Fisher, P.E., Roadway Standards Engineer  
Andrew Holloway, P.E., Transportation Engineer

**South Carolina Department of Transportation**

Mark H. Anthony, P.E., Letting Preparation Engineer  
Jason Hall, P.E., Engineer

**South Dakota Department of Transportation**

Sam Weisgram, Engineering Manager  
Drew Miller, Standards Engineer

**Utah Department of Transportation**

Shawn Debenham, Traffic and Safety Specialist  
Kelly Ash, Traffic Operations Engineer  
Clinton McCleery, Barrier & Attenuation Specialist

**Virginia Department of Transportation**

Charles Patterson, P.E., Standards/Special Design Section  
Manager  
Andrew Zickler, P.E., Complex Bridge Design and ABC  
Support Program Manager  
Bangfei Han, P.E., Senior Engineer  
Junyi Meng, P.E., Senior Structural Engineer

**Wisconsin Department of Transportation**

Erik Emerson, P.E., Standards Development Engineer  
Rodney Taylor, P.E., Roadway Design Standards Unit  
Supervisor

**Wyoming Department of Transportation**

William Wilson, P.E., Architectural and Highway Standards  
Engineer

**Federal Highway Administration**

David Mraz, Division Bridge Engineer, Nebraska Division  
Office

SI* (MODERN METRIC) CONVERSION FACTORS				
APPROXIMATE CONVERSIONS TO SI UNITS				
Symbol	When You Know	Multiply By	To Find	Symbol
<b>LENGTH</b>				
in.	inches	25.4	millimeters	mm
ft	feet	0.305	meters	m
yd	yards	0.914	meters	m
mi	miles	1.61	kilometers	km
<b>AREA</b>				
in <sup>2</sup>	square inches	645.2	square millimeters	mm <sup>2</sup>
ft <sup>2</sup>	square feet	0.093	square meters	m <sup>2</sup>
yd <sup>2</sup>	square yard	0.836	square meters	m <sup>2</sup>
ac	acres	0.405	hectares	ha
mi <sup>2</sup>	square miles	2.59	square kilometers	km <sup>2</sup>
<b>VOLUME</b>				
fl oz	fluid ounces	29.57	milliliters	mL
gal	gallons	3.785	liters	L
ft <sup>3</sup>	cubic feet	0.028	cubic meters	m <sup>3</sup>
yd <sup>3</sup>	cubic yards	0.765	cubic meters	m <sup>3</sup>
NOTE: volumes greater than 1,000 L shall be shown in m <sup>3</sup>				
<b>MASS</b>				
oz	ounces	28.35	grams	g
lb	pounds	0.454	kilograms	kg
T	short ton (2,000 lb)	0.907	megagrams (or "metric ton")	Mg (or "t")
<b>TEMPERATURE (exact degrees)</b>				
°F	Fahrenheit	5(F-32)/9 or (F-32)/1.8	Celsius	°C
<b>ILLUMINATION</b>				
fc	foot-candles	10.76	lux	lx
fl	foot-Lamberts	3.426	candela per square meter	cd/m <sup>2</sup>
<b>FORCE &amp; PRESSURE or STRESS</b>				
lbf	poundforce	4.45	newtons	N
lbf/in <sup>2</sup>	poundforce per square inch	6.89	kilopascals	kPa
APPROXIMATE CONVERSIONS FROM SI UNITS				
Symbol	When You Know	Multiply By	To Find	Symbol
<b>LENGTH</b>				
mm	millimeters	0.039	inches	in.
m	meters	3.28	feet	ft
m	meters	1.09	yards	yd
km	kilometers	0.621	miles	mi
<b>AREA</b>				
mm <sup>2</sup>	square millimeters	0.0016	square inches	in <sup>2</sup>
m <sup>2</sup>	square meters	10.764	square feet	ft <sup>2</sup>
m <sup>2</sup>	square meters	1.195	square yard	yd <sup>2</sup>
ha	hectares	2.47	acres	ac
km <sup>2</sup>	square kilometers	0.386	square miles	mi <sup>2</sup>
<b>VOLUME</b>				
ml	milliliter	0.034	fluid ounces	fl oz
L	liters	0.264	gallons	gal
m <sup>3</sup>	cubic meters	35.314	cubic feet	ft <sup>3</sup>
m <sup>3</sup>	cubic meters	1.307	cubic yards	yd <sup>3</sup>
<b>MASS</b>				
g	grams	0.035	ounces	oz
kg	kilograms	2.202	pounds	lb
Mg (or "t")	megagrams (or "metric ton")	1.103	short ton (2,000 lb)	T
<b>TEMPERATURE (exact degrees)</b>				
°C	Celsius	1.8C+32	Fahrenheit	°F
<b>ILLUMINATION</b>				
lx	lux	0.0929	foot-candles	fc
cd/m <sup>2</sup>	candela per square meter	0.2919	foot-Lamberts	fl
<b>FORCE &amp; PRESSURE or STRESS</b>				
N	newtons	0.225	poundforce	lbf
kPa	kilopascals	0.145	poundforce per square inch	lbf/in <sup>2</sup>

\*SI is the symbol for the International System of Units. Appropriate rounding should be made to comply with Section 4 of ASTM E380.

## TABLE OF CONTENTS

TECHNICAL REPORT DOCUMENTATION PAGE .....	i
DISCLAIMER STATEMENT .....	ii
UNCERTAINTY OF MEASUREMENT STATEMENT .....	ii
ACKNOWLEDGEMENTS .....	ii
SI* (MODERN METRIC) CONVERSION FACTORS .....	iv
TABLE OF CONTENTS.....	v
LIST OF FIGURES .....	vii
LIST OF TABLES.....	ix
1 INTRODUCTION .....	1
1.1 Background .....	1
1.2 Objective .....	3
1.3 Scope.....	3
2 STATE DOT SURVEY .....	4
3 DESIGN AND ANALYSIS .....	7
3.1 Design Criteria.....	7
3.2 Post Design .....	8
3.3 Anchorage Design.....	9
4 DYNAMIC COMPONENT TESTING CONDITIONS .....	11
4.1 Purpose.....	11
4.2 Scope.....	11
4.3 Equipment and Instrumentation .....	11
4.3.1 Bogie Vehicle.....	11
4.3.2 Accelerometers .....	12
4.3.3 Retroreflective Optic Speed Trap .....	13
4.3.4 Digital Photography .....	13
4.4 End of Test Determination.....	14
4.5 Data Processing.....	14
5 DYNAMIC COMPONENT TESTING – ROUND 1.....	15
5.1 Scope.....	15
5.2 Results.....	30
5.2.1 Test No. AGTRB-1 .....	30
5.2.2 Test No. AGTRB-2.....	32
5.2.3 Test No. AGTRB-3 .....	34
5.2.4 Test No. AGTRB-4.....	36
5.2.5 Test No. AGTRB-5.....	38

5.3 Discussion.....	40
6 DYNAMIC COMPONENT TESTING – ROUND 2.....	42
6.1 Scope.....	42
6.2 Results.....	53
6.2.1 Test No. AGTRB-6.....	53
6.2.2 Test No. AGTRB-7.....	55
6.3 Discussion.....	57
7 DYNAMIC COMPONENT TESTING – ROUND 3.....	59
7.1 Scope.....	59
7.2 Results.....	67
7.2.1 Test No. AGTRB-8.....	67
7.2.2 Test No. AGTRB-9.....	69
7.3 Discussion.....	71
8 SUMMARY AND CONCLUSIONS .....	73
9 REFERENCES .....	75
10 APPENDICES .....	77
Appendix A. State DOT Survey .....	78
Appendix B. Bogie Test Results.....	86

## LIST OF FIGURES

Figure 1. Cantilevered Beam Retrofit for First Post Adjacent to Concrete Parapet [1] .....	1
Figure 2. Dual Post and Beam Retrofit for Straddling an Obstruction [1] .....	2
Figure 3. Photographs of Actual AGT Installations with Obstructed AGT Posts .....	5
Figure 4. Photographs of AGTs Installed on Slopes.....	5
Figure 5. Photographs of AGT Posts Within Asphalt or Concrete Pavements .....	6
Figure 6. Force-Displacement Data for Tests MGSATB-5 and MGSATB-6 [9].....	7
Figure 7. Weakening Holes in Post Compression Flange.....	8
Figure 8. Base Plate Bending Allowing Post Rotation.....	9
Figure 9. Rigid-Frame Bogie Vehicles on Guidance Tracks.....	12
Figure 10. Dynamic Component Testing Matrix and Setup – Round 1 .....	16
Figure 11. Test Article Details, Round 1 – Assembly A .....	17
Figure 12. Test Article Details, Round 1 – Assembly B .....	18
Figure 13. Test Article Details, Round 1 – Assembly C .....	19
Figure 14. Test Article Details, Round 1 – Assembly D .....	20
Figure 15. Test Article Details, Round 1 – Assembly E.....	21
Figure 16. Test Article Details, Round 1 – Assembly F.....	22
Figure 17. Test Article Details, Round 1 – Assembly G .....	23
Figure 18. Test Article Details, Round 1 – Assembly H .....	24
Figure 19. Test Article Details, Round 1 – Assembly I.....	25
Figure 20. Test Article Details, Round 1 – Base Plates.....	26
Figure 21. Test Article Details, Round 1 – Post Segments.....	27
Figure 22. Test Article Details, Round 1 – Anchorage Hardware .....	28
Figure 23. Test Article Details, Round 1 – Bill of Materials.....	29
Figure 24. Time-Sequential and Post-Impact Photographs, Test No. AGTRB-1.....	31
Figure 25. Force vs. Deflection and Energy vs. Deflection, Test No. AGTRB-1 .....	32
Figure 26. Time-Sequential and Post-Impact Photographs, Test No. AGTRB-2.....	33
Figure 27. Force vs. Deflection and Energy vs. Deflection, Test No. AGTRB-2 .....	34
Figure 28. Time-Sequential and Post-Impact Photographs, Test No. AGTRB-3.....	35
Figure 29. Force vs. Deflection and Energy vs. Deflection, Test No. AGTRB-3 .....	36
Figure 30. Time-Sequential and Post-Impact Photographs, Test No. AGTRB-4.....	37
Figure 31. Force vs. Deflection and Energy vs. Deflection, Test No. AGTRB-4 .....	38
Figure 32. Time-Sequential and Post-Impact Photographs, Test No. AGTRB-5.....	39
Figure 33. Force vs. Deflection and Energy vs. Deflection, Test No. AGTRB-5 .....	40
Figure 34. Force vs. Deflection Comparison, Component Testing - Round 1 .....	41
Figure 35. Energy vs. Deflection Comparison, Component Testing - Round 1 .....	41
Figure 36. Dynamic Component Testing Matrix and Setup – Round 2 .....	43
Figure 37. Test Article Details, Round 2 – Assembly J.....	44
Figure 38. Test Article Details, Round 2 – Assembly K .....	45
Figure 39. Test Article Details, Round 2 – Assembly L.....	46
Figure 40. Test Article Details, Round 2 – Assembly M.....	47
Figure 41. Test Article Details, Round 2 – Assembly N .....	48
Figure 42. Test Article Details, Round 2 – Base Plates.....	49
Figure 43. Test Article Details, Round 2 – Post Segments.....	50
Figure 44. Test Article Details, Round 2 – Anchorage Hardware .....	51
Figure 45. Test Article Details, Round 2 – Bill of Materials.....	52

Figure 46. Time-Sequential and Post-Impact Photographs, Test No. AGTRB-6.....	54
Figure 47. Force vs. Deflection and Energy vs. Deflection, Test No. AGTRB-6 .....	55
Figure 48. Time-Sequential and Post-Impact Photographs, Test No. AGTRB-7.....	56
Figure 49. Force vs. Deflection and Energy vs. Deflection, Test No. AGTRB-7 .....	57
Figure 50. Force vs. Deflection Comparison, Round 2 Bogie Tests .....	58
Figure 51. Energy vs. Deflection Comparison, Round 2 Bogie Tests.....	58
Figure 52. Photographs of the Test Installations for Test Nos. AGTRB-8 and AGTRB-9.....	59
Figure 53. Dynamic Component Testing Matrix and Setup – Round 3 .....	60
Figure 54. Dynamic Component Testing Setup – Test No. AGTRB-8 .....	61
Figure 55. Test Article Details, Round 3 – Post Assembly .....	62
Figure 56. Test Article Details, Round 3 – Post and Base plate.....	63
Figure 57. Test Article Details, Round 3 – Concrete Slabs .....	64
Figure 58. Test Article Details, Round 3 – Anchorage Hardware.....	65
Figure 59. Test Article Details, Round 3 – Bill of Materials.....	66
Figure 60. Time-Sequential and Post-Impact Photographs, Test No. AGTRB-8.....	68
Figure 61. Force vs. Deflection and Energy vs. Deflection, Test No. AGTRB-8 .....	69
Figure 62. Time-Sequential and Post-Impact Photographs, Test No. AGTRB-9.....	70
Figure 63. Force vs. Deflection and Energy vs. Deflection, Test No. AGTRB-9 .....	71
Figure 64. Concrete Breakout Cone Shape [11] .....	72
Figure 65. Anchor Location for Test No. AGTRB-8.....	72
Figure B-1. Test No. AGTRB-1 Results (SLICE-1).....	87
Figure B-2. Test No. AGTRB-1 Results (SLICE-2).....	88
Figure B-3. Test No. AGTRB-2 Results (SLICE-1).....	89
Figure B-4. Test No. AGTRB-2 Results (SLICE-2).....	90
Figure B-5. Test No. AGTRB-3 Results (SLICE-1).....	91
Figure B-6. Test No. AGTRB-3 Results (SLICE-2).....	92
Figure B-7. Test No. AGTRB-4 Results (SLICE-1).....	93
Figure B-8. Test No. AGTRB-4 Results (SLICE-2).....	94
Figure B-9. Test No. AGTRB-5 Results (SLICE-1).....	95
Figure B-10. Test No. AGTRB-5 Results (SLICE-2).....	96
Figure B-11. Test No. AGTRB-6 Results (SLICE-1).....	97
Figure B-12. Test No. AGTRB-6 Results (SLICE-2).....	98
Figure B-13. Test No. AGTRB-7 Results (SLICE-1).....	99
Figure B-14. Test No. AGTRB-7 Results (SLICE-2).....	100
Figure B-15. Test No. AGTRB-8 Results (SLICE-1).....	101
Figure B-16. Test No. AGTRB-8 Results (SLICE-2).....	102
Figure B-17. Test No. AGTRB-9 Results (SLICE-1).....	103
Figure B-18. Test No. AGTRB-9 Results (SLICE-2).....	104

## LIST OF TABLES

Table 1. Summary of Survey Responses .....	4
Table 2. Summary of Cameras used Per Test.....	13
Table 3. Summary of Post Assemblies .....	15
Table 4. Test Matrix, Dynamic Component Testing - Round 1 .....	15
Table 5. Results Summary, Component Testing - Round 1 .....	40
Table 6. Summary of Post Assemblies – Round 2.....	42
Table 7. Results Summary, Component Testing - Round 2 .....	58

## 1 INTRODUCTION

### 1.1 Background

Utility and drainage structures, such as intake tops, underground pipes, and surface flumes, are commonly found along the roadside. When these structures are located adjacent to the ends of a bridge, they can prevent the proper placement of guardrail posts within the approach guardrail transition (AGT). Previous studies have suggested that omitting even a single post from an AGT can be detrimental to the safety performance of the system by increasing deflections, pocketing, and vehicle snag [1]. Thus, AGT retrofit options are necessary to properly treat these sites where the AGTs cannot be installed in their original, as-tested configurations.

In 2012, MwRSF conducted a study on retrofitting existing AGTs at locations where a transition post could not be properly installed [1]. These retrofits included a horizontal beam mounted to the backside of the rigid buttress/bridge rail as a surrogate for the first transition post adjacent to the parapet, as shown in Figure 1, and a dual post and beam structure that could be used to straddle an obstruction anywhere within the AGT, as shown in Figure 2. However, some installations are troubled with obstructions that either prevent multiple posts from being properly installed or prevent these retrofits from being installed properly. For example, a large drainage basin or a pipe running parallel to the roadway would prevent multiple posts from being properly installed. Therefore, a need exists to develop additional AGT retrofits for installation sites where obstructions prevent proper installation.

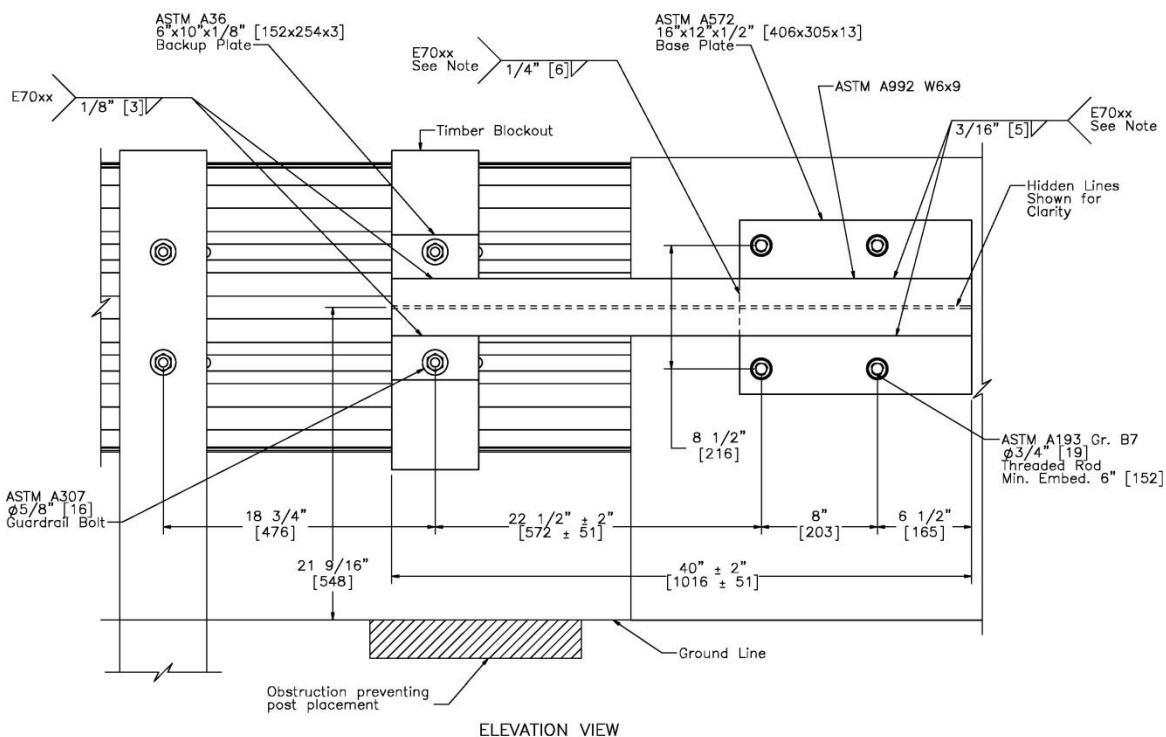


Figure 1. Cantilevered Beam Retrofit for First Post Adjacent to Concrete Parapet [1]

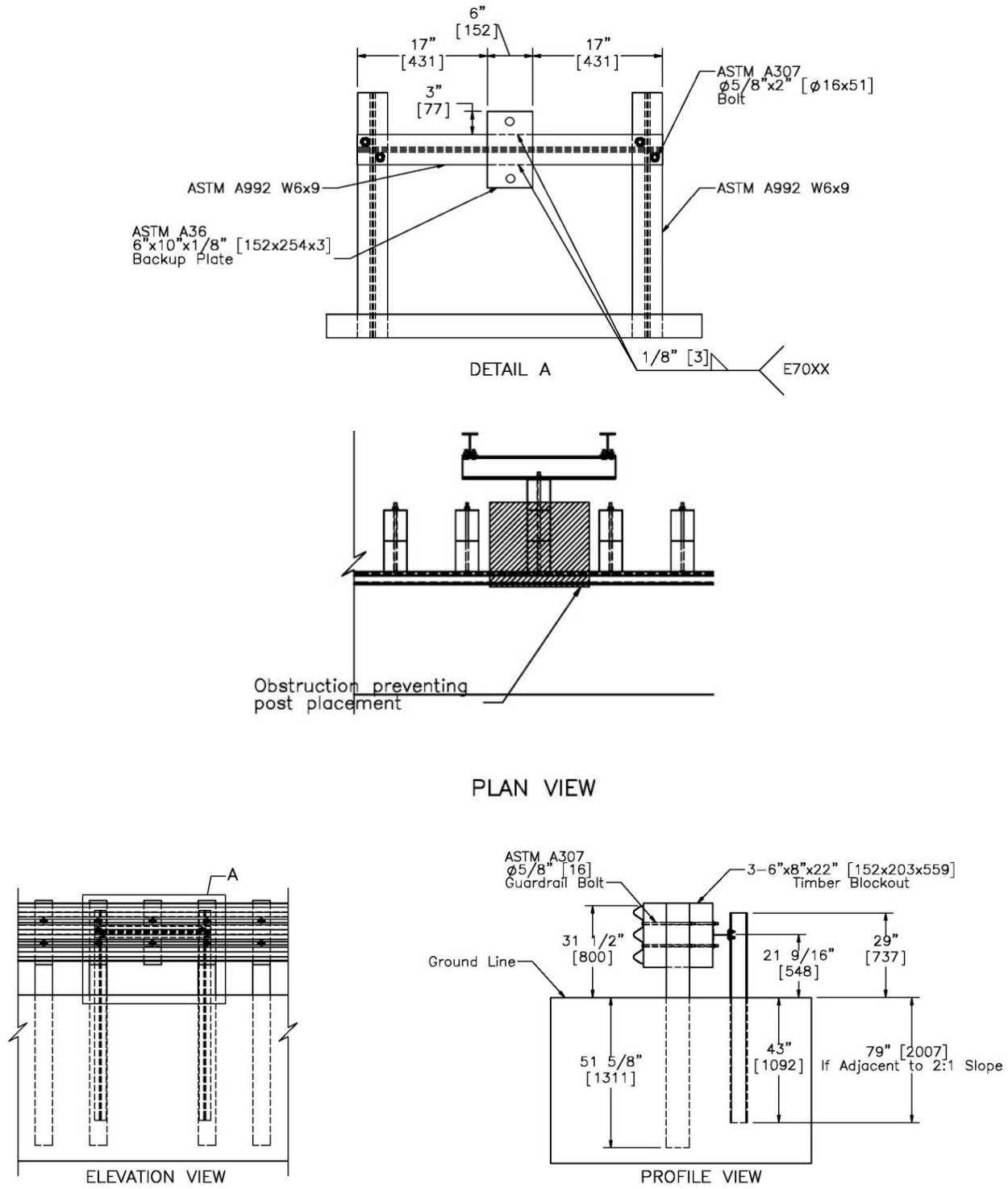


Figure 2. Dual Post and Beam Retrofit for Straddling an Obstruction [1]

## 1.2 Objective

The objective of this project was to develop additional retrofit options for AGTs where obstructions prevent the proper installation of the guardrail posts. The new retrofit options developed herein were to address obstructions that the previous retrofits did not cover, as well as address obstructions that prevented multiple posts from being installed within an AGT. The retrofitted AGTs should remain crashworthy to Test Level 3 (TL-3) of American Association of State Highway and Transportation Officials' (AASHTO's) *Manual for Assessing Safety Hardware (MASH)* [2]. Phase I of the project, documented herein, was to develop retrofit designs through computer simulation, and dynamic component testing. The proposed retrofits developed in Phase I would be evaluated via crash testing in Phase II of the project.

## 1.3 Scope

Research efforts began with a survey of the sponsoring state departments of transportation (DOTs) to gain an understanding of the types of hazards and obstructions that were preventing AGTs from being installed in nominal configurations. From this survey, a surface-mounted post was selected as the desired retrofit to address many real-world site issues. A surface-mounted AGT post design was then developed through engineering analysis and computer simulations. The surface-mounted post design was then refined through dynamic component testing. The finalized post configuration was recommended for MASH crash testing for a complete performance evaluation.

## 2 STATE DOT SURVEY

To better understand the obstructions and site conditions that were preventing the proper installation of AGT posts, a survey/questionnaire was sent to the State DOTs that sponsored this research project. The survey sought to identify the types and sizes of the obstructions, estimate the number of affect posts and their locations within an AGT, learn about current practices for retrofitting AGT installations when post obstructions are present, and gather photographs of actual AGT installations. A copy of the survey is provided in Appendix A.

Table 1 contains a summary of the survey responses that were received from 11 State DOTs. Ten DOTs expressed that they regularly have obstructions near bridge ends that prevent the installation of AGT posts. The most common obstructions were drainage structures, utility lines, and wingwalls. These obstructions were most likely to be located within 10 ft of the bridge (as measured from the end of the bridge rail or buttress) and the number of posts affected by these obstructions was typically limited to three or less. Photographs of actual AGT installations provided by survey respondents are shown in Figure 3.

Table 1. Summary of Survey Responses

AGT Installation Issue	Number of DOTs Observing Issue*
Site constraints preventing AGT post installation	10
Site constraints allowing only partial embedment of AGT posts	7
Ground slopes on or near AGT post locations	7
Asphalt/concrete pavements covering AGT location	5

\*11 total DOT responses

The survey responses also revealed that AGT posts often had to be installed on soil fill slopes or within concrete/asphalt pavements. Previous studies have shown guardrail posts installed on or adjacent to steep slopes have reduced strengths due to the lack of soil behind the post [3-5]. Reduced post strengths within AGTs would result in increased system deflections and vehicle snag [1]. Conversely, asphalt and concrete pavements prevent guardrail posts from rotating through the soil, thereby increasing post resistive strengths and leading to vehicle snag on posts and increased stresses in the guardrail [6-8]. Thus, both of these ground conditions can be detrimental to the performance of an AGT. Examples of actual AGTs installed in these conditions provided by survey respondents are shown in Figures 4 and 5.

Various retrofit design configurations to remedy these non-ideal site conditions were discussed with the project sponsor. Ultimately, the development of a surface-mounted AGT post was selected as the retrofit that best addressed these installation issues. A surface-mounted post would not interfere with subsurface structures, drainage pipes, or utility lines. Further, a surface-mounted post could be directly attached to concrete pavements and could be placed adjacent to steep slopes.



Figure 3. Photographs of Actual AGT Installations with Obstructed AGT Posts



Figure 4. Photographs of AGTs Installed on Slopes



Figure 5. Photographs of AGT Posts Within Asphalt or Concrete Pavements

### 3 DESIGN AND ANALYSIS

#### 3.1 Design Criteria

Following the DOT survey discussed in Chapter 2, the scope of the project was changed to focus on the development of a surface-mounted post as a retrofit option for obstructed AGT posts. MASH-crashworthy, thrie-beam AGTs typically utilize one of two post configurations: (1) W6x9 posts spaced at 18 $\frac{3}{4}$  in. (quarter post spacing) or (2) W6x15 posts spaced at 37 $\frac{1}{2}$  in. (half post spacing). Running concurrent to the project described herein, another Midwest Pooled Fund project was focused on the development of a surface-mounted W6x9 post for use with the Midwest Guardrail System (MGS). To avoid duplication of research efforts, it was decided that the surface-mounted AGT post would focus on retrofitting a W6x15 AGT post.

The primary function for the retrofit post was to replicate the strength of the original W6x15 AGT post. In other words, the surface-mounted retrofit post was required to provide similar force-deflection characteristics to the W6x15 embedded in soil. In a previous study, 7-ft long W6x15 posts had been evaluated through dynamic impact testing with a rigid frame bogie vehicle [9]. In test nos. MGSATB-5 and MGSATB-6, W6x15 posts embedded 54 in. into compacted soil were impacted by an 1,800-lb bogie at a speed of 20 mph and at a height of 25 in. Force-Displacement plots from these bogie tests are shown in Figure 6. Through 15 in. of displacement, the average forces from these two tests were 16.9 kips and 17.9 kips, respectively. Thus, the target strength for the new surface-mounted, AGT post was an average of 17 kips through 10 in. of displacement.

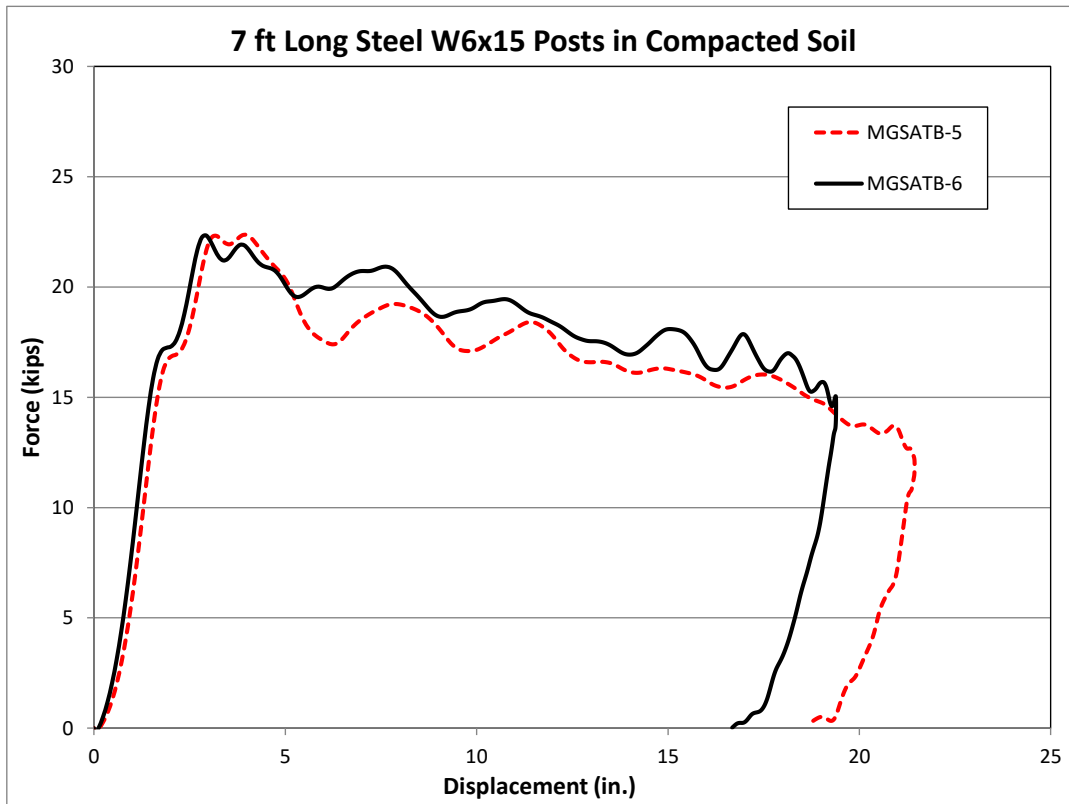


Figure 6. Force-Displacement Data for Tests MGSATB-5 and MGSATB-6 [9]

The AGT retrofit post was to be assembled from an ASTM A992 W6x15 post and an ASTM A572 base plate. The retrofit post was to utilize the same section as the original AGT post to avoid confusion as to which posts the new surface-mounted post could replace. The material specification for the base plate was selected to match the yield strength of W6x15 post (50 ksi).

A minimum depth of 8 in. and a minimum compressive strength of 4,000 psi were selected for the concrete slab that would be supporting the new retrofit post. Accordingly, the threaded rods used to anchor the retrofit post were limited to an embedment depth of 6 in. within the concrete slab. Finally, to avoid costly repairs, the concrete and anchor rods were to remain undamaged when the post was impacted/loaded. Thus, retrofit posts within an impacted/damaged AGT could be replaced with new posts using the same anchors.

### 3.2 Post Design

Recall, the surface-mounted retrofit post was required to have an average strength of 17 kips through 10 in. of lateral displacement. However, a W6x15 post attached to a rigid base plate would provide a higher strength than this desired value. Calculating a posts strength using the plastic section modulus of  $Z_x = 10.8 \text{ in.}^3$ , a yield strength of  $f_y = 50 \text{ ksi}$ , and an effective load height of 24 in. results in 23 kips to bend the post backward. Having a post strength 35 percent higher than desired could lead to vehicle snag and excessive decelerations. Further, increased post strengths would be more demanding on the anchorage hardware and concrete slab that were to remain undamaged. Thus, the post needed to be weakened.

Various methods and mechanisms were explored to weaken the strength of the retrofit post. One mechanism was to put holes, chamfers, or cuts in the compression flange of the post, as shown in Figure 7. The reduced section would cause localized flange buckling under lower loads while still allowing plastic bending resistance after yielding. Placing holes or cuts in the tension flange was not desired as they could lead to tensile rupture of the flange and a significant loss of strength.

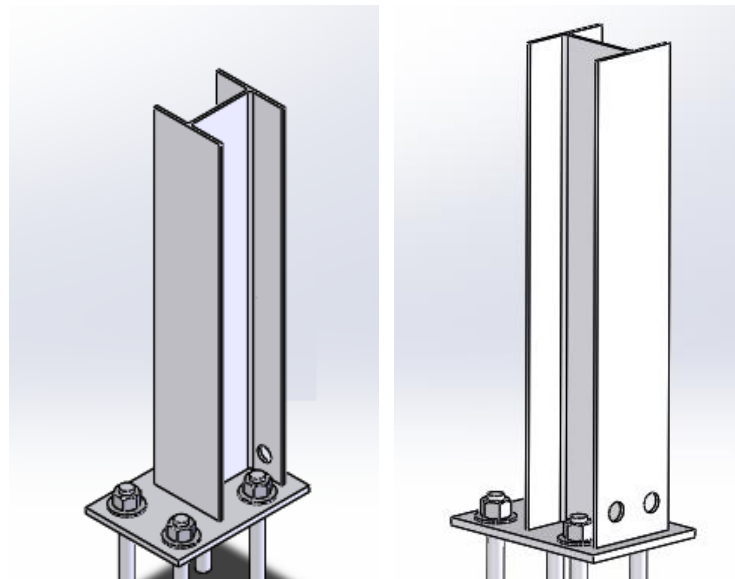


Figure 7. Weakening Holes in Post Compression Flange

Various weld patterns were also explored as a post-weakening mechanism. One weakening concept was to only weld the front flange and web of the post to the base plate. The unwelded compression flange would then be susceptible to localized buckling, and hopefully, a reduced strength to bend the post. Welds on the tension flange were considered crucial to developing bending strength in the post, so only the welds on the compression flange were omitted for this weakening concept.

Finally, varying the thickness and size of the base plate was also considered as a weakening mechanism for the retrofit post. A thinner/smaller base plate would bend during loading to the post and allow the post to rotate backwards, as shown in Figure 8. All of the post weakening mechanisms discussed in this section were explored via dynamic impact testing, as documented in Chapters 5 through 7.



Figure 8. Base Plate Bending Allowing Post Rotation

The weld required to provide adequate strength for the front flange was also to be evaluated. In a previous study, a standard  $\frac{1}{4}$ -in. fillet weld showed insufficient strength to attach a W6x9 post to a base plate. When this W6x9 culvert post assembly was subjected to dynamic impact testing, the weld on the front flange failed. Ultimately, a 3-pass,  $\frac{3}{8}$ -in. fillet weld was necessary to prevent premature failure along the front flange of the W6x9 culvert post [10]. It was unclear if a similar 3-pass weld would be necessary for the W6x15 post assembly designed herein. Thus, dynamic testing would be conducted on posts with various welds along the front flange of the post.

### 3.3 Anchorage Design

As discussed in Section 3.1, the anchorage for the surface-mounted, retrofit post was to be designed for 8 in. thick concrete slabs, thus limiting the anchor embedment depth to 6 in. Additionally, both the anchor rods and the concrete slab were to remain undamaged during impact events. Thus, the anchor rods and their spacing needed to be designed to prevent failure.

The anchor rods themselves had to be strong enough to prevent tensile failure as lateral loads to the post translated to tensile load in the anchors. The post was designed for a lateral impact load of 17 kips, but the lateral distance between the anchor rods and the post would dictate the magnitude of the tensile load in the rods (i.e., a greater lateral distance results in a greater moment arm and a reduced tensile demand on the anchor rods). However, the base plate was not to extend in front of the thrie beam and oversized base plates would add unnecessary cost to the retrofit post. Additionally, the longitudinal spacing between anchor rods (lateral width of the base plate) had to be sufficient to avoid concrete breakout failure in the slab. Thus, the size of the anchor rods, the spacing between anchor rods, and the lateral distance between the anchor rods and the post had to be optimized.

The base plate and anchor rod configurations were optimized by varying the anchor locations, calculating their tensile demand, and estimating the anchorage tensile strength using Chapter 17 of ACI 318 [11], which provides strength analysis procedures for anchor rupture and concrete breakout. Ultimately, the optimized anchor configuration was designed with  $\frac{7}{8}$ -in. diameter ASTM A193 B7 threaded rods spaced 8 in. apart and at a distance of  $5\frac{1}{2}$  in. from the front flange of the W6x15 post. The base plate configuration was 11 in. wide by 16 in. deep. Dynamic component testing was used to determine the necessary thickness of the base plate, as documented in Chapters 5 through 7.

## 4 DYNAMIC COMPONENT TESTING CONDITIONS

### 4.1 Purpose

Dynamic component tests were conducted on various configurations of the surface-mounted, retrofit AGT post to evaluate the strength and robustness of the configurations. The desired performance for the retrofit post was an average resistance force of 17 kips over 10 in. of displacement. Additionally, the post should deflect in a controlled manner without any failure or damage to the anchor rods or concrete slab. For each round of component testing, multiple retrofit post configurations were fabricated, and the testing was conducted with an iterative approach where the post configuration selected for a given test was based on the results of the previous tests. Not all of the fabricated posts were tested.

### 4.2 Scope

A total of nine dynamic component tests were conducted over 3 rounds of testing. Each test consisted of a bogie vehicle impacting one of the design variations for the surface-mounted, retrofit post. The targeted impact conditions were a speed of 18 mph and an angle of 90 degrees, creating a classical “head-on” or full frontal impact and strong axis bending. The bogie impact head contacted the posts at a height of 25 in. above ground line. Each retrofit post configuration was comprised of a W6x15 post welded to a base plate, and the post assembly was anchored to the concrete tarmac using epoxy anchored threaded rods. Details on the various post configurations are provided in the test chapters for each round of component testing.

### 4.3 Equipment and Instrumentation

Equipment and instrumentation utilized to collect and record data during the dynamic bogie tests included a bogie vehicle, accelerometers, a retroreflective speed trap, high-speed and standard-speed digital video cameras.

#### 4.3.1 Bogie Vehicle

A rigid-frame bogie was used to impact the posts. A variable height, detachable impact head was used in the testing. The bogie head was constructed of 8-in. diameter,  $\frac{1}{2}$ -in. thick standard steel pipe, with  $\frac{3}{4}$ -in. neoprene belting wrapped around the pipe to prevent local damage to the post from the impact. The impact head was bolted to the bogie vehicle, creating a rigid frame with an impact height of 25 in. Tests AGTRB-1 through AGTRB-7 used bogie no. 4 with a weight of 2,540 lb, while test nos. AGTRB-8 and AGTRB-9 used bogie no. 3 with a weight of 2,302 lb. Both bogie vehicles equipped with the impact head are shown in Figure 9.

A pickup truck with a reverse-cable tow system was used to propel the bogie to a target impact speed of 18 mph. When the bogie approached the end of the guidance system, it was released from the tow cable, allowing it to be free rolling when it impacted the post. A radio-controlled brake system was installed on the bogie, allowing it to be brought safely to rest after the test.



(a) Bogie No. 4 – Tests AGTRB-1 through AGTRB-7



(b) Bogie No. 3 – Tests AGTRB-8 and AGTRB-9

Figure 9. Rigid-Frame Bogie Vehicles on Guidance Tracks

#### 4.3.2 Accelerometers

Two accelerometer systems were mounted on the bogie vehicle near its center of gravity (c.g.) to measure the acceleration in the longitudinal, lateral, and vertical directions. However, only the longitudinal acceleration was processed and reported.

The two systems, the SLICE-1 and SLICE-2 units, were modular data acquisition systems manufactured by Diversified Technical Systems, Inc. of Seal Beach, California. Triaxial acceleration and angular rate sensor modules were mounted inside the bodies of custom-built SLICE 6DX event data recorders equipped with 7GB of non-volatile flash memory and recorded data at 10,000 Hz to the onboard microprocessor. The accelerometers had a range of  $\pm 500\text{g}$ 's in each of three directions (longitudinal, lateral, and vertical) and a 1,650 Hz (CFC 1000) anti-aliasing

filter. The SLICE MICRO Triax ARS had a range of 1,500 degrees/sec in each of three directions (roll, pitch, and yaw). The raw angular rate measurements were downloaded, converted to the proper Euler angles for analysis, and plotted. The “SLICEWare” computer software program and a customized Microsoft Excel worksheet were used to analyze and plot the accelerometer data.

#### 4.3.3 Retroreflective Optic Speed Trap

A retroreflective optic speed trap was used to determine the speed of the bogie vehicle before impact. Three retroreflective targets, spaced at approximately 18-in. intervals, were applied to the side of the bogie vehicle. When the emitted beam of light was reflected by the targets and returned to the Emitter/Receiver, a signal was sent to the data acquisition computer, recording at 10,000 Hz, as well as the external LED box activating the LED flashes. The speed was then calculated using the spacing between the retroreflective targets and the time between the signals. LED lights and high-speed digital video analysis are used as a backup if vehicle speeds cannot be determined from the electronic data.

#### 4.3.4 Digital Photography

AOS high-speed digital video cameras, GoPro digital video cameras, and Panasonic digital cameras were used to document each test. The AOS high-speed cameras had a frame rate of 500 frames per second, the GoPro video cameras had a frame rate of 120 frames per second, and the Panasonic digital video cameras had a frame rate of 120 frames per second. The cameras were placed laterally from the post, with a view perpendicular to the bogie’s direction of travel. A summary of the number of video cameras used in each test is shown in Table 2.

Table 2. Summary of Cameras used Per Test

Test	Number of Cameras		
	AOS	GoPro	Panasonic
AGTRB-1	1	3	1
AGTRB-2	1	3	1
AGTRB-3	1	3	1
AGTRB-4	1	3	1
AGTRB-5	1	3	1
AGTRB-6	1	1	3
AGTRB-7	1	1	3
AGTRB-8	1	0	4
AGTRB-9	1	0	4

#### **4.4 End of Test Determination**

When the impact head initially contacts the test article, the force exerted by the bogie vehicle is directly perpendicular. However, as the post rotates, the bogie's orientation and path move away from perpendicular. This introduces two sources of error: (1) the contact force between the impact head and the post has a vertical component and (2) the impact head slides upward along the test article. Therefore, only the initial portion of the accelerometer trace should be used since variations in the data become significant as the system rotates and the bogie overrides the system. Additionally, guidelines were established to define the end of test time using the high-speed video of the impact. The first occurrence of either of the following events was used to determine the end of the test: (1) the test article fractured or (2) the bogie overrode or lost contact with the test article.

#### **4.5 Data Processing**

The electronic accelerometer data obtained in dynamic testing was filtered using the SAE Class 60 Butterworth filter conforming to the SAE J211/1 specification [12]. The pertinent acceleration signal was extracted from the bulk of the data signals. The processed acceleration data was then multiplied by the mass of the bogie to get the impact force using Newton's Second Law. Next, the acceleration trace was integrated to find the change in velocity versus time. Initial velocity of the bogie, calculated from the retroreflective optic speed trap data, was then used to determine the bogie's velocity and the calculated velocity trace was integrated to find the bogie's displacement. This displacement is also the displacement of the post. Combining the previous results, a force vs. deflection curve was plotted for each test. Finally, integration of the force vs. deflection curve provided the energy vs. deflection curve for each test.

## 5 DYNAMIC COMPONENT TESTING – ROUND 1

### 5.1 Scope

For Round 1 of dynamic component testing, nine different configurations of the surface-mounted, retrofit AGT post were fabricated. However, the selection of which post assembly to evaluate was done iteratively for each test based on the results from the previous tests. Thus, only five tests were conducted during Round 1. The remaining four post assemblies were not anticipated to provide the desired performance, so they were discarded.

Each of the post assemblies included a 31-in. tall W6x15 post welded to a steel base plate of varying sizes. Each post assembly was anchored by two Ø7/8-in. threaded rods, which were embedded into the tarmac using epoxy adhesive. The two anchor rods were spaced 8 in. apart and 5½ in. in front of the front flange of the post.

Round 1 of component testing sought to evaluate a baseline post with no weakening mechanisms (Assembly A) and posts with various weakening mechanisms including holes and chamfers in the compression flange, various weld patterns, base plate thicknesses, and base plate lengths. All nine post assemblies are described in Table 3 and detailed in Figures 10 through 23. The test matrix describing which post assembly was evaluated during each test listed in Table 4.

Table 3. Summary of Post Assemblies

Assembly	Base plate Dimensions	Base plate Thickness	Front Flange Fillet Weld	Back Flange Fillet Weld	Compression Flange Weakening
A	16" x 11"	1"	3-Pass 3/8"	1/4"	-
B	16" x 11"	1"	3-Pass 3/8"	None	-
C	16" x 11"	3/4"	3-Pass 3/8"	1/4"	-
D	16" x 11"	3/4"	3-Pass 3/8"	None	-
E	16" x 11"	3/4"	1/4"	1/4"	-
F	16" x 11"	1"	1/4"	None	-
G	14" x 11"	3/4"	3-Pass 3/8"	None	-
H	16" x 11"	1"	3-Pass 3/8"	1/4"	Ø1½" holes
I	16" x 11"	1"	3-Pass 3/8"	1/4"	1½" chamfers

- = not applicable

Table 4. Test Matrix, Dynamic Component Testing - Round 1

Test	Assembly
AGTRB-1	A
AGTRB-2	B
AGTRB-3	E
AGTRB-4	H
AGTRB-5	I

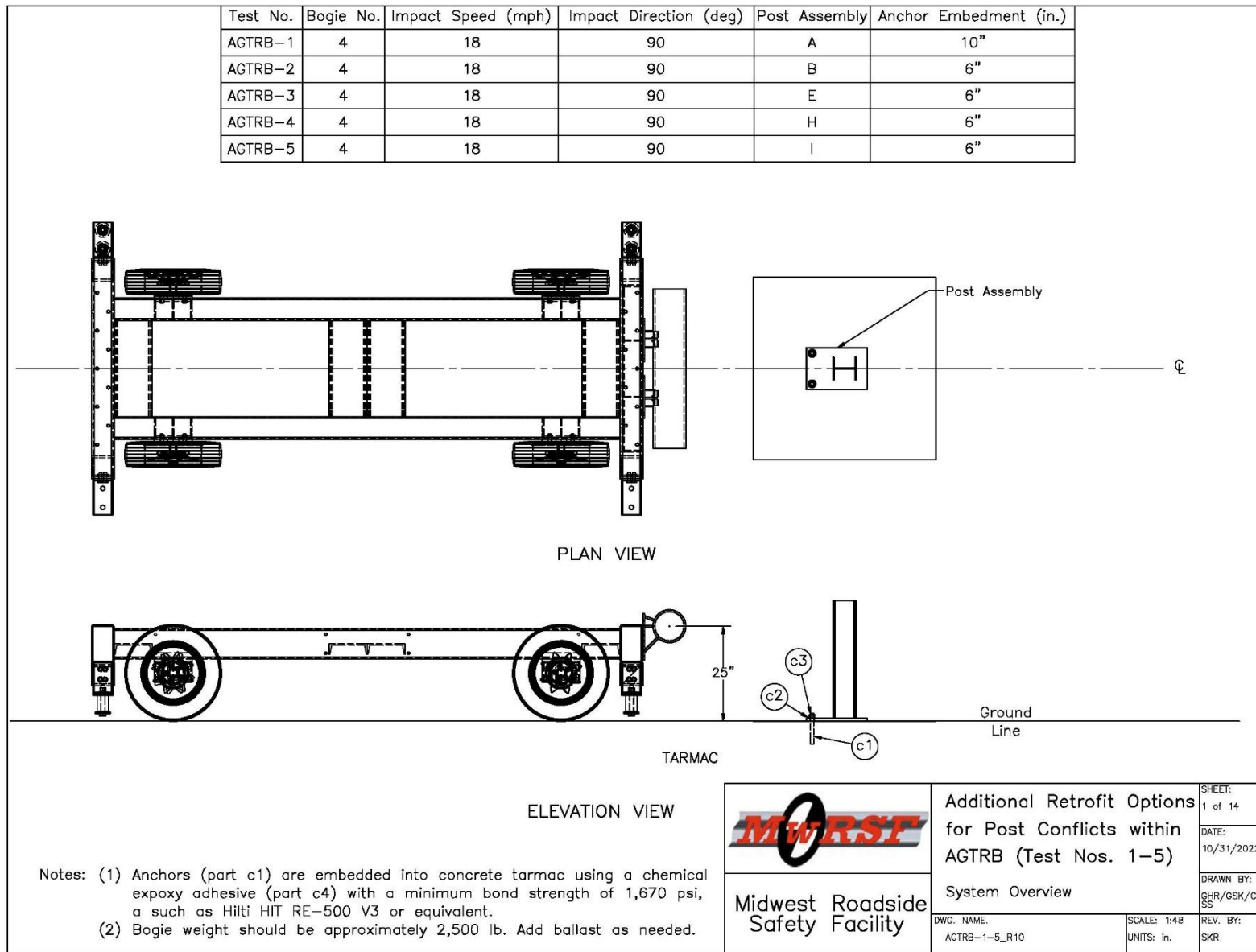


Figure 10. Dynamic Component Testing Matrix and Setup – Round 1

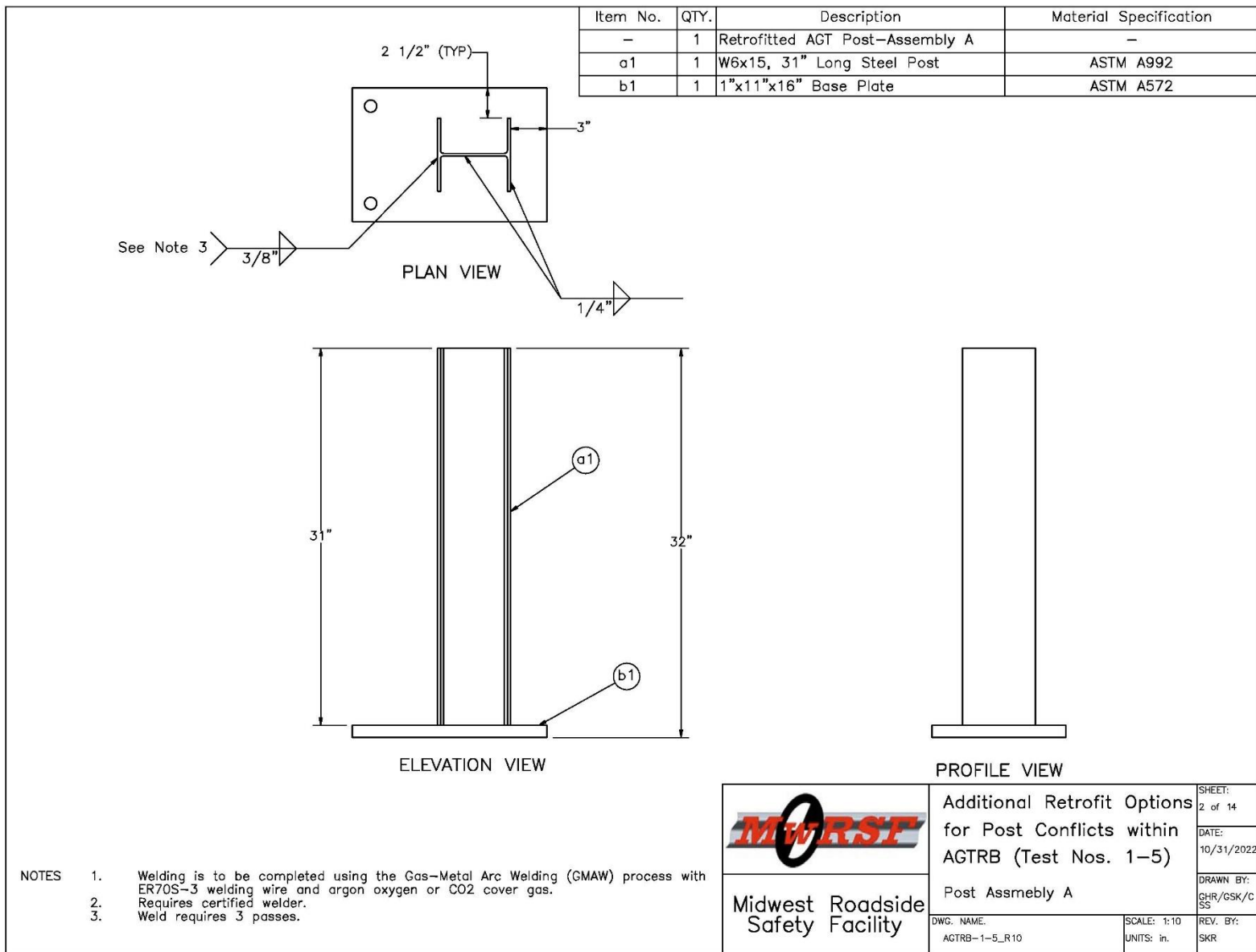


Figure 11. Test Article Details, Round 1 – Assembly A

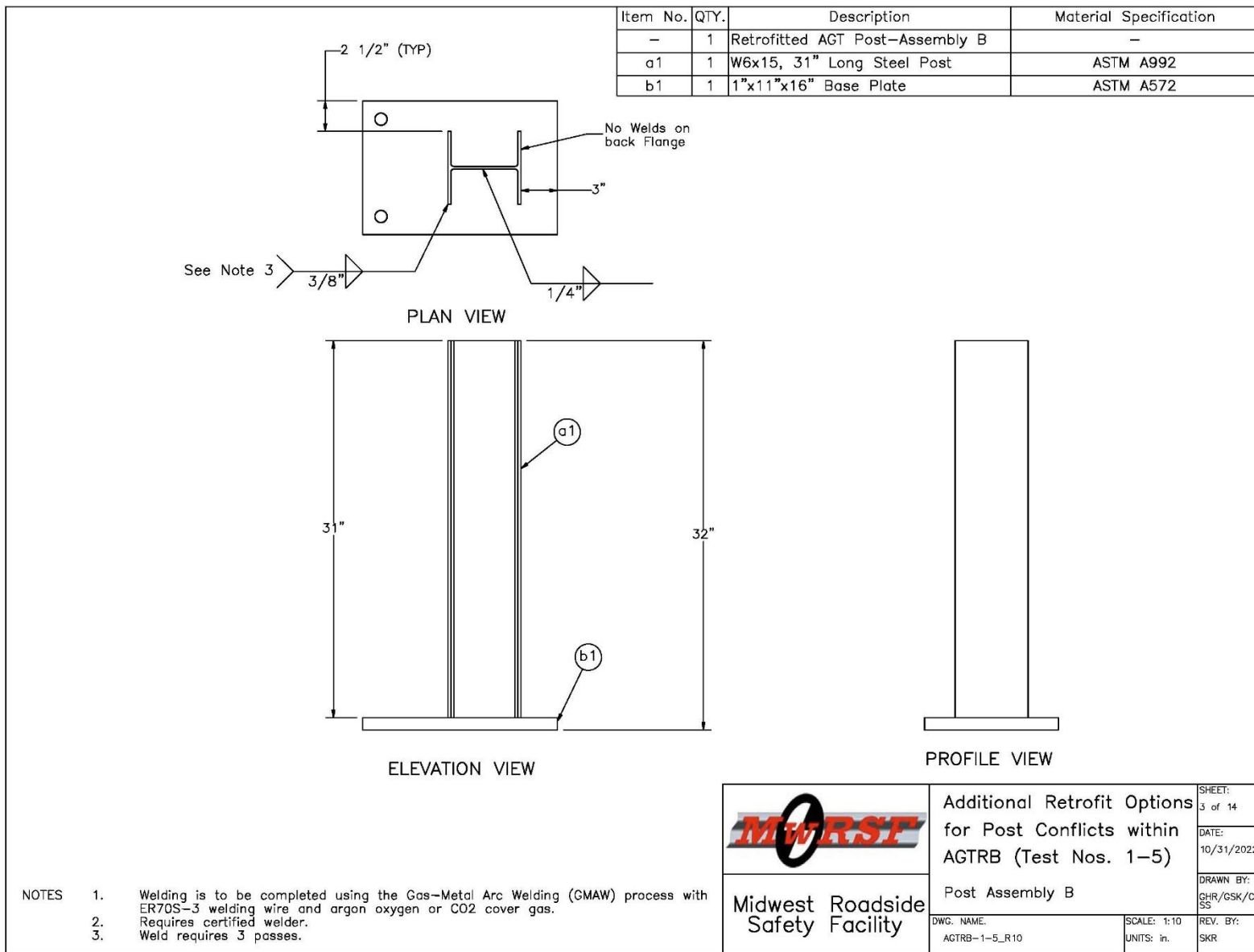


Figure 12. Test Article Details, Round 1 – Assembly B

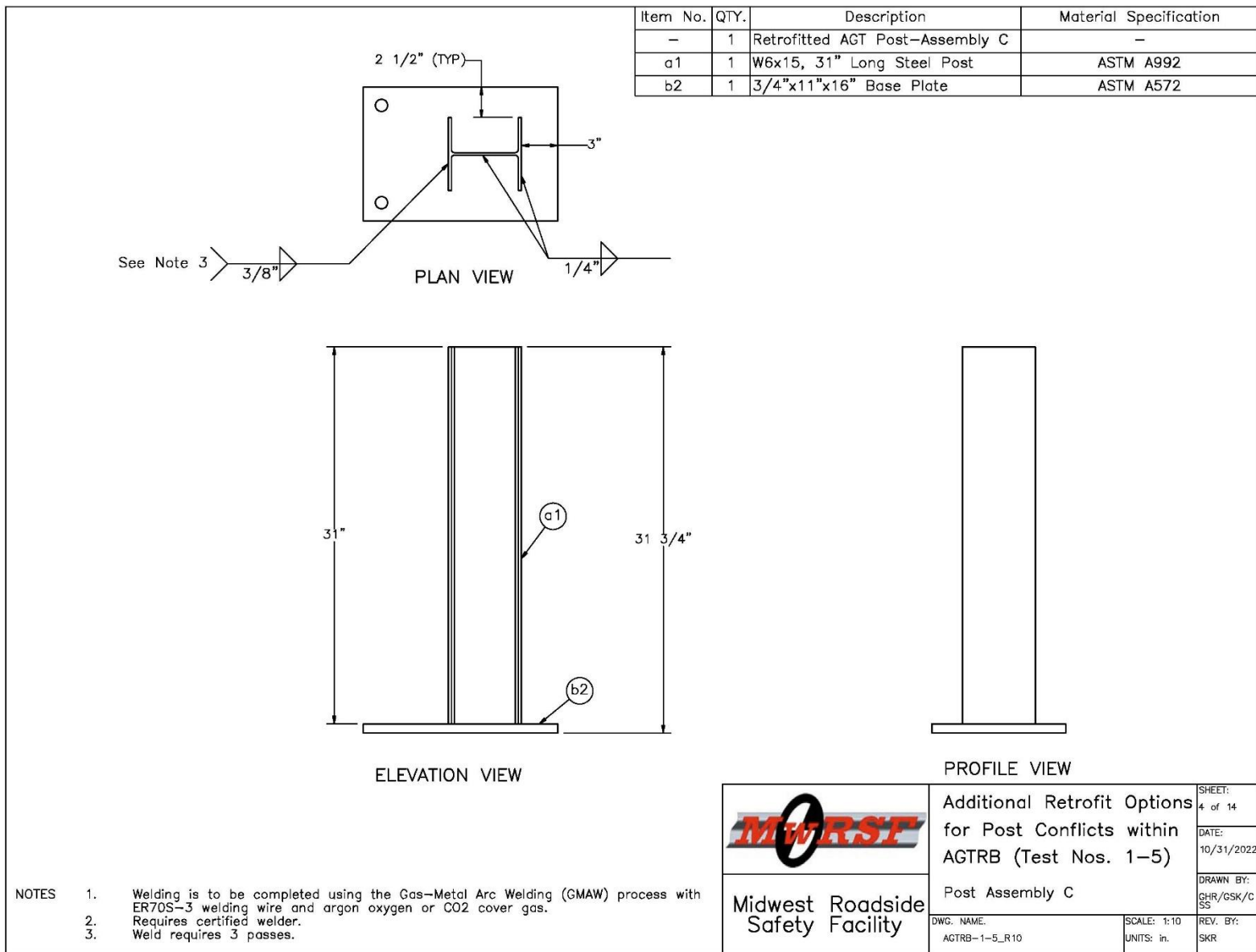


Figure 13. Test Article Details, Round 1 – Assembly C

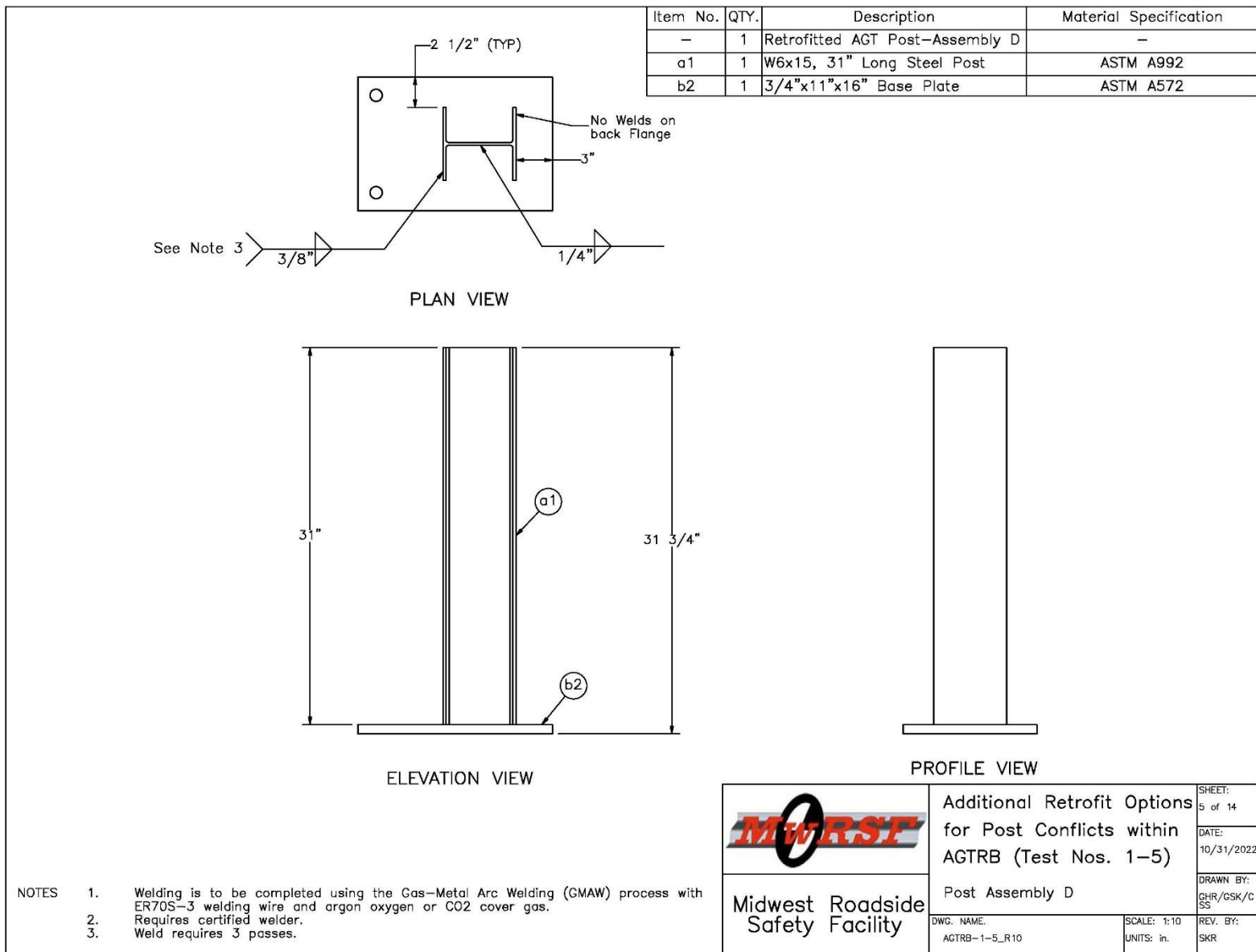


Figure 14. Test Article Details, Round 1 – Assembly D

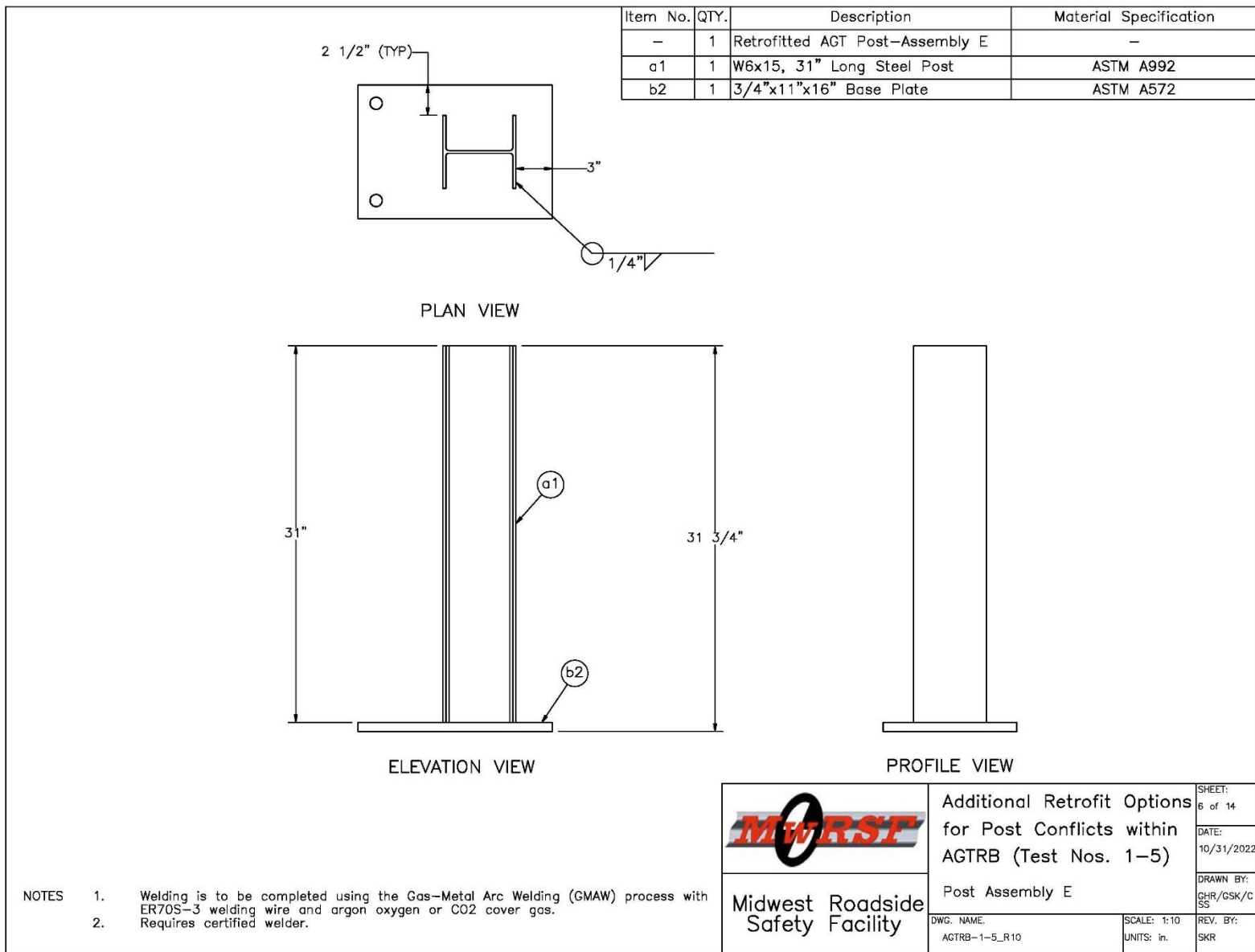


Figure 15. Test Article Details, Round 1 – Assembly E

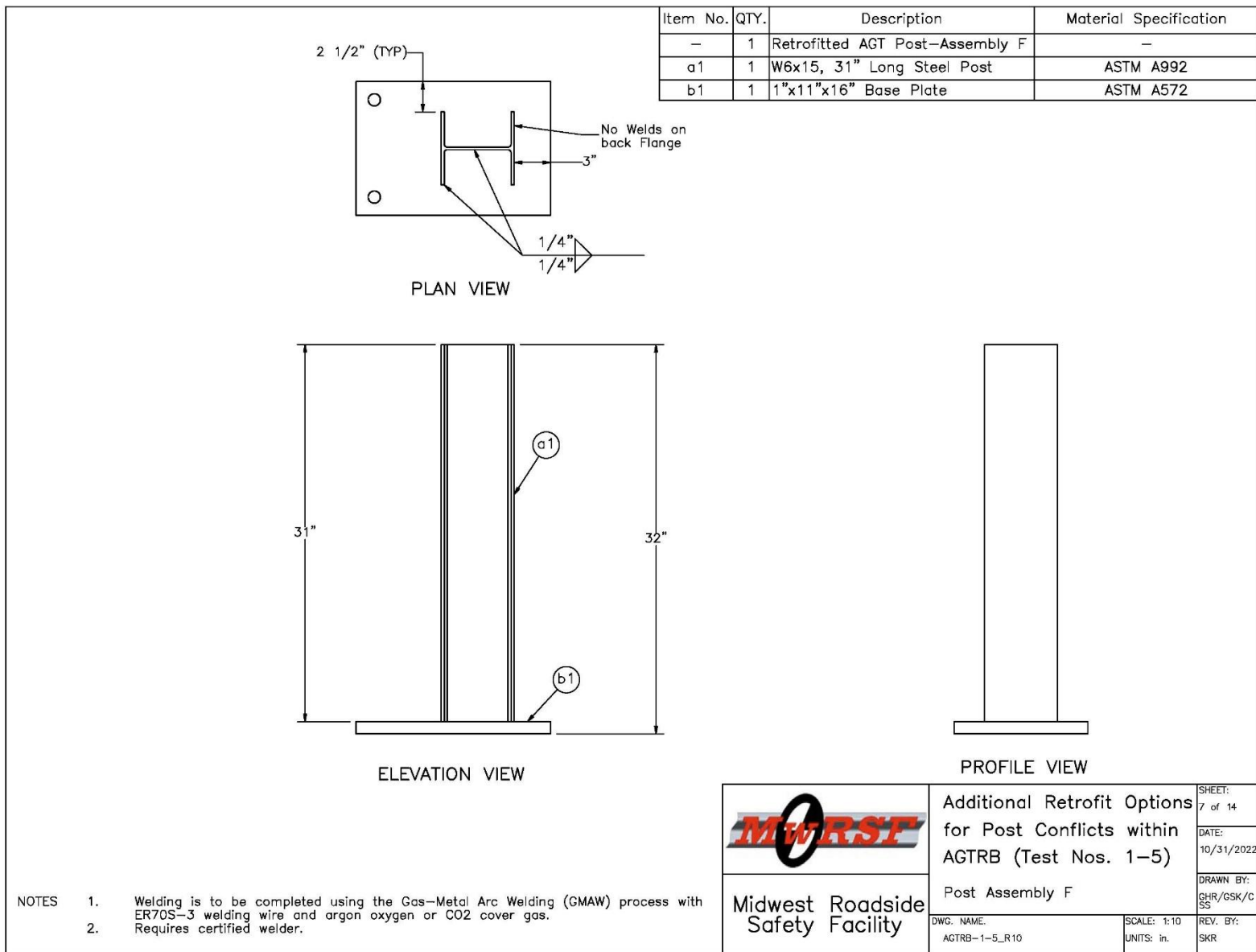


Figure 16. Test Article Details, Round 1 – Assembly F

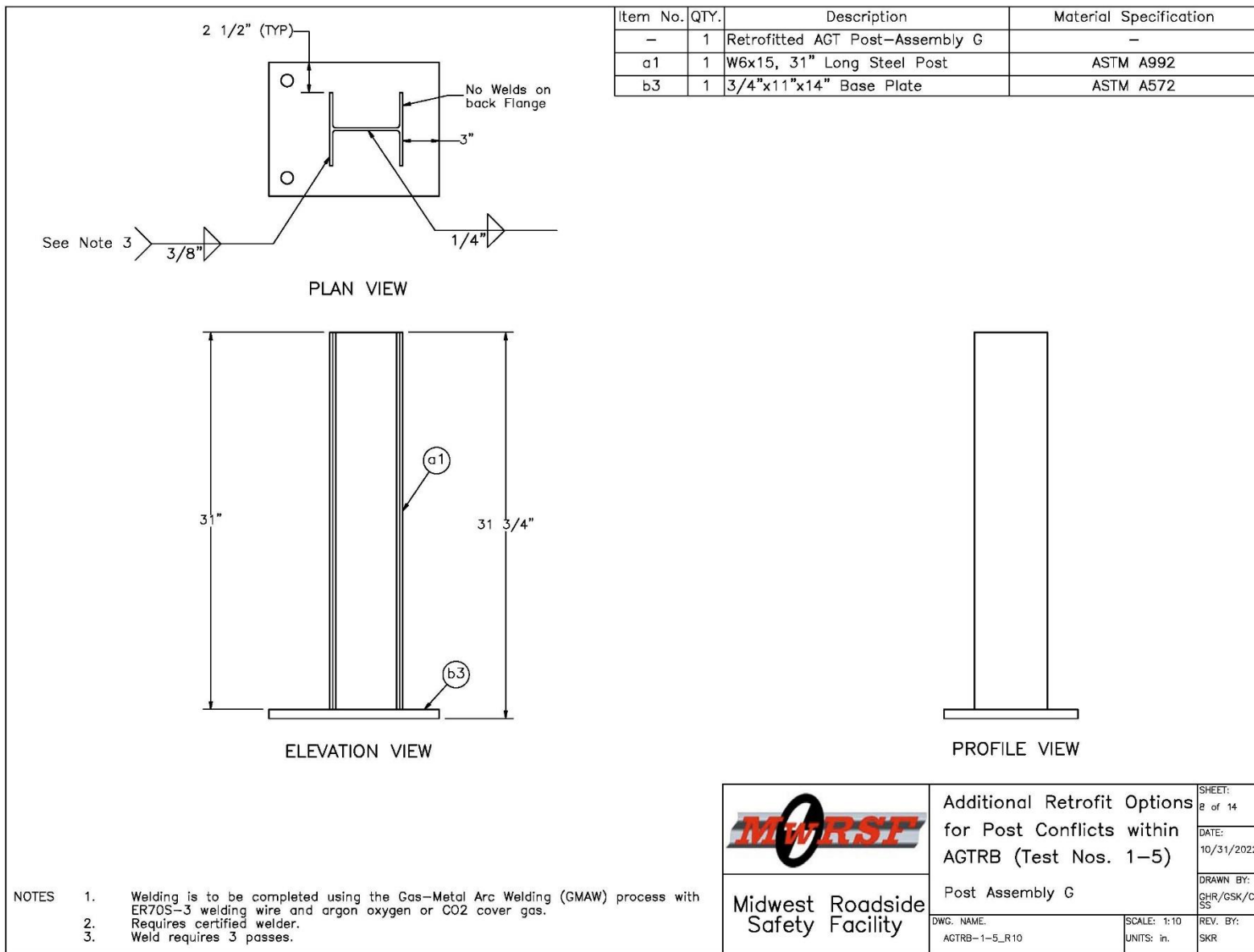


Figure 17. Test Article Details, Round 1 – Assembly G

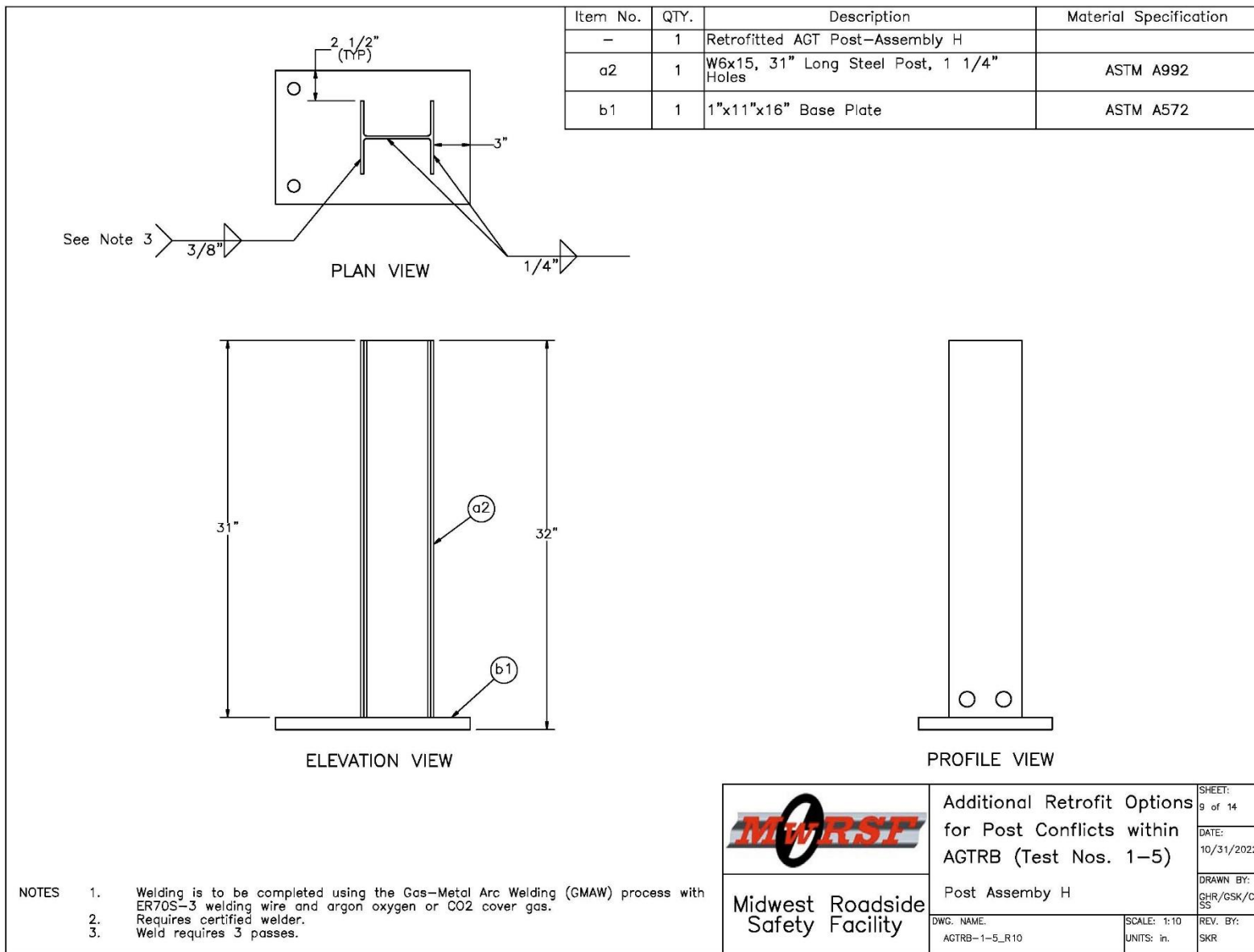


Figure 18. Test Article Details, Round 1 – Assembly H

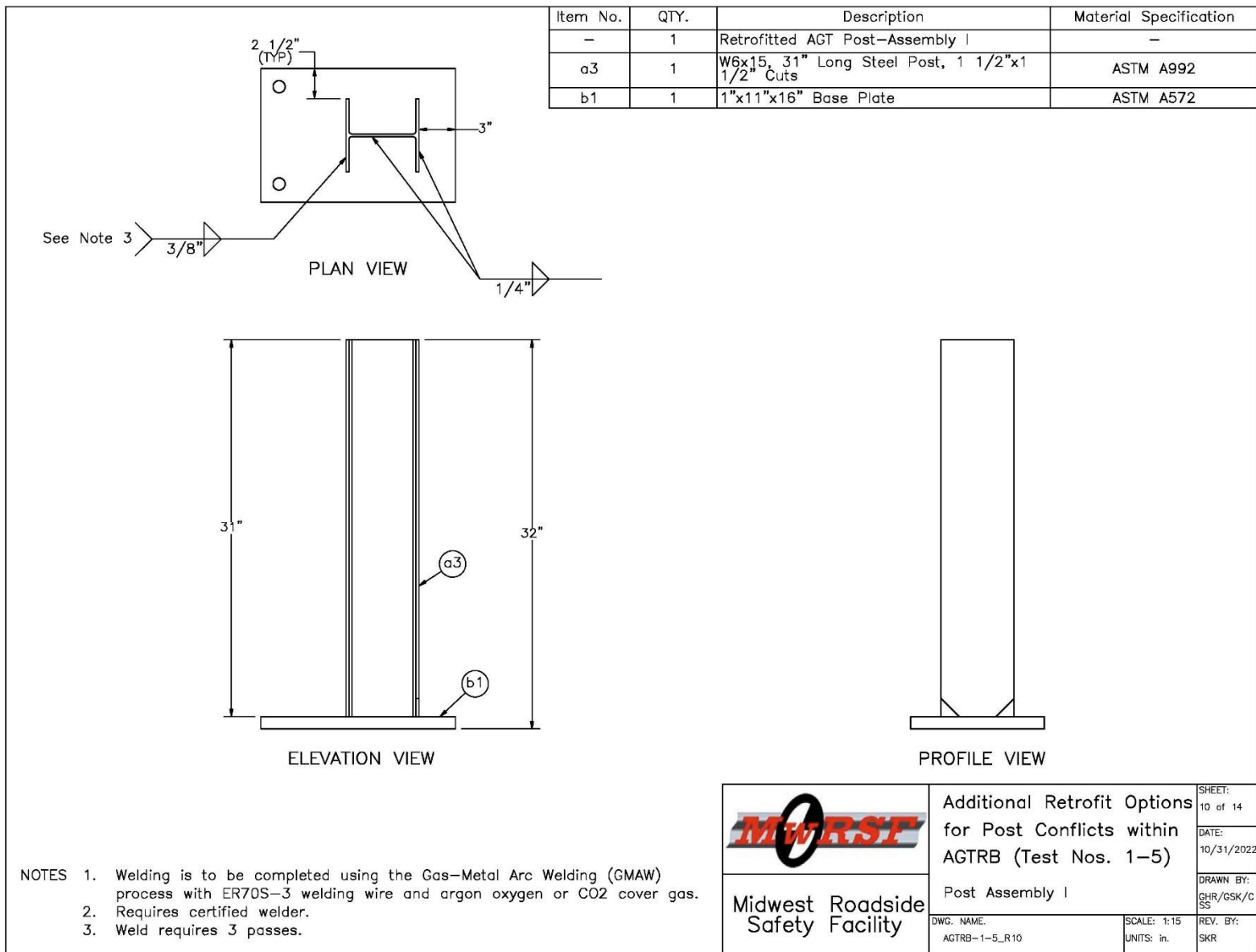


Figure 19. Test Article Details, Round 1 – Assembly I

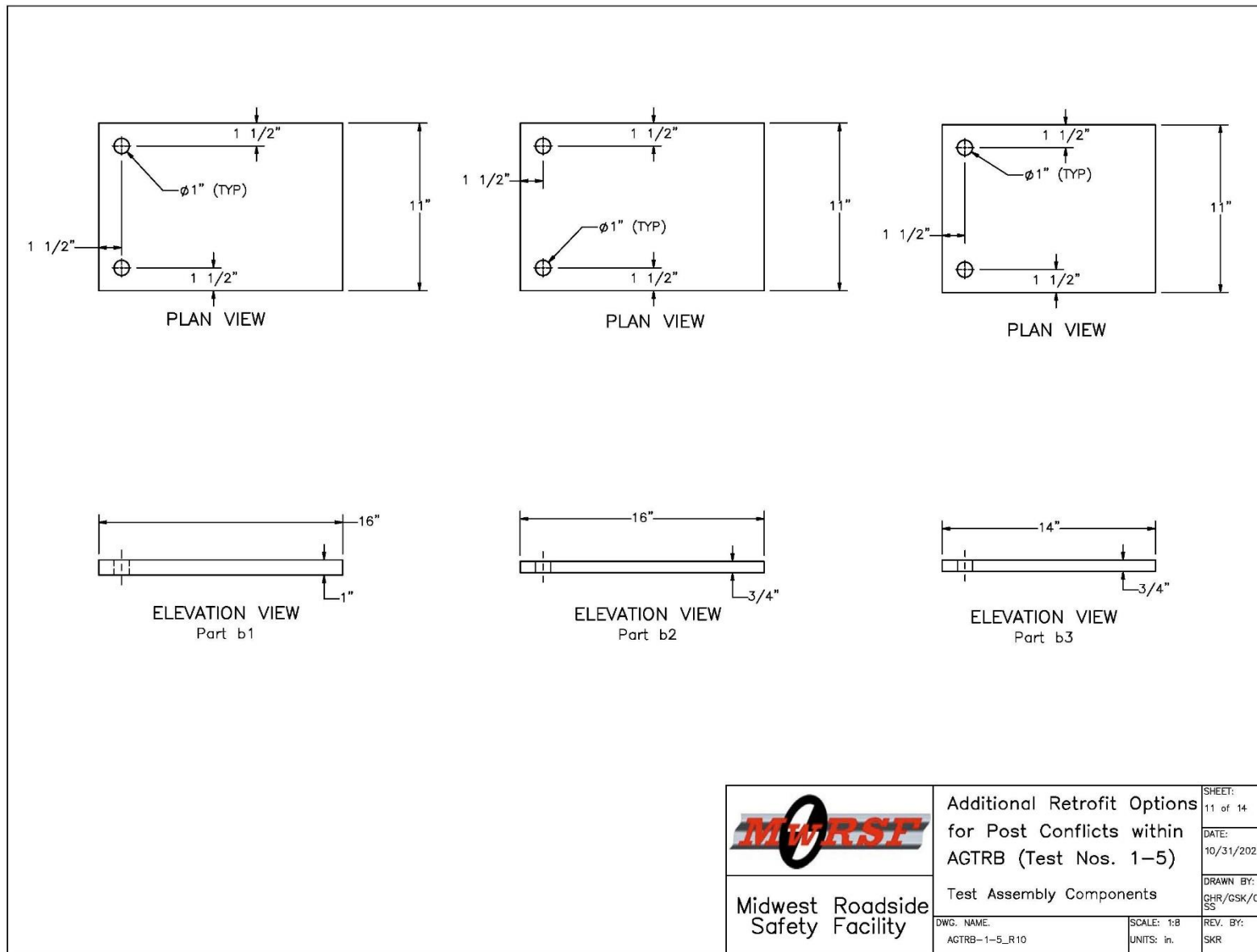


Figure 20. Test Article Details, Round 1 – Base Plates

 <b>Midwest Roadside Safety Facility</b>	Additional Retrofit Options for Post Conflicts within AGTRB (Test Nos. 1–5)		DRAWN BY: GHR/GSK/CSS
	Test Assembly Components		
DWG. NAME: AGTRB-1-5_R10	SCALE: 1:8 UNITS: in.	REV. BY: SKR	

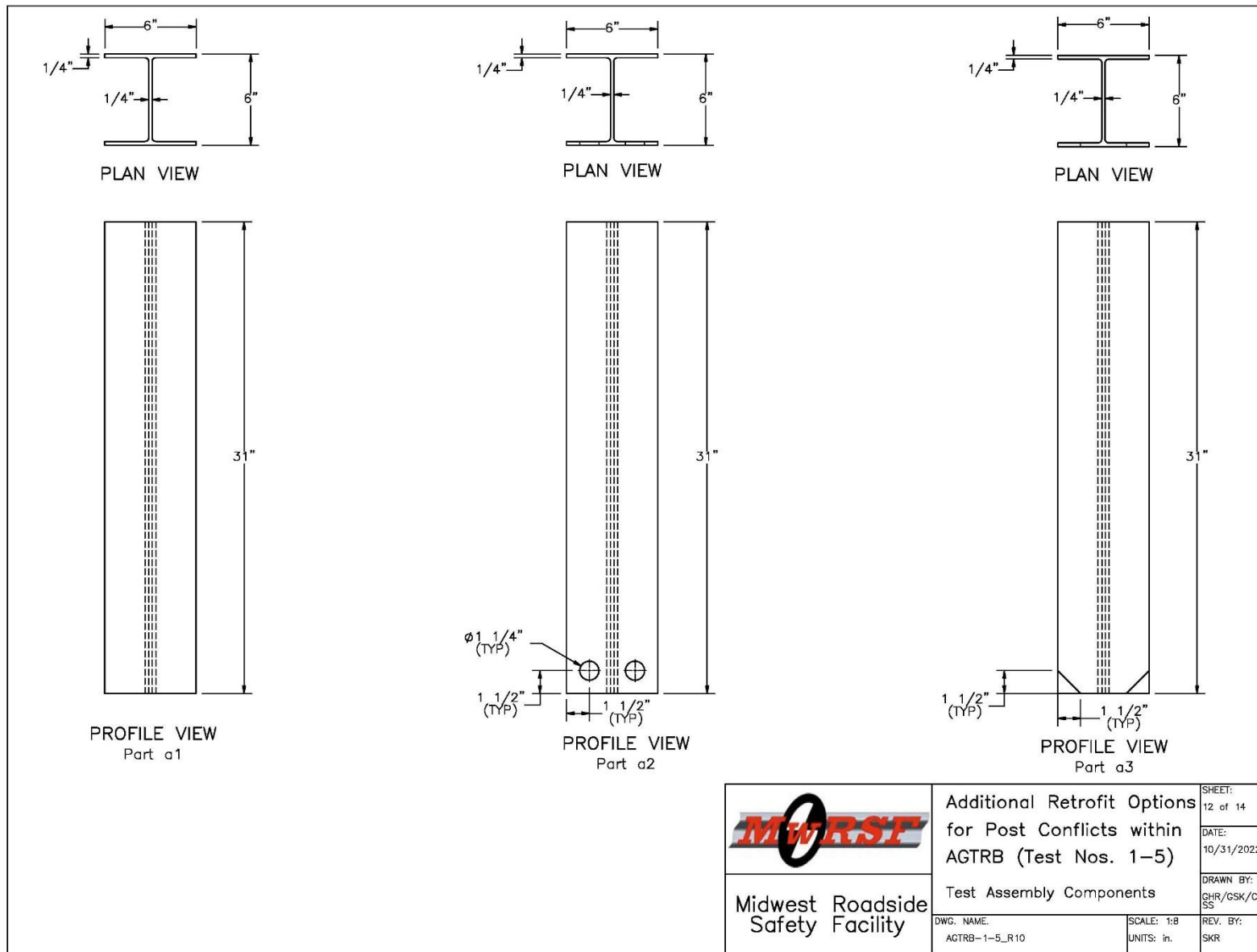


Figure 21. Test Article Details, Round 1 – Post Segments

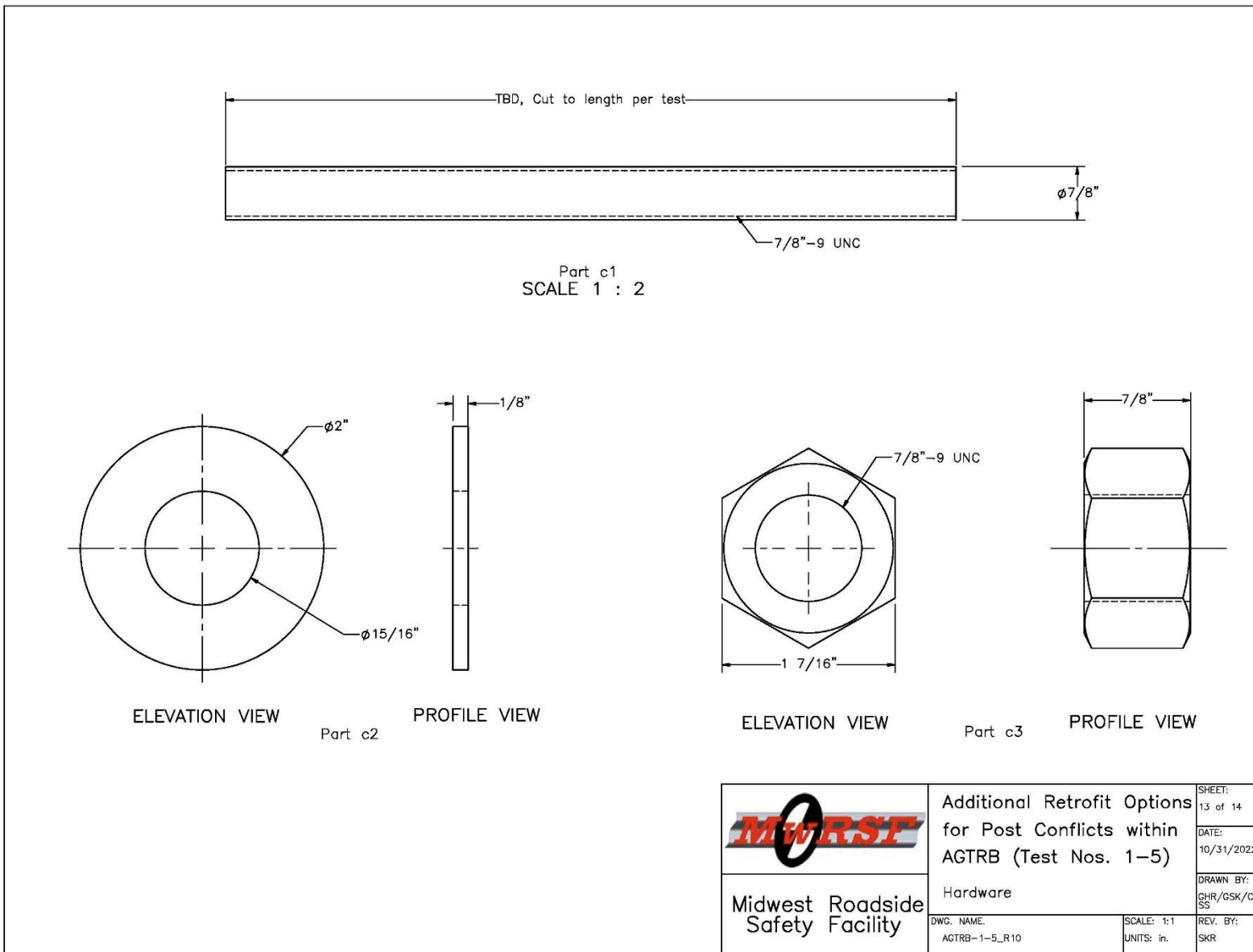


Figure 22. Test Article Details, Round 1 – Anchorage Hardware

Item No.	QTY.	Description	Material Specification
a1	7	W6x15, 31" Long Steel Post	ASTM A992
a2	1	W6x15, 31" Long Steel Post, 1 1/4" Holes	ASTM A992
a3	1	W6x15, 31" Long Steel Post, 1 1/2"x1 1/2" Cuts	ASTM A992
b1	5	1"x11"x16" Base Plate	ASTM A572
b2	3	3/4"x11"x16" Base Plate	ASTM A572
b3	1	3/4"x11"x14" Base Plate	ASTM A572
c1 (1)	*	7/8-9 UNC, Threaded Rod, Length TBD	ASTM A193 Grade B7
c2	12	7/8" Dia., Plain Round Washer	ASTM F844
c3	12	7/8"-9 UNC Heavy Hex Nut	ASTM A194 Grade 2H or Equivalent
c4	—	Chemical Epoxy	Hilti HIT RE-500 V3

Note: (1) 12 ft of threaded rod is needed to allow for enough for test series. Individual rod lengths to be cut as needed for each test, equal to the embedment depth plus 2 in.

 <b>Midwest Roadside Safety Facility</b>	<b>Additional Retrofit Options for Post Conflicts within AGTRB (Test Nos. 1-5)</b>		
	SHEET: 14 of 14 DATE: 10/31/2022 DRAWN BY: GHR/GSK/CSS DWG. NAME: AGTRB-1-5_R10 SCALE: None UNITS: in. REV. BY: SKR		
Bill of Materials			

Figure 23. Test Article Details, Round 1 – Bill of Materials

## 5.2 Results

Round 1 of physical testing included five dynamic component tests. Descriptions of each test, including sequential and post-test photographs, are contained in the following sections. Data from both accelerometers was processed for each test. Although the two accelerometers produced similar results, the values described herein were calculated from the SLICE-1 data in order to provide a common basis for comparing the test results. Test results from both accelerometers and for all tests are provided in Appendix B.

### 5.2.1 Test No. AGTRB-1

Test no. AGTRB-1 was conducted on a post assembly without any post weakening mechanisms, a thick base plate, and anchors epoxied into the concrete at a depth of 10 in. (4 in. further than design requirements). Test AGTRB-1 served as a baseline test to measure the force-displacement results for an unmodified post with a thick, near-rigid base plate.

During test no. AGTRB-1, the bogie impacted Post Assembly A at a speed of 18.3 mph causing the post to yield and bend backward. The bogie overrode the top of the post at a displacement of 15.0 in. Upon post-test examination, post bending was the result of compression flange buckling and plastic bending in the base plate. Neither weld nor anchor failure occurred. Time sequential photographs and post-impact photographs are shown in Figure 24.

Force-deflection and energy-deflection curves were created from the accelerometer data and are shown in Figure 25. A peak force of 32.9 kips occurred at a displacement of 3.2 in., and the post assembly provided an average force of 25.2 kips through 10 in. of displacement. As anticipated, the measured resistance force was significantly higher than the desired 17 kips over 10 in. of displacement.

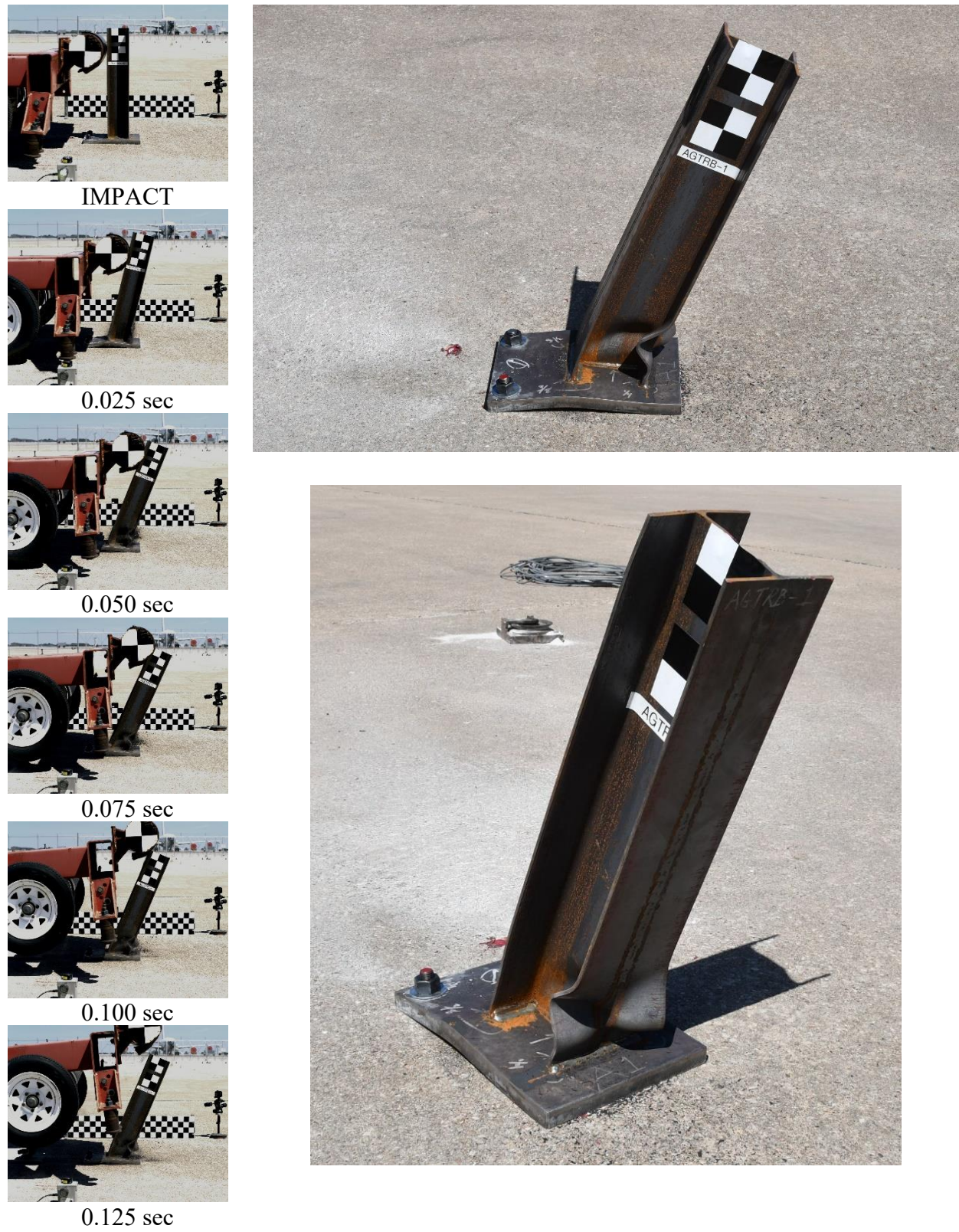


Figure 24. Time-Sequential and Post-Impact Photographs, Test No. AGTRB-1

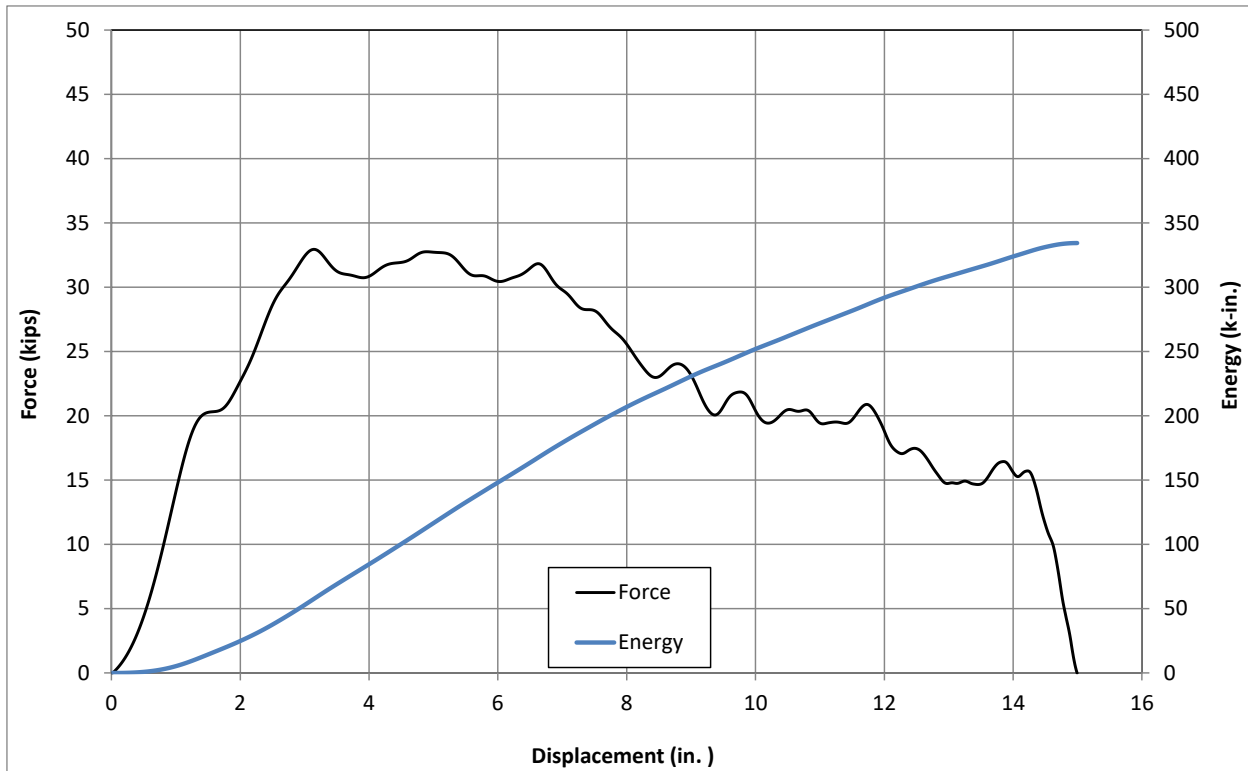


Figure 25. Force vs. Deflection and Energy vs. Deflection, Test No. AGTRB-1

### 5.2.2 Test No. AGTRB-2

Test no. AGTRB-2 was conducted on Post Assembly B, which had a 1-in. thick base plate and no welding of the post's compression flange. During test no. AGTRB-2, the bogie impacted the post assembly at a speed of 17.2 mph causing the post to yield and bend backward. The bogie overrode the top of the post at a displacement of 17.6 in. Post bending was found to be the result of compression flange buckling and plastic bending of the base plate. There was no damage to the anchor rods or the supporting concrete slab. Time sequential photographs and post-impact photographs are shown in Figure 26.

Force-deflection and energy-deflection curves were created from the accelerometer data and are shown in Figure 27. A peak force of 31.4 kips occurred at a displacement of 3.6 in., and the post assembly provided an average force of 21.0 kips through 10 in. of displacement. Thus, Post Assembly B provided a 17 percent reduction in force, as compared to the baseline, Assembly A. However, 21.0 kips was still 19 percent higher than the targeted 17-kip resistance.



Figure 26. Time-Sequential and Post-Impact Photographs, Test No. AGTRB-2

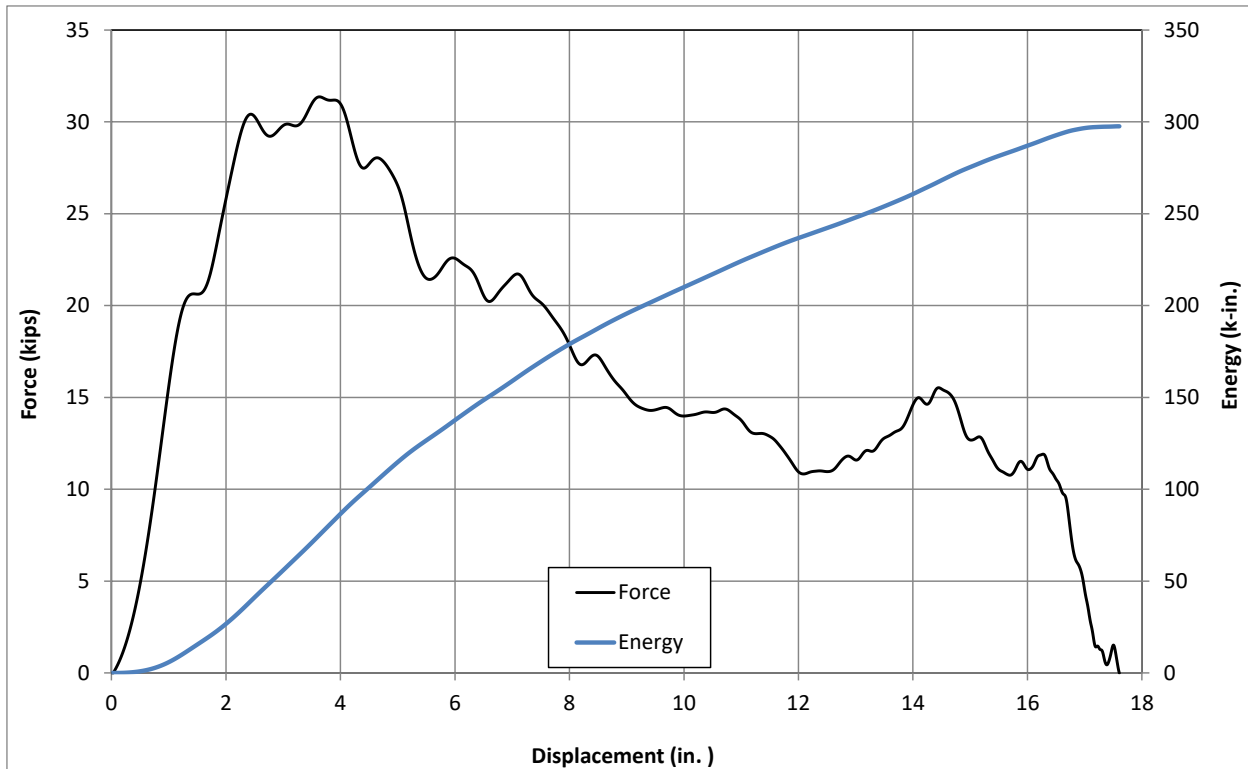


Figure 27. Force vs. Deflection and Energy vs. Deflection, Test No. AGTRB-2

### 5.2.3 Test No. AGTRB-3

Test no. AGTRB-3 was conducted on Post Assembly E, which utilized a thinner,  $\frac{3}{4}$ -in. thick base plate and single pass  $\frac{1}{4}$ -in. fillet weld all around the base of the post. During test no. AGTRB-3, the bogie impacted the post assembly at a speed of 18.2 mph causing the base plate to bend upward and allow the post to rotate backward. As the base plate deformed, it caused a combination of tensile and bending to the anchor rods. This prying action eventually resulted in both anchor rods fracturing around 9-10 in. of displacement and allowed the post assembly to displace freely. Minimal deformations were observed on the post, but the base plate was significantly bent. Both anchor rods fractured near ground line under the base plate. Time sequential photographs and post-impact photographs are shown in Figure 28.

Force-deflection and energy-deflection curves were created from the accelerometer data and are shown in Figure 29. A peak force of 31.6 kips occurred at a displacement of 8.1 in., and the post assembly provided an average force of 19.9 kips through 10 in. of displacement. Post Assembly E provided a lower resistance force than the two previous tests, but the fracture of the anchor bolts was detrimental to its performance.

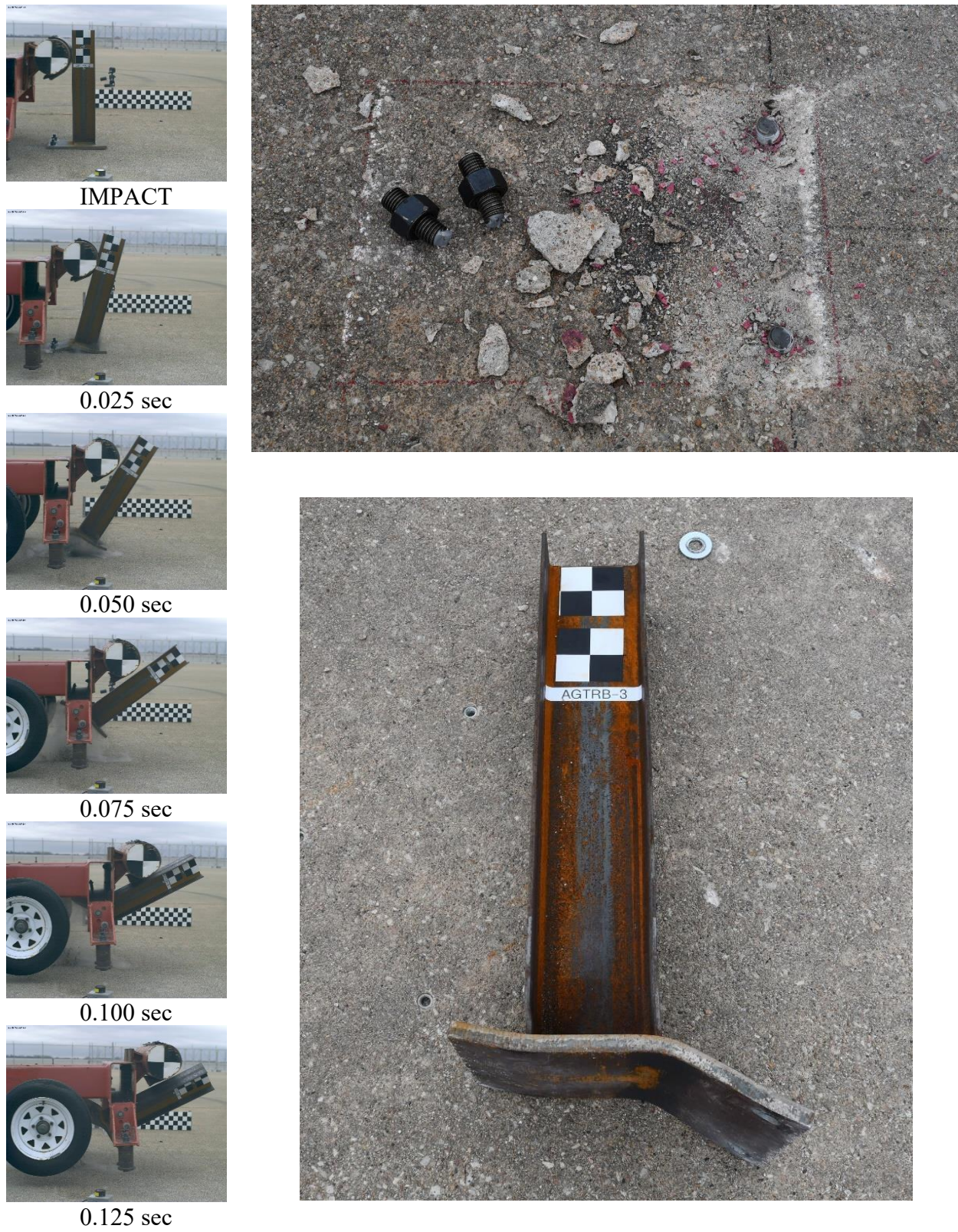


Figure 28. Time-Sequential and Post-Impact Photographs, Test No. AGTRB-3

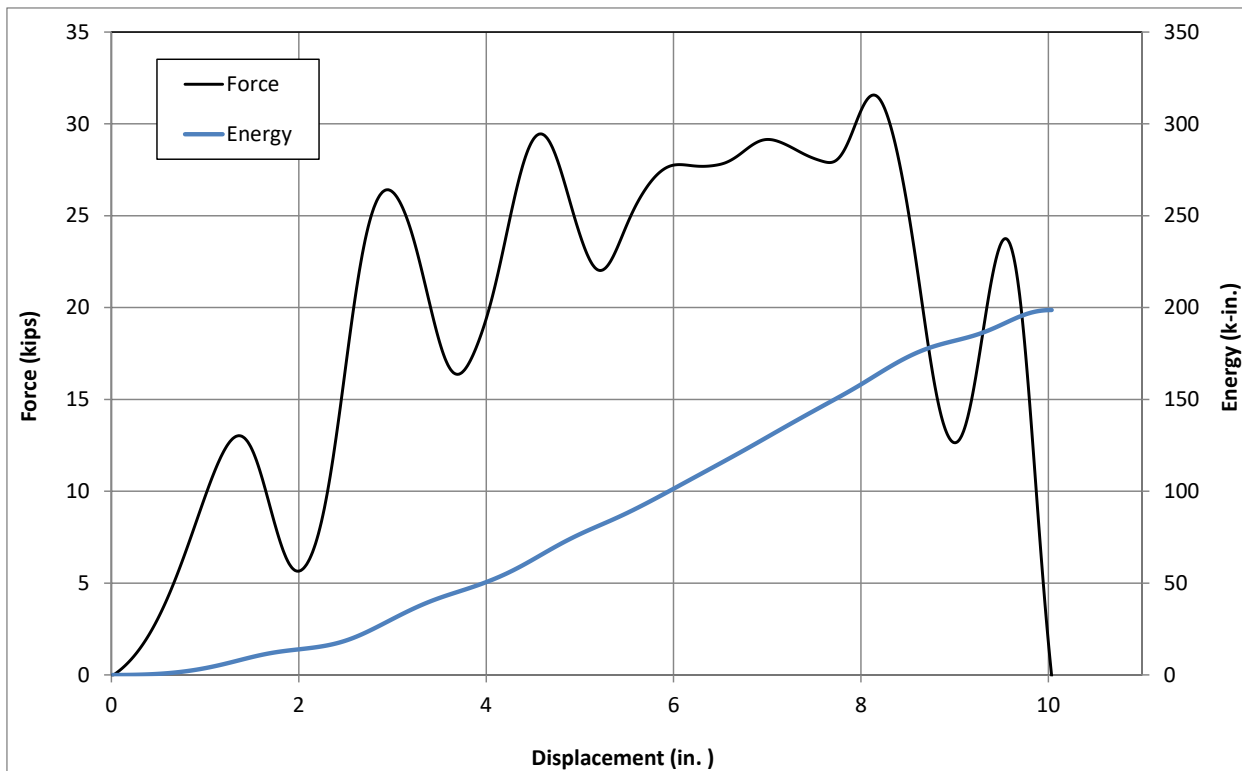


Figure 29. Force vs. Deflection and Energy vs. Deflection, Test No. AGTRB-3

#### 5.2.4 Test No. AGTRB-4

Test no. AGTRB-4 was conducted on Post Assembly H, which consisted of a 1-in. thick base plate and a post with two 1 $\frac{1}{4}$ -in. diameter holes in the compression flange. During test no. AGTRB-4, the bogie impacted the post assembly at a speed of 19.0 mph causing the post to yield and bend backward. The bogie eventually overrode the top of the post at a displacement of 18.3 in. Upon post-test examination, post bending was initiated by localized buckling in the compression flange adjacent to the weakening holes. Additionally, the base plate was bent slightly upward. There was no observed weld or anchor failure. Time sequential photographs and post-impact photographs are shown in Figure 30.

Force-deflection and energy-deflection curves were created from the accelerometer data and are shown in Figure 31. A peak force of 33.6 kips occurred at a displacement of 3.2 in., and the post assembly provided an average force of 23.3 kips through 10 in. of displacement. Although the post plastically deformed in a controlled and predictable manner, the resistance forces were significantly higher than the targeted 17 kips.



Figure 30. Time-Sequential and Post-Impact Photographs, Test No. AGTRB-4

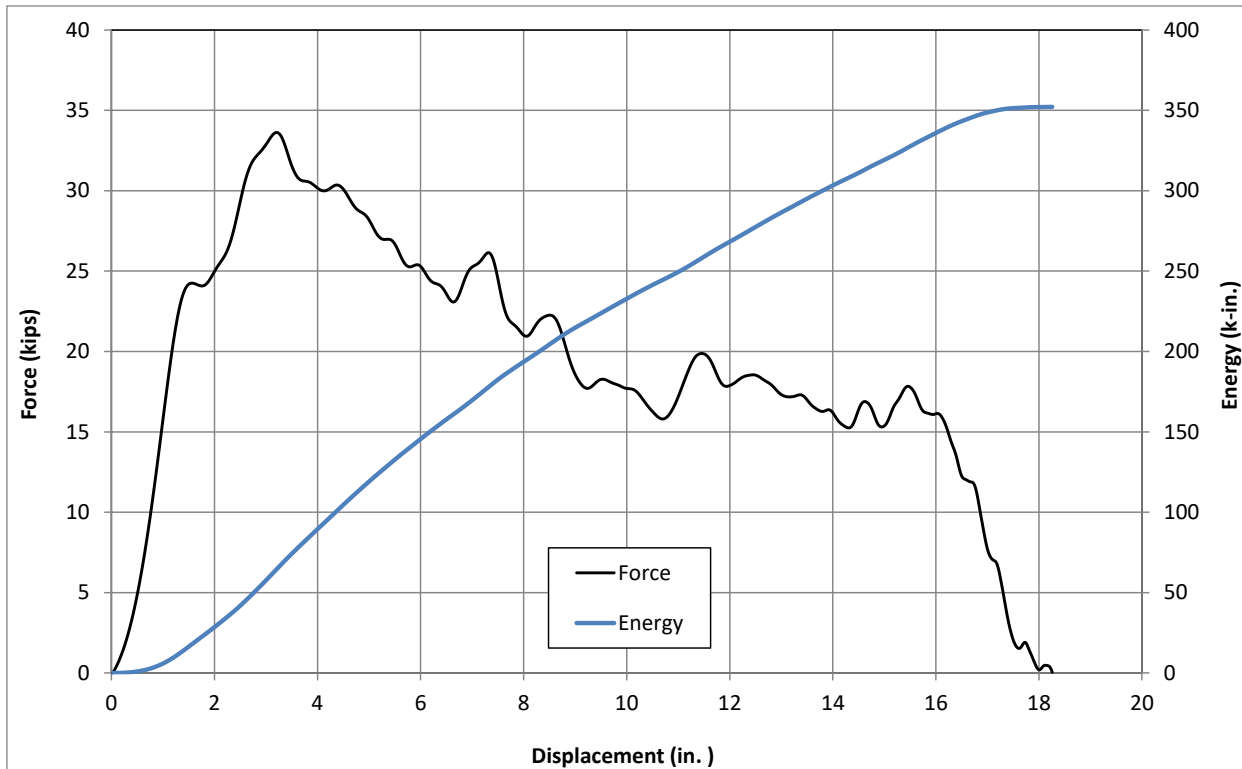


Figure 31. Force vs. Deflection and Energy vs. Deflection, Test No. AGTRB-4

### 5.2.5 Test No. AGTRB-5

Test no. AGTRB-5 was conducted on Post Assembly I, which consisted of a 1-in. thick base plate and a post with 1½-in. x 1½-in. chamfers cut from the bottom edges of the compression flange. During test no. AGTRB-5, the bogie impacted the post assembly at a speed of 18.2 mph causing the post to yield and bend backward. The bogie eventually overrode the top of the post at a displacement of 14.8 in. Post bending was the result of compression flange buckling and slight bending of the base plate. There was no observed failure to the welds or anchors. Time sequential photographs and post-impact photographs are shown in Figure 32.

Force-deflection and energy-deflection curves were created from the accelerometer data and are shown in Figure 33. A peak force of 36.1 kips occurred at a displacement of 5.1 in., and the post assembly provided an average force of 26.7 kips through 10 in. of displacement. Although Post Assembly I bent backward without failure to the anchor rods, the chamfers did not initiate flange buckling as intended. Thus, the resistance forces were well above the targeted 17 kips, and the flange buckling in Post Assembly I was not as pronounced as that observed for Post Assembly H with the holes in the flange.



Figure 32. Time-Sequential and Post-Impact Photographs, Test No. AGTRB-5

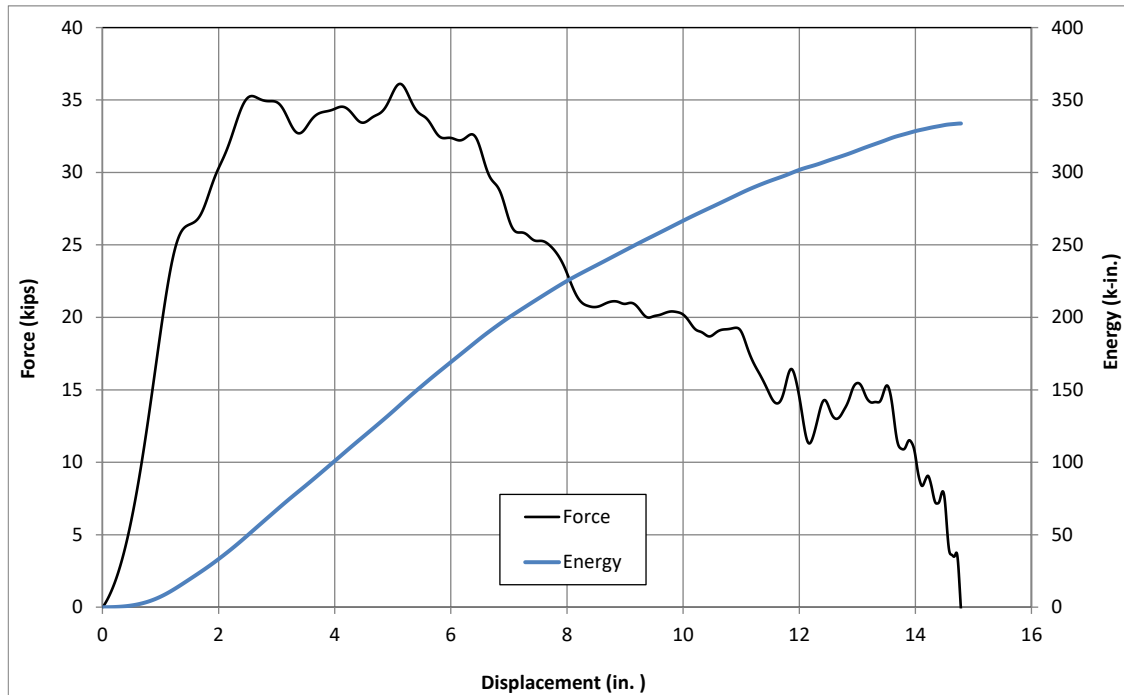


Figure 33. Force vs. Deflection and Energy vs. Deflection, Test No. AGTRB-5

### 5.3 Discussion

Round 1 of component testing began with a test of a “baseline” post assembly that had no post weakening mechanisms. Predictably, the retrofit post assembly provided a much higher force than the desired 17 kips over 10 in. of displacement. Unfortunately, the other four tests, which all contained weakening mechanisms, only slightly reduced the resistance forces. All of the tests resulted in forces significantly higher than the desired 17 kips. The only post assembly to result in an average force below 20 kips was Post Assembly E with a thinner base plate. However, the test on Post Assembly E resulted in fracture of the anchor rods. Thus, none of the retrofit AGT posts evaluated in Round 1 of dynamic component testing satisfied the design objectives. A summary of Round 1 testing results is provided in Table 5, while force vs. displacement and energy vs. displacement curves for the tests are shown in Figure 34 and 35, respectively. Note, test nos. MGSATB-5 and 6, which are shown in Figures 34 and 35, were the bogie tests conducted on W6x15 posts in soil that provided the target resistance force of 17 kips over 10 in. of displacement.

Table 5. Results Summary, Component Testing - Round 1

Test No.	Post Assembly and Weakening Mechanism	$F_{ave}$ @ 10 in. (kips)	Failure Description
AGTRB-1	A – baseline	25.2	Post Bending, Flange Buckling
AGTRB-2	B – no flange weld	21.0	Post Bending, Flange Buckling
AGTRB-3	E – Thin (3/4") base plate	19.9	Base Plate Bending, Anchor Fracture
AGTRB-4	H – Ø1 1/4" holes	23.9	Post Bending, Flange Buckling
AGTRB-5	I – 1 1/2" chamfers	26.7	Post Bending, Flange Buckling

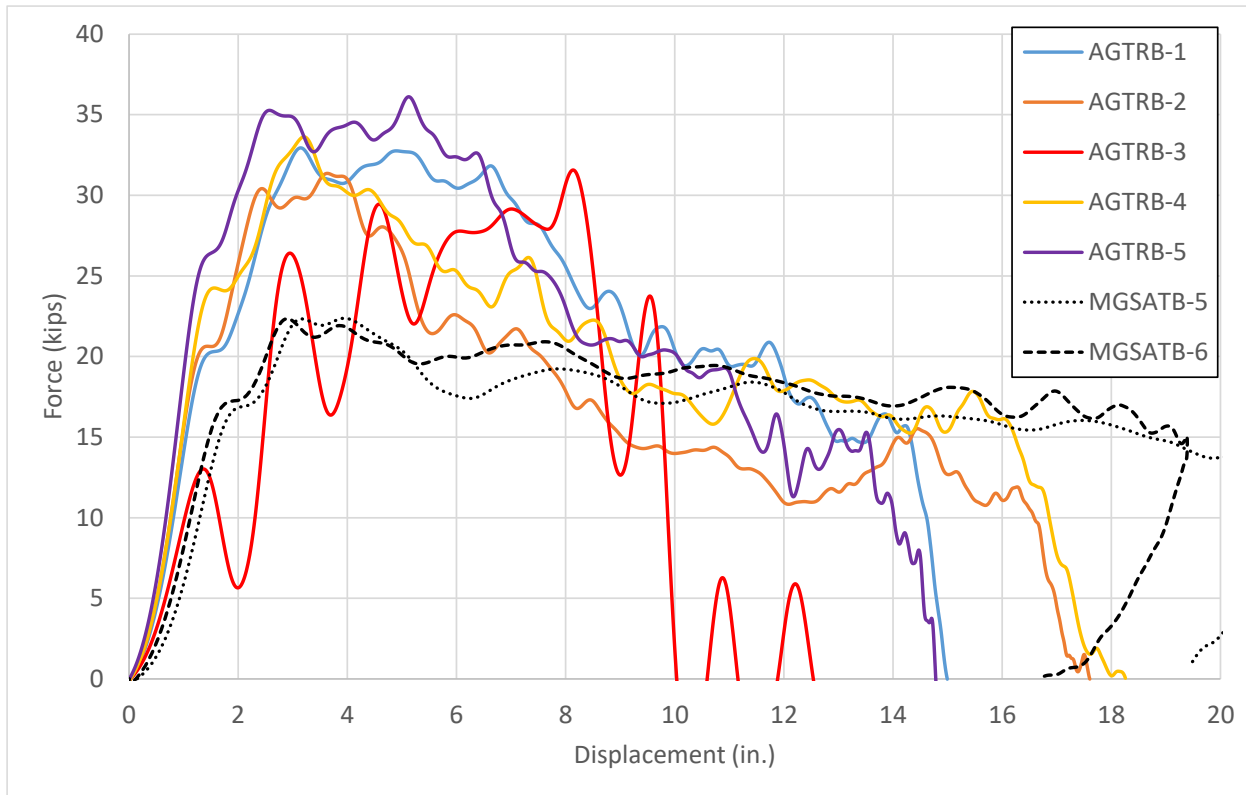


Figure 34. Force vs. Deflection Comparison, Component Testing - Round 1

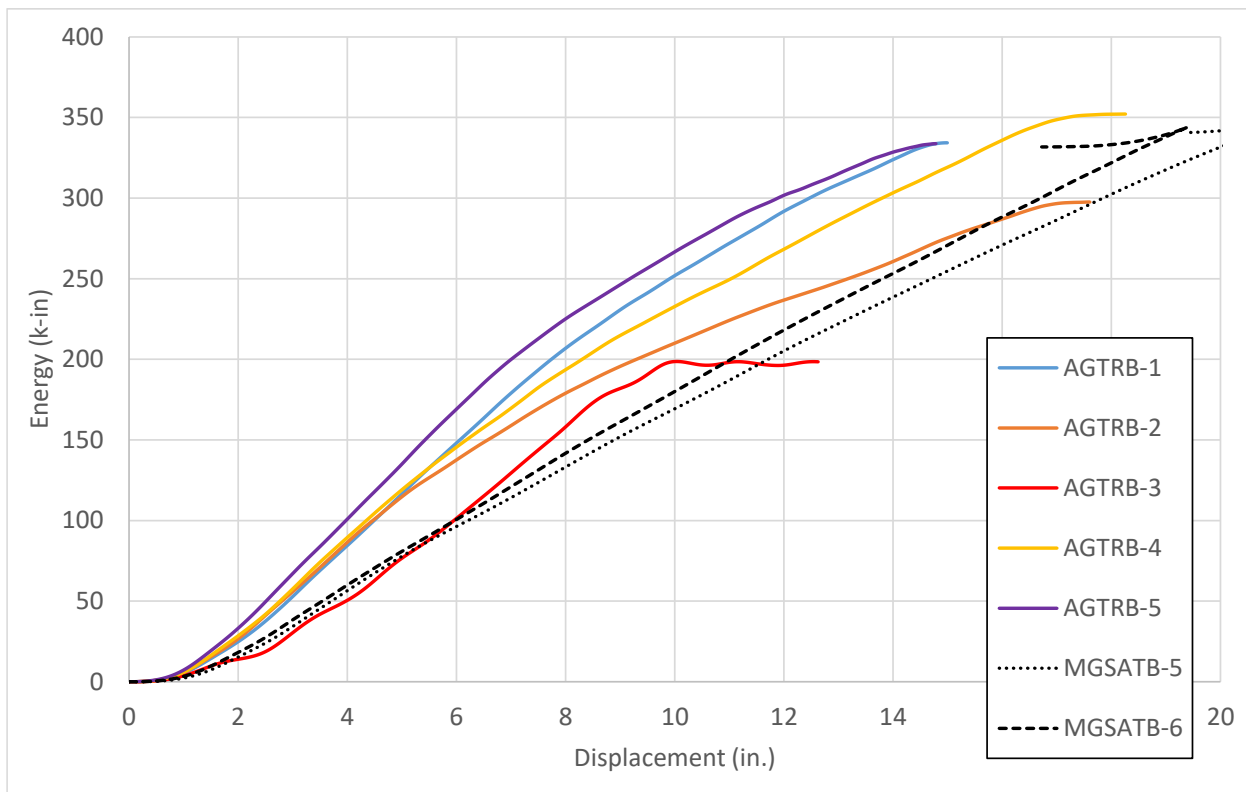


Figure 35. Energy vs. Deflection Comparison, Component Testing - Round 1

## 6 DYNAMIC COMPONENT TESTING – ROUND 2

### 6.1 Scope

After reviewing the results from Round 1 of dynamic component testing, additional configurations for the surface mounted, retrofit post were developed to further weaken the post and prevent anchorage failure. These additional configurations included increasing the diameter of the anchor bolts, slotting the base plate to allow more movement, slotting the holes in the compression flange to initiate buckling earlier, and placing holes in both the compression and tension flanges of the post.

For Round 2 of component testing, five different configurations of the surface-mounted, retrofit AGT post were fabricated. However, the selection of which post assembly to evaluate was done iteratively for each test based on the results from the previous tests. Thus, only two tests were conducted during Round 2. The remaining three post assemblies were discarded. A summary of the five post assemblies is provided in Table 6 and CAD details are shown in Figures 36 through 45. Figure 36 also contains the test matrix showing which post assembly was evaluated during each test.

Each post assembly consisted of a 31-in. long W6x15 post welded to a base plate of varying thicknesses. It should be noted that in Round 1 of component testing, the weld pattern on the front flange was varied to investigate the required size/strength of the weld to prevent rupture during dynamic loading. Test no. AGTRB-3 with Post Assembly E showed that a single-pass,  $\frac{1}{4}$ -in. fillet weld provided enough strength to develop the full strength of the post. Thus, for Round 2 of testing,  $\frac{1}{4}$ -in. fillet welds were used exclusively to connect the post to the base plate.

Table 6. Summary of Post Assemblies – Round 2

Assembly	Base Plate Thickness	Base Plate Holes/Slots	Anchor Rod Diameter	Compression Flange Weakening	Tension Flange Weakening
J	$\frac{3}{4}$ "	Holes	$\varnothing 1$ "	-	-
K	$\frac{3}{4}$ "	Slots	$\varnothing 1$ "	-	-
L	$\frac{3}{4}$ "	Holes	$\varnothing 1\frac{1}{8}$ "	-	-
M	1"	Holes	$\varnothing \frac{7}{8}$ "	$\varnothing 1\frac{1}{4}$ " x 3" slots	-
N	1"	Holes	$\varnothing \frac{7}{8}$ "	$\varnothing 1\frac{1}{4}$ " holes	$\varnothing 1\frac{1}{4}$ " holes

- = not applicable

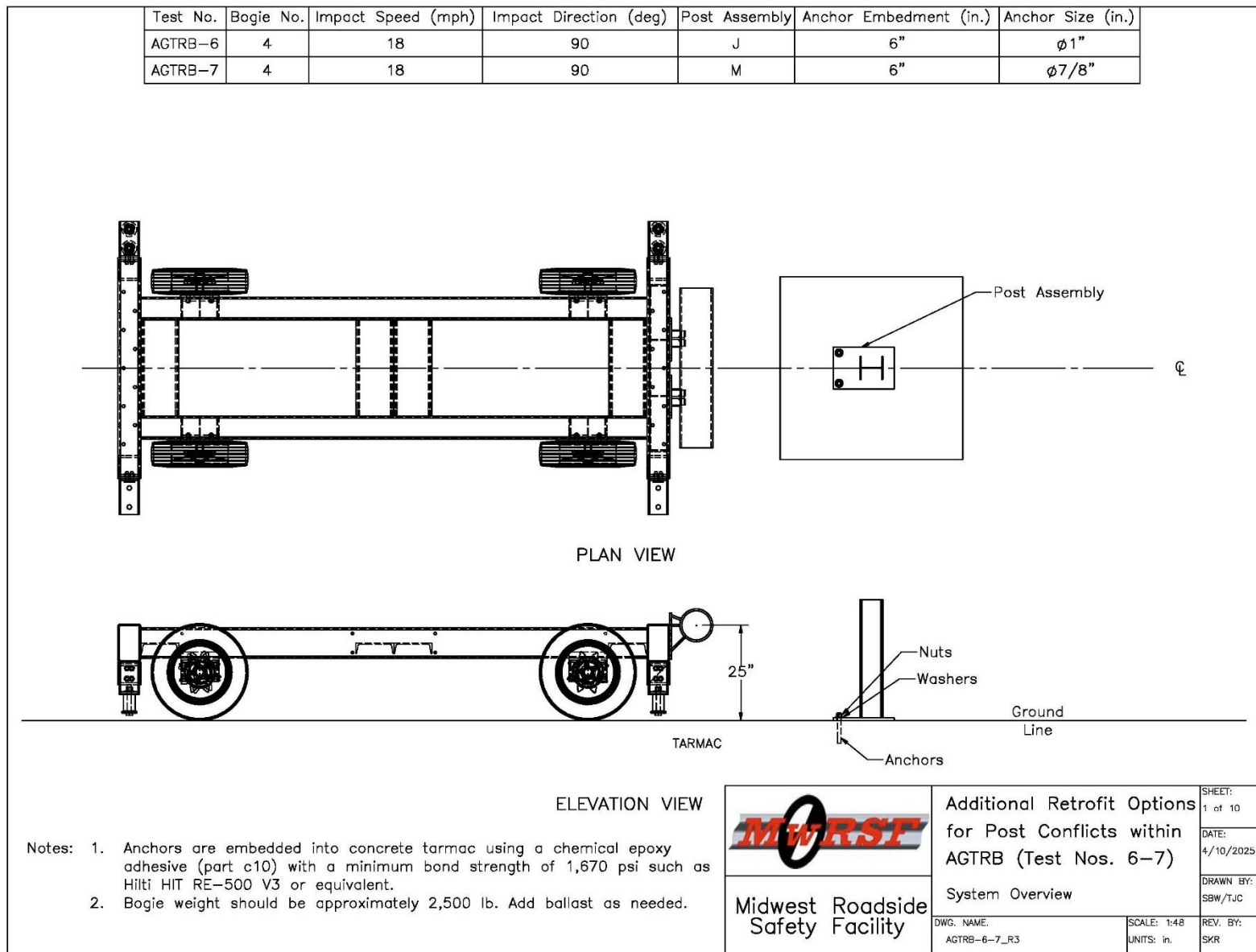


Figure 36. Dynamic Component Testing Matrix and Setup – Round 2

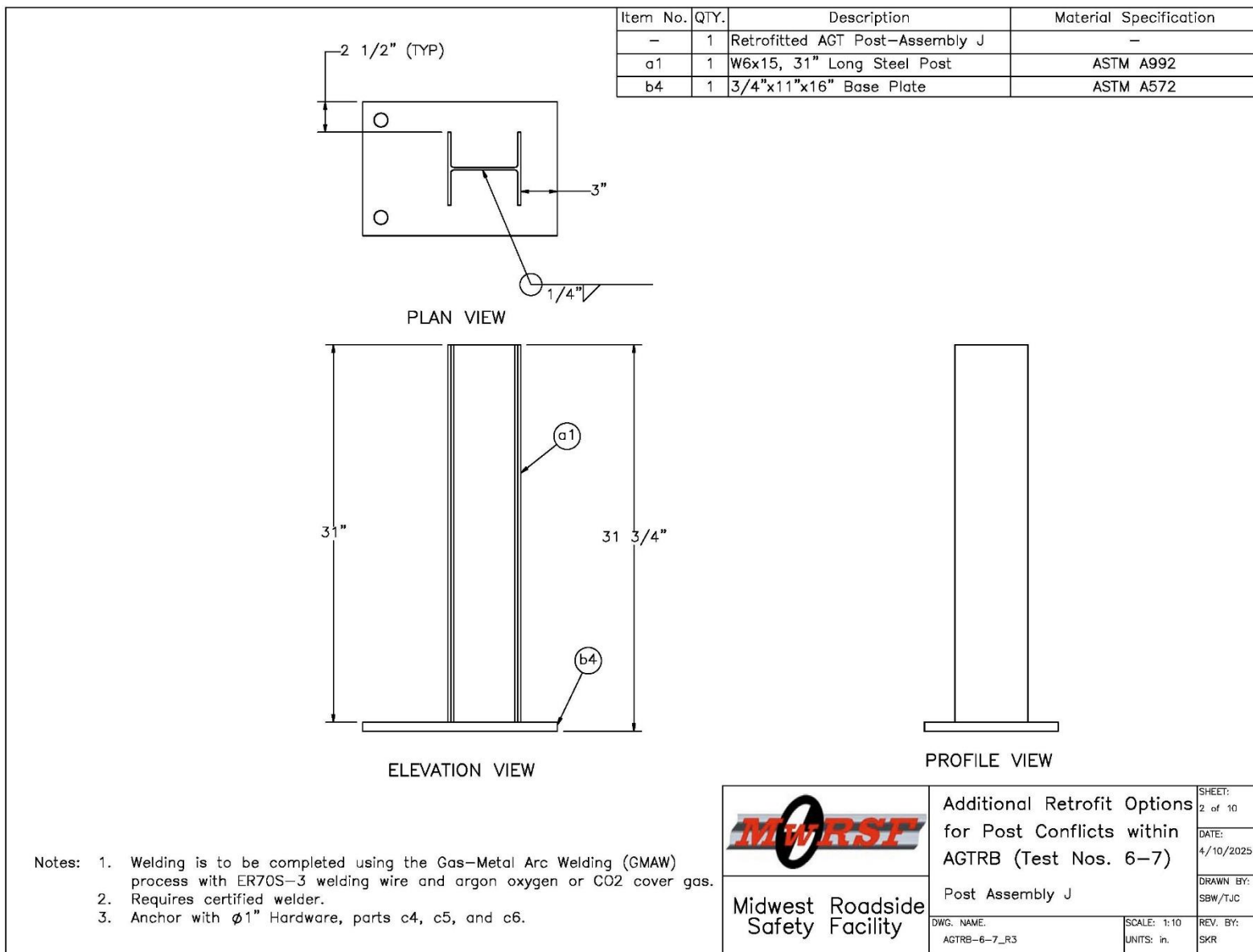


Figure 37. Test Article Details, Round 2 – Assembly J

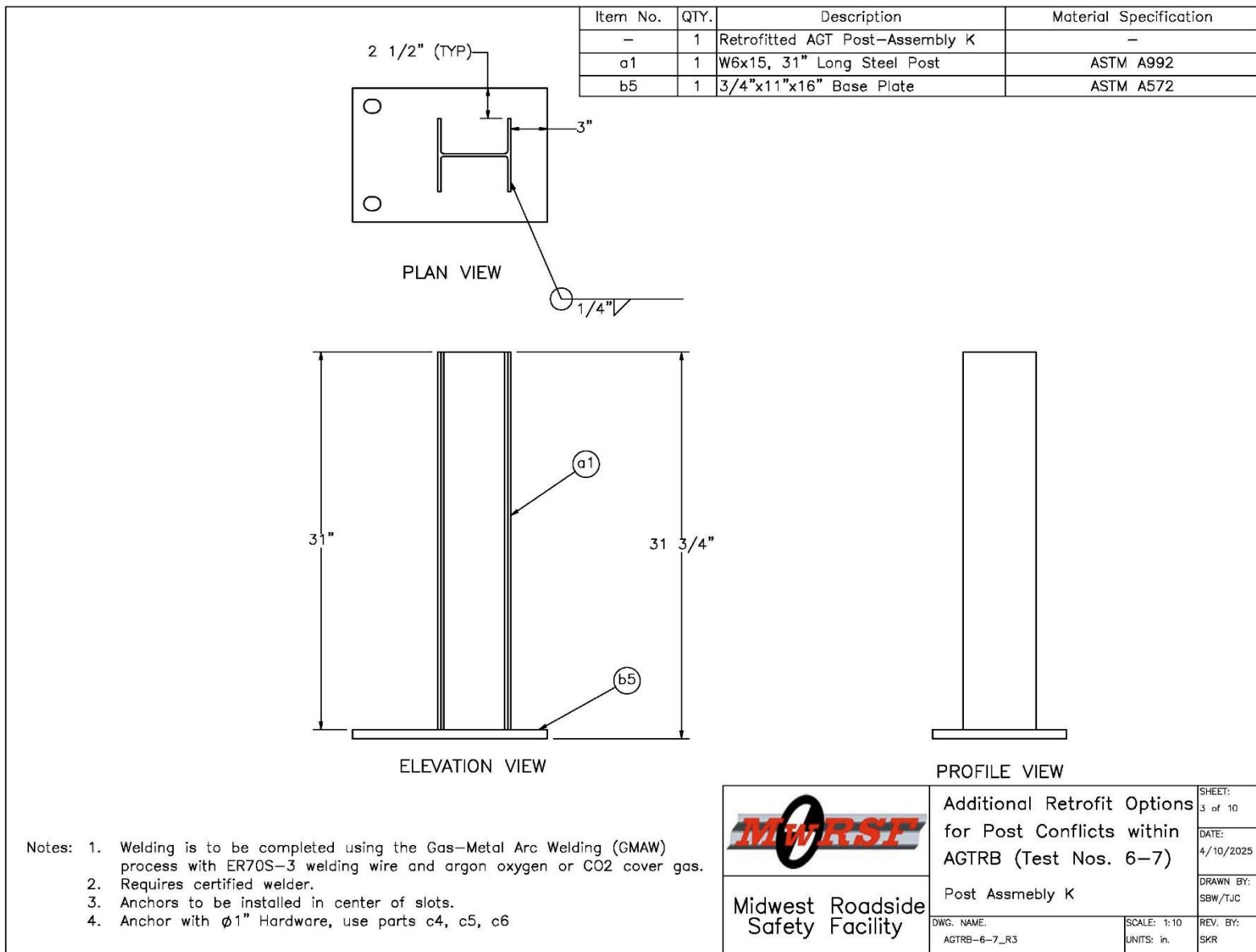


Figure 38. Test Article Details, Round 2 – Assembly K

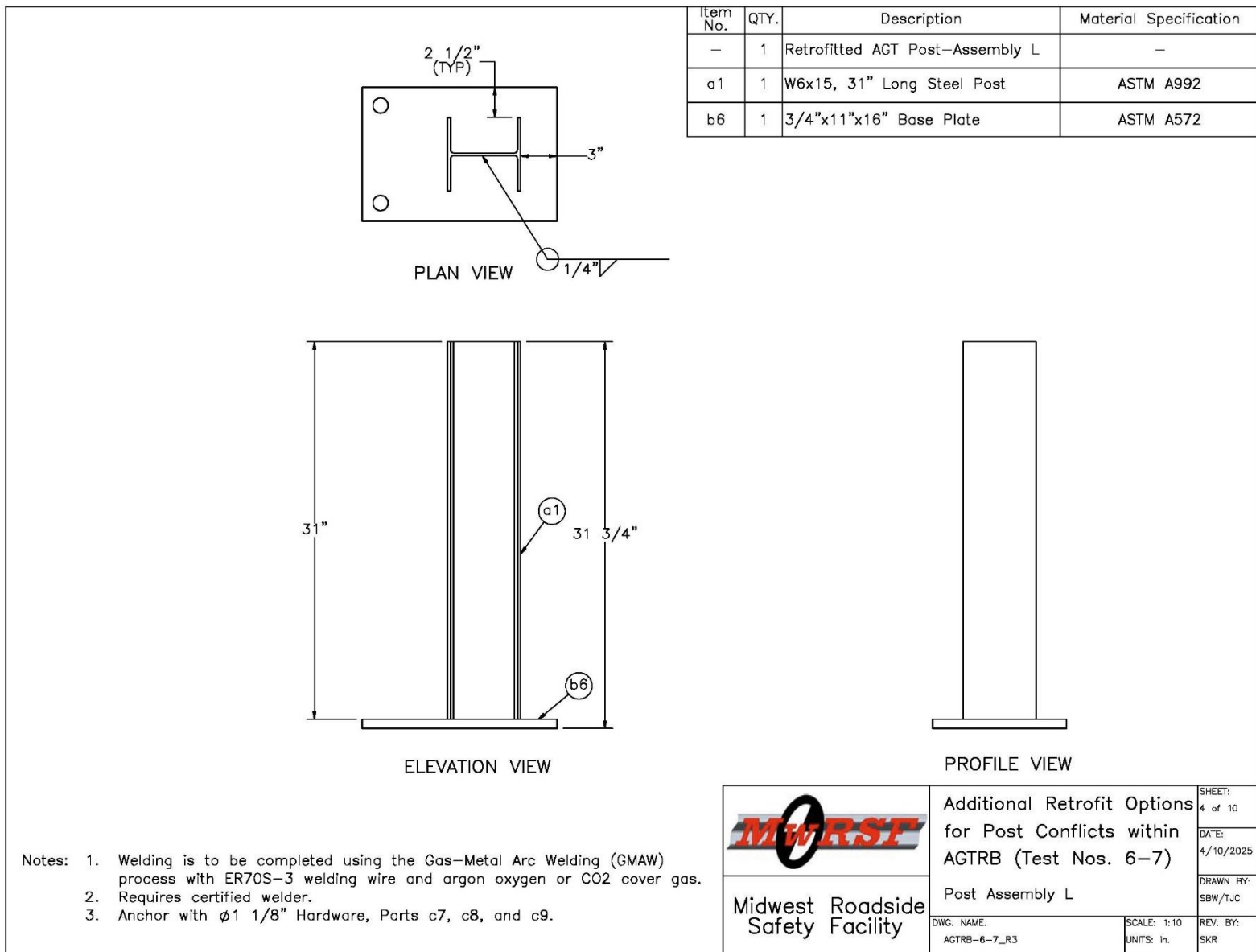


Figure 39. Test Article Details, Round 2 – Assembly L

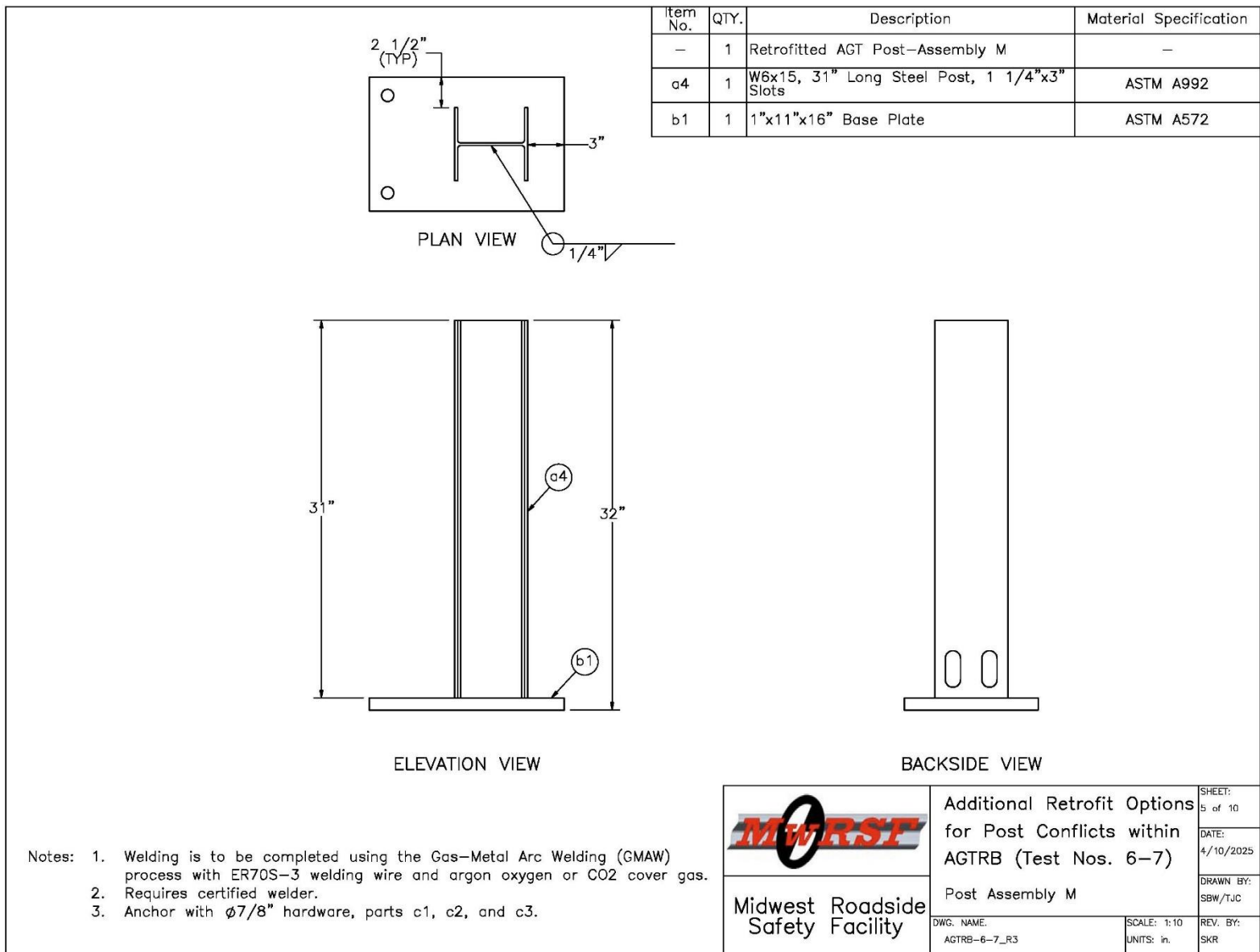


Figure 40. Test Article Details, Round 2 – Assembly M

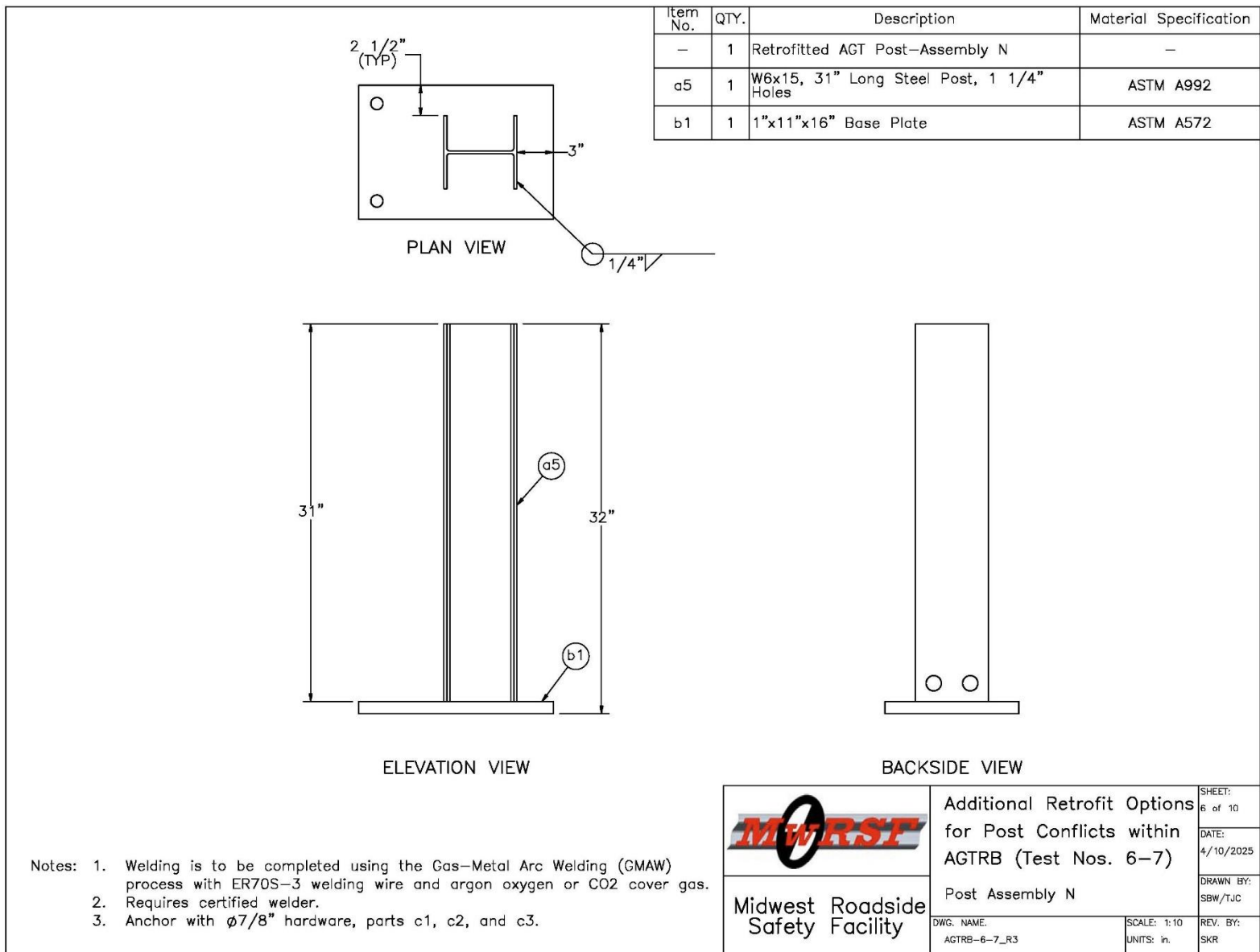


Figure 41. Test Article Details, Round 2 – Assembly N

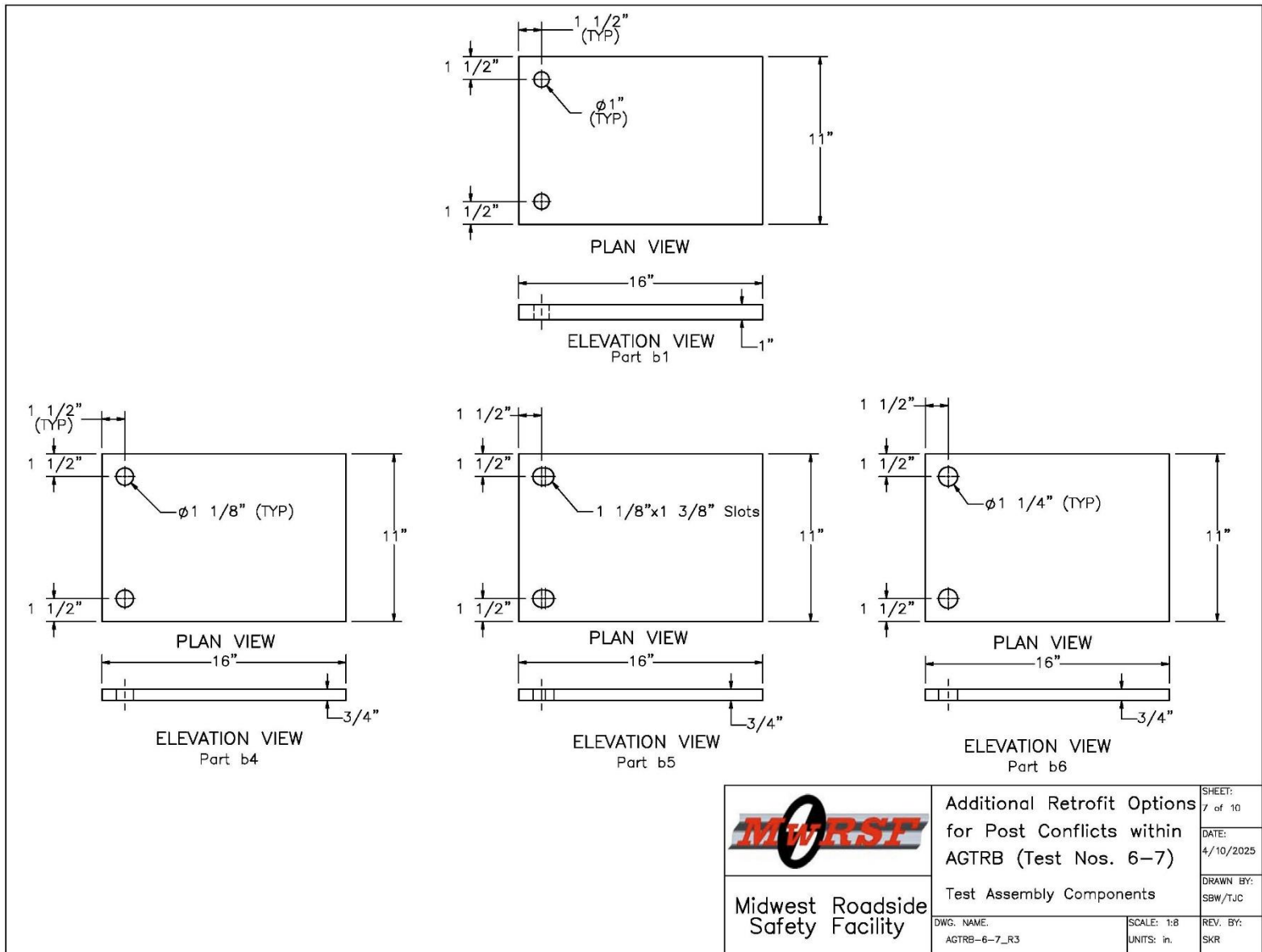


Figure 42. Test Article Details, Round 2 – Base Plates



Additional Retrofit Options  
for Post Conflicts within  
AGTRB (Test Nos. 6–7)

Test Assembly Components

DWG. NAME:  
AGTRB-6-7-R3

SCALE: 1:8  
UNITS: in.

DATE:  
4/10/2025

DRAWN BY:  
SBW/TJC

REV. BY:  
SKR

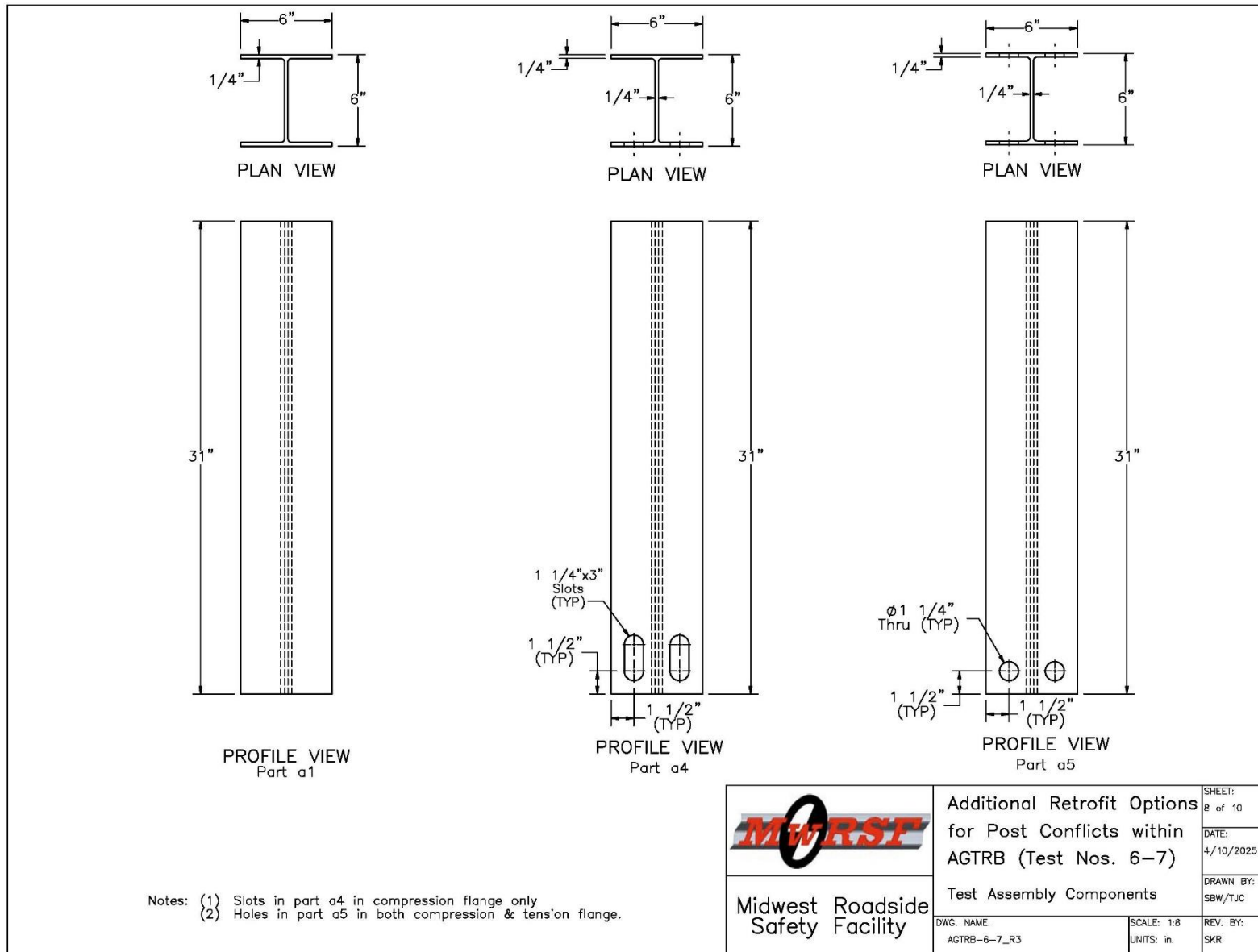


Figure 43. Test Article Details, Round 2 – Post Segments

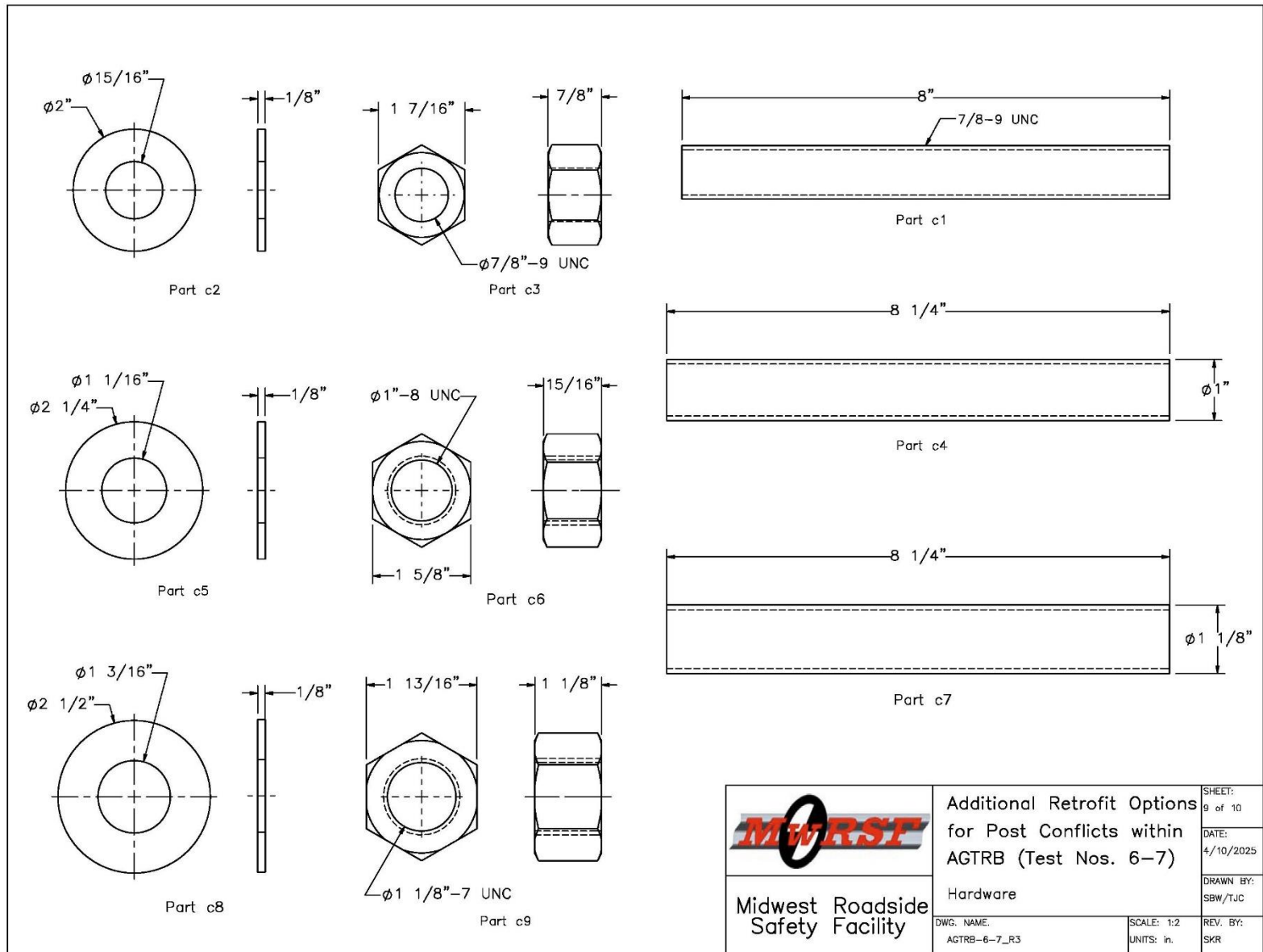


Figure 44. Test Article Details, Round 2 – Anchorage Hardware

 <b>Midwest Roadside Safety Facility</b>	<b>Additional Retrofit Options for Post Conflicts within AGTRB (Test Nos. 6-7)</b>		<b>Sheet:</b> 9 of 10  <b>Date:</b> 4/10/2025  <b>Drawn By:</b> SBW/TJC  <b>Rev. By:</b> SKR
	<b>Hardware</b> <b>Dwg. Name:</b> AGTRB-6-7-R3	<b>Scale:</b> 1:2 <b>Units:</b> in.	

Item No.	QTY.	Description	Material Specification
a1	3	W6x15, 31" Long Steel Post	ASTM A992
a4	1	W6x15, 31" Long Steel Post, 1 1/4"x3" Slots	ASTM A992
a5	1	W6x15, 31" Long Steel Post, 1 1/4" Holes	ASTM A992
b1	2	1"x11"x16" Base Plate	ASTM A572
b4	1	3/4"x11"x16" Base Plate	ASTM A572
b5	1	3/4"x11"x16" Base Plate	ASTM A572
b6	1	3/4"x11"x16" Base Plate	ASTM A572
c1	4	7/8"-9 UNC, 8" Long Threaded Rod	ASTM A193 Grade B7
c2	4	7/8" Dia., Plain Round Washer	ASTM F844
c3	4	7/8"-9 UNC Heavy Hex Nut	ASTM A194 Grade 2H or Equivalent
c4	4	1"-8 UNC, Threaded Rod, 8 1/4" Long	ASTM A193 Grade B7
c5	4	1" Dia., Plain Round Washer	ASTM F844
c6	4	1"-8 UNC Heavy Hex Nut	ASTM A194 Grade 2H or Equivalent
c7	2	1 1/8"-7 UNC, Threaded Rod, 8 1/4" Long	ASTM A193 Grade B7
c8	2	1 1/8" Dia., Plain Round Washer	ASTM F844
c9	2	1 1/8"-7 UNC Heavy Hex Nut	ASTM A194 Grade 2H or Equivalent
c10	-	Chemical Epoxy	Hilti HIT RE-500 V3

 <b>Midwest Roadside Safety Facility</b>	<b>Additional Retrofit Options for Post Conflicts within AGTRB (Test Nos. 6-7)</b>		<b>SHEET:</b> 10 of 10 <b>DATE:</b> 4/10/2025 <b>DRAWN BY:</b> SBW/TJC  <b>Bill of Materials</b>
	<b>DWG. NAME:</b> AGTRB-6-7_R3	<b>SCALE:</b> None <b>UNITS:</b> in.	

Figure 45. Test Article Details, Round 2 – Bill of Materials

## 6.2 Results

Round 1 of physical testing included five dynamic component tests. Descriptions of each test, including sequential and post-test photographs, are contained in the following sections. Data from both accelerometers was processed for each test. Although the two accelerometers produced similar results, the values described herein were calculated from the SLICE-1 data in order to provide a common basis for comparing the test results. Test results from both accelerometers and for all tests are provided in Appendix B.

### 6.2.1 Test No. AGTRB-6

Test no. AGTRB-6 was conducted on Post Assembly J, which consisted of a W6x15 post welded to a  $\frac{3}{4}$ -in. thick base plate. This post assembly was similar to that evaluated in test no. AGTRB-3. However, the diameter of the anchor rods was increased to 1 in. to prevent the anchor fracture observed in the previous test.

During test no. AGTRB-6, the bogie impacted the post assembly at a speed of 17.5 mph causing the base plate to bend and the post to rotate backward. The bogie eventually overrode the top of the post at a displacement of 12.2 in. Upon post-test examination, minor bending and compression flange buckling was observed on the post, while the base plate was significantly bent. Although the anchor rods did not fracture the base plate did apply prying loads which cause the rods to bend slightly and for the surrounding concrete to spall. Time sequential photographs and post-impact photographs are shown in Figure 46.

Force-deflection and energy-deflection curves were created from the accelerometer data and are shown in Figure 47. A peak force of 34.8 kips occurred at a displacement of 7.2 in., and an average force of 26.0 kips occurred through 10 in. of displacement. These force levels were higher than anticipated and may be the result of the larger anchors preventing further displacement of the base plate.

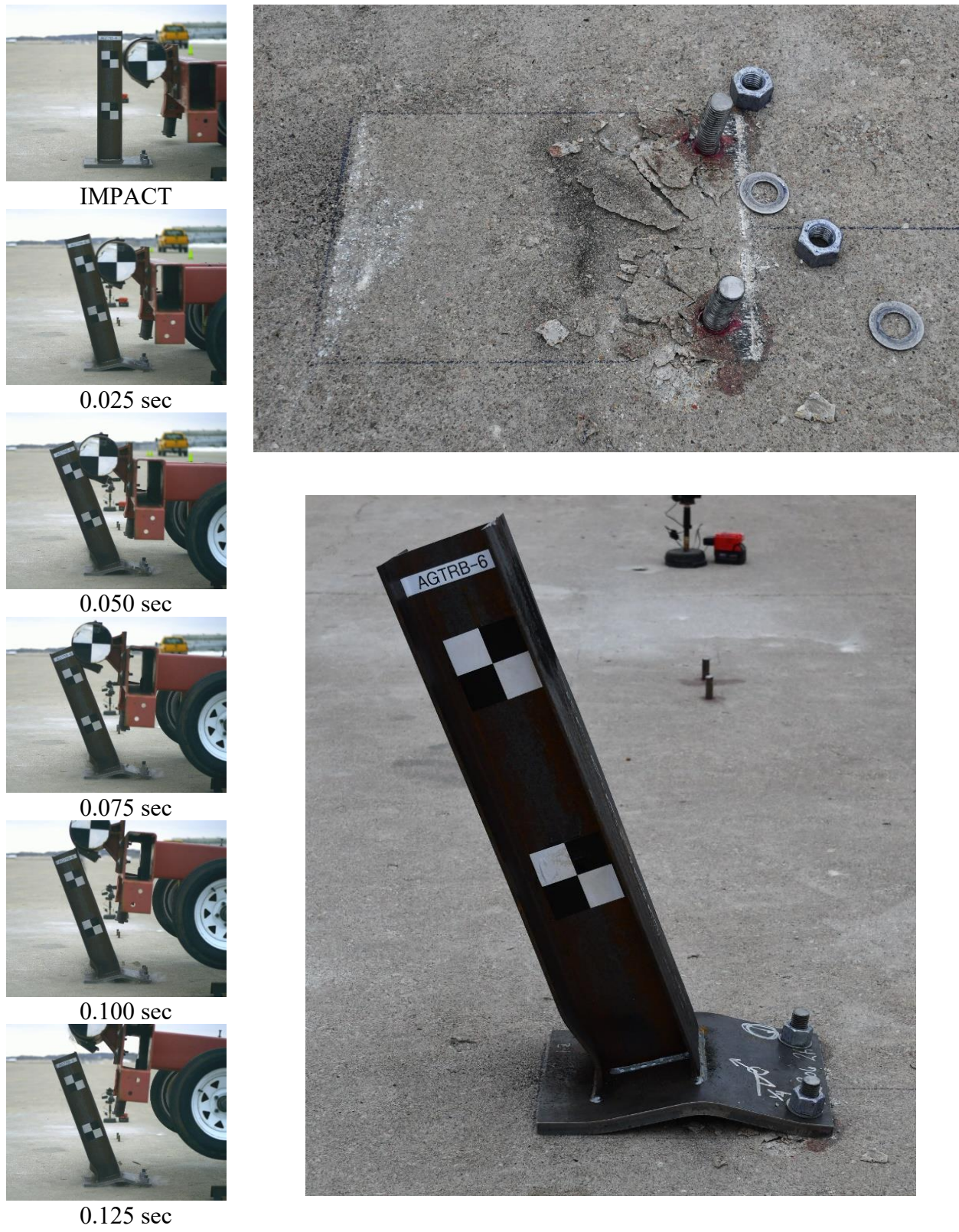


Figure 46. Time-Sequential and Post-Impact Photographs, Test No. AGTRB-6

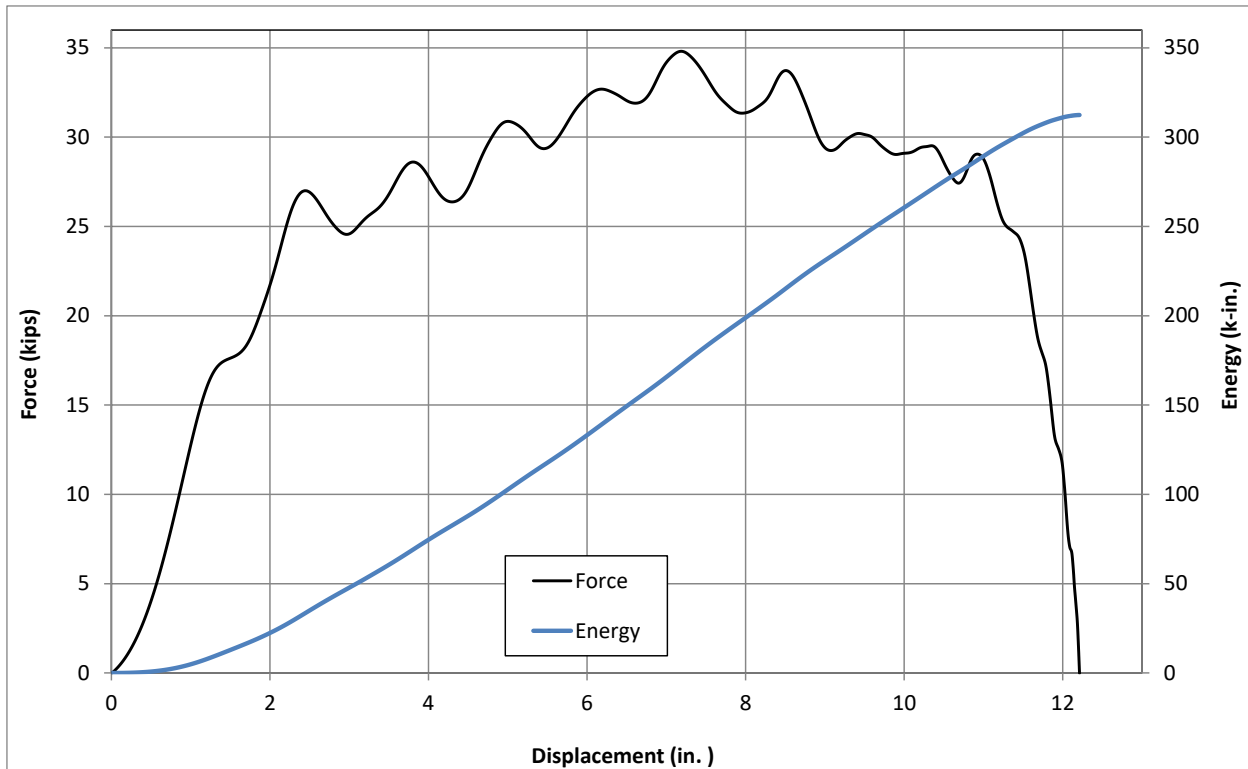


Figure 47. Force vs. Deflection and Energy vs. Deflection, Test No. AGTRB-6

### 6.2.2 Test No. AGTRB-7

Test no. AGTRB-7 was conducted on Post Assembly M, which consisted of a W6x15 post with two 1 $\frac{1}{4}$ -in. x 3 in. slots in the bottom of the compression flange. During test no. AGTRB-7, the bogie impacted the post assembly at a speed of 18.4 mph causing the post to yield and bend backward. The bogie eventually overrode the top of the post at a displacement of 19.8 in. Upon post-test examination, severe buckling of the compression flange was observed adjacent to the slots and the base plate was minimally bent. No weld or anchor failure was observed. Time sequential photographs and post-impact photographs are shown in Figure 48.

Force-deflection and energy-deflection curves were created from the accelerometer data and are shown in Figure 49. A peak force of 29.6 kips occurred at a displacement of 2.5 in., however, after the post yielded, the resistance force dropped and an average force of 19.2 kips occurred through 10 in. of displacement.

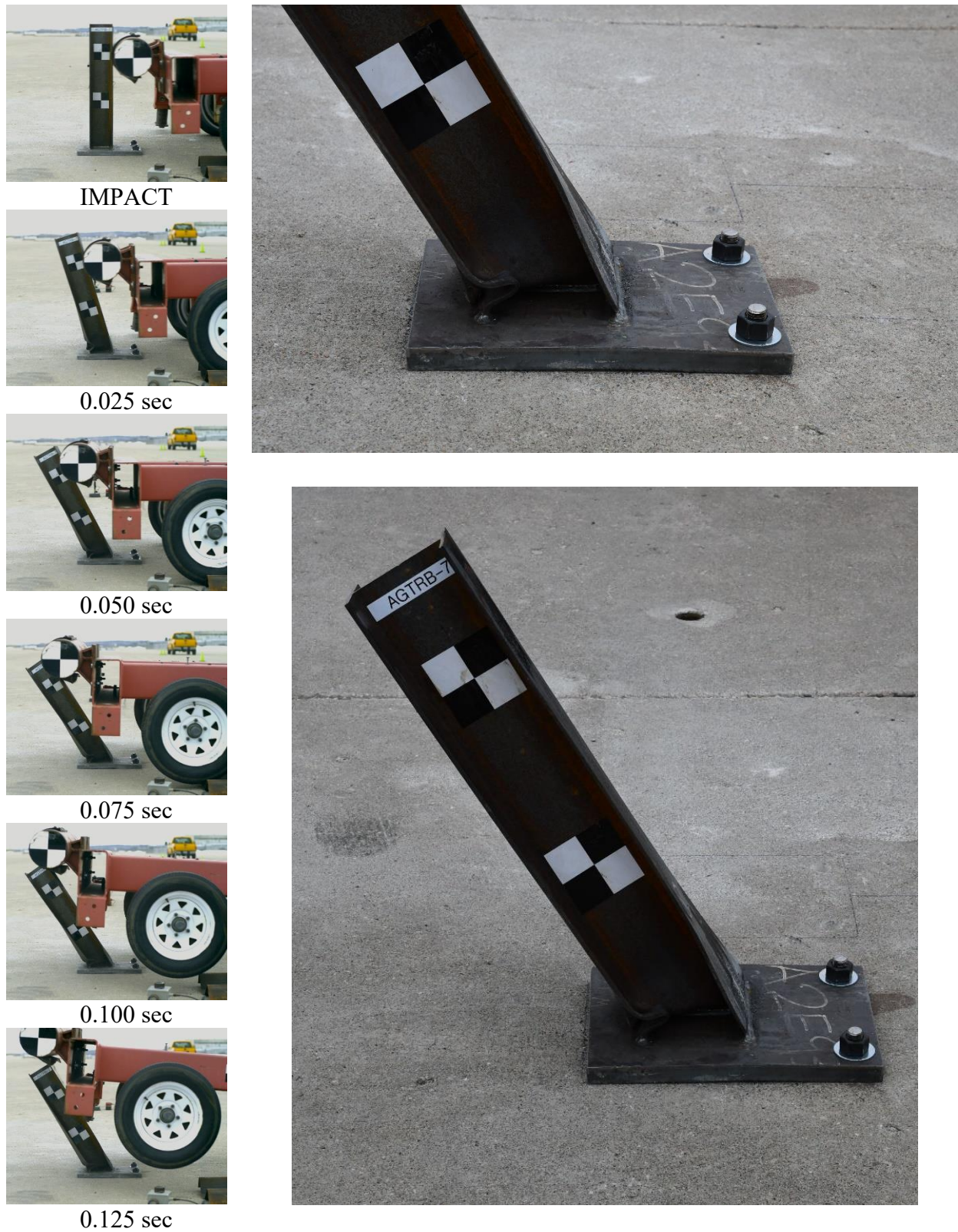


Figure 48. Time-Sequential and Post-Impact Photographs, Test No. AGTRB-7

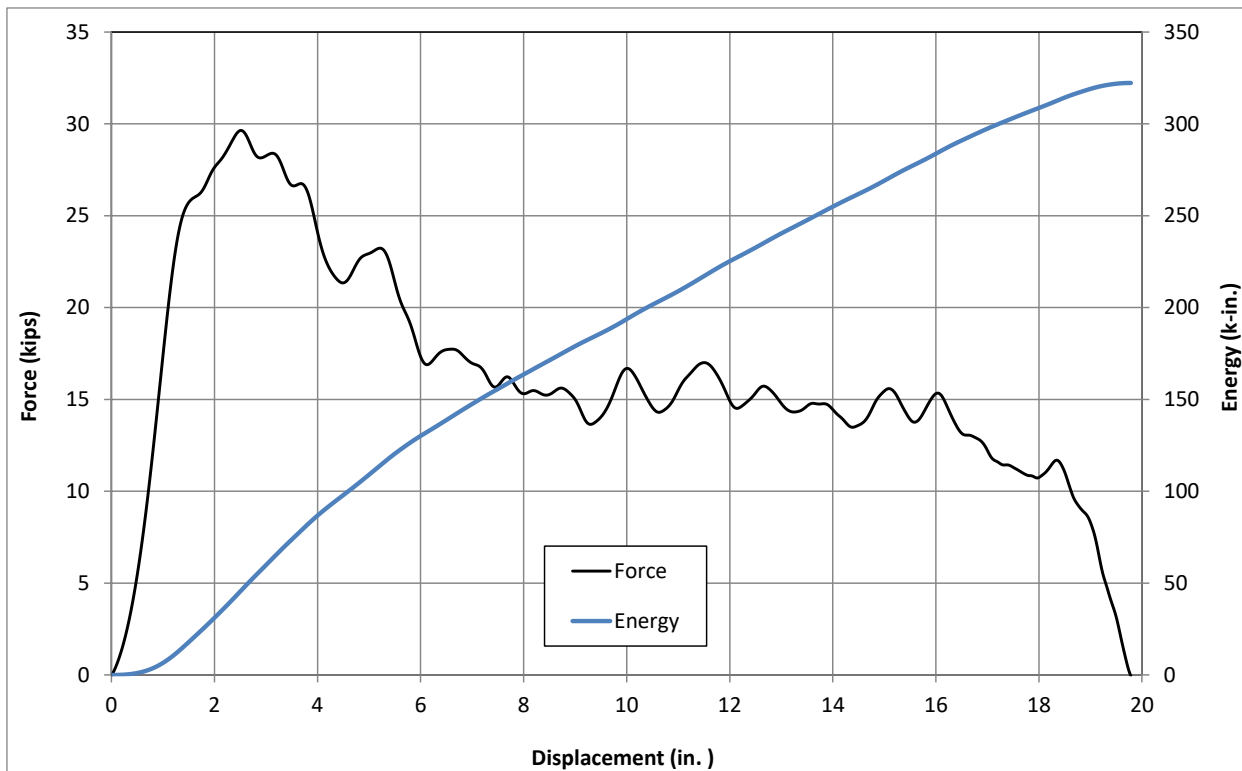


Figure 49. Force vs. Deflection and Energy vs. Deflection, Test No. AGTRB-7

### 6.3 Discussion

Round 2 of testing consisted of two dynamic component tests. In test no. AGTRB-6, a thinner  $\frac{3}{4}$ -in. base plate was used in combination with larger 1-in. diameter anchor rods to prevent anchor fracture. Unfortunately, the larger anchors may have limited the base plate from deforming, thereby stiffening the post assembly and resulting in forces well above the targeted 17 kips.

Test no. AGTRB-7 was conducted on a post with two  $1\frac{1}{4}$ -in. x 3-in. slots cut into the compression flange of the post. These slots helped initiate flange buckling and allowed the post to bend backward in a controlled and steady manner. The average force over 10 in. was 19.2 kips, which was a little higher than targeted, but only by 12 percent. Additionally, the post assembly's performance in terms of a steady and consistent resistance force following yielding and the lack of anchorage damage were preferable. Thus, Post Assembly M was selected for further evaluation.

A summary of Round 2 testing is provided in Table 7, while force vs. displacement and energy vs. displacement curves for the tests are shown in Figure 50 and 51, respectively. Note, Test nos. MGSATB-5 and 6, which are shown in Figures 50 and 51, were the bogie tests conducted on W6x15 posts in soil that provided the target resistance force of 17 kips over 10 in. of displacement.

Table 7. Results Summary, Component Testing - Round 2

Test No.	Post Assembly and Weakening Mechanism	$F_{ave}$ @ 10 in. (kips)	Failure Description
AGTRB-6	J – $\frac{3}{4}$ " base plate, Ø1" rods	26.0	Base Plate Bending, Rod Bending
AGTRB-7	M – Ø1 $\frac{1}{4}$ " x 3" slots	19.2	Post Bending, Flange Buckling

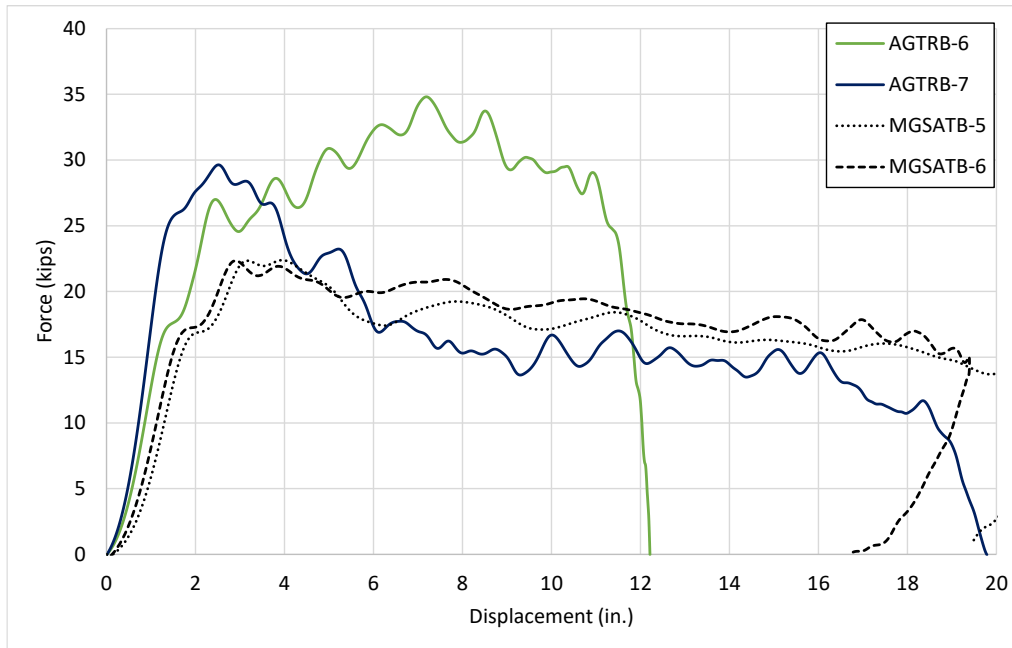


Figure 50. Force vs. Deflection Comparison, Round 2 Bogie Tests

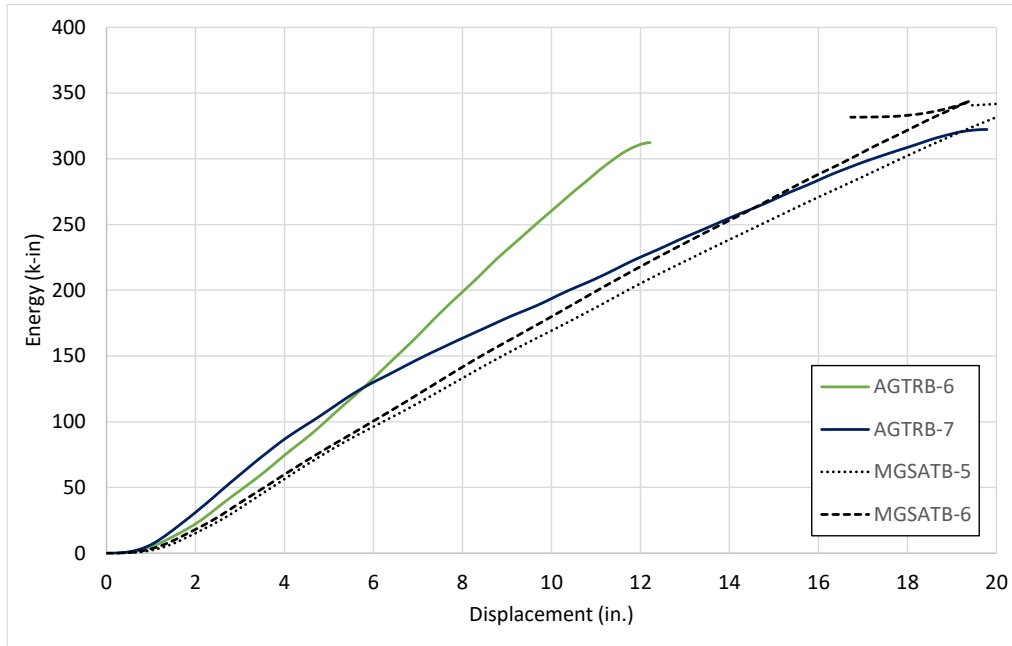


Figure 51. Energy vs. Deflection Comparison, Round 2 Bogie Tests

## 7 DYNAMIC COMPONENT TESTING – ROUND 3

### 7.1 Scope

All of the component test performed during Rounds 1 and 2 were conducted with the retrofit posts mounted to the test site tarmac, a very large concrete slab. After Post Assembly M was selected as the desired surface-mounted, retrofit post design, Round 3 of component testing was conducted to evaluate the requirements for the concrete slab supporting the new retrofit post.

Anchorage for the retrofit post was designed with a 6-in. embedment depth in order to be compatible with concrete slabs with a minimum thickness of 8 in. However, the length and width requirements for the slab needed to be defined. Most AGTs consisting of W6x15 posts use a post spacing of 37½ in. Recognizing that the retrofit post may need to be used for more than one post location, the maximum slab length that could be attributed to a single post was 37½ in. For testing purposes, a conservative width of 36 in. was selected.

Ideally, the slab width would be held to a minimum to limit installation costs. Roadside designers would want to limit the extent of the slab behind the posts to avoid any ground obstructions and/or slopes, similar to those observed during the DOT survey in Chapter 2. Limiting the extend of the slab in front of the posts would prevent conflicts with roadway or shoulder pavements. However, the slab needed to extend far enough in front of the anchor rods to prevent premature failure due to concrete breakout. Taking all of this into consideration, a two ft width was selected. Note, this width resulted in the slab extending 4 in. in front of the face of the three beam guardrail. Thus, Round 3 of component testing was conducted with the AGT posts mounted to 3-ft long by 2-ft wide by 8 in. deep concrete slabs.

Two dynamic component tests were conducted in Round 3 of testing. Both tests were conducted with the selected retrofit post design (Post Assembly M) mounted to identical reinforced concrete slabs measuring 36 in. x 24 in. x 8 in. Test no. AGTRB-8 was conducted with the slab tied to the adjacent concrete using three ½-in. diameter dowel rod, while test no. AGTRB-9 was conducted with a free standing slab. Photographs of the test articles are shown in Figure 52, and CAD details for Round 3 of component testing are shown in Figures 53 through 59.



Test No. AGTRB-8 (Doweled)



Test No. AGTRB-9 (Freestanding)

Figure 52. Photographs of the Test Installations for Test Nos. AGTRB-8 and AGTRB-9

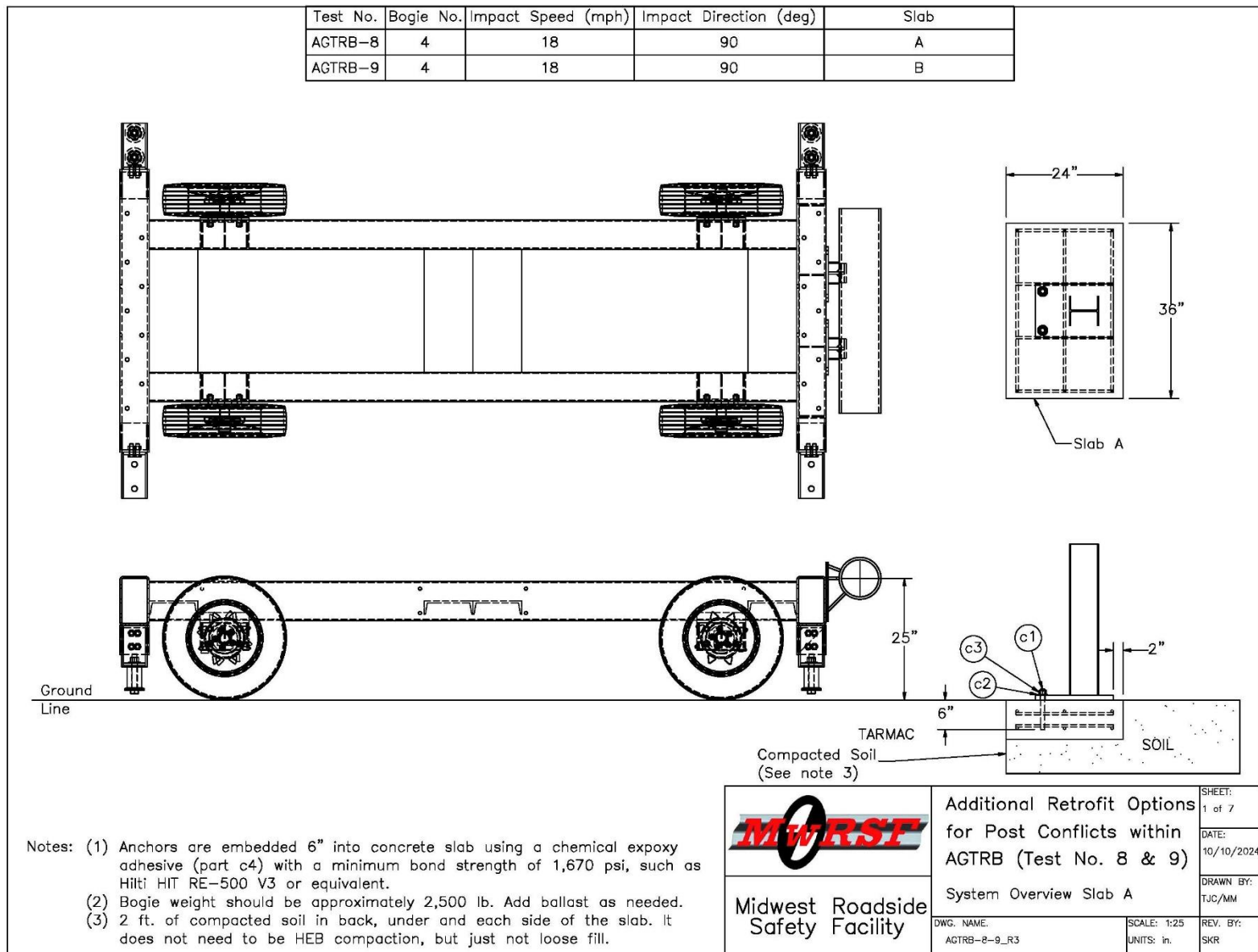


Figure 53. Dynamic Component Testing Matrix and Setup – Round 3

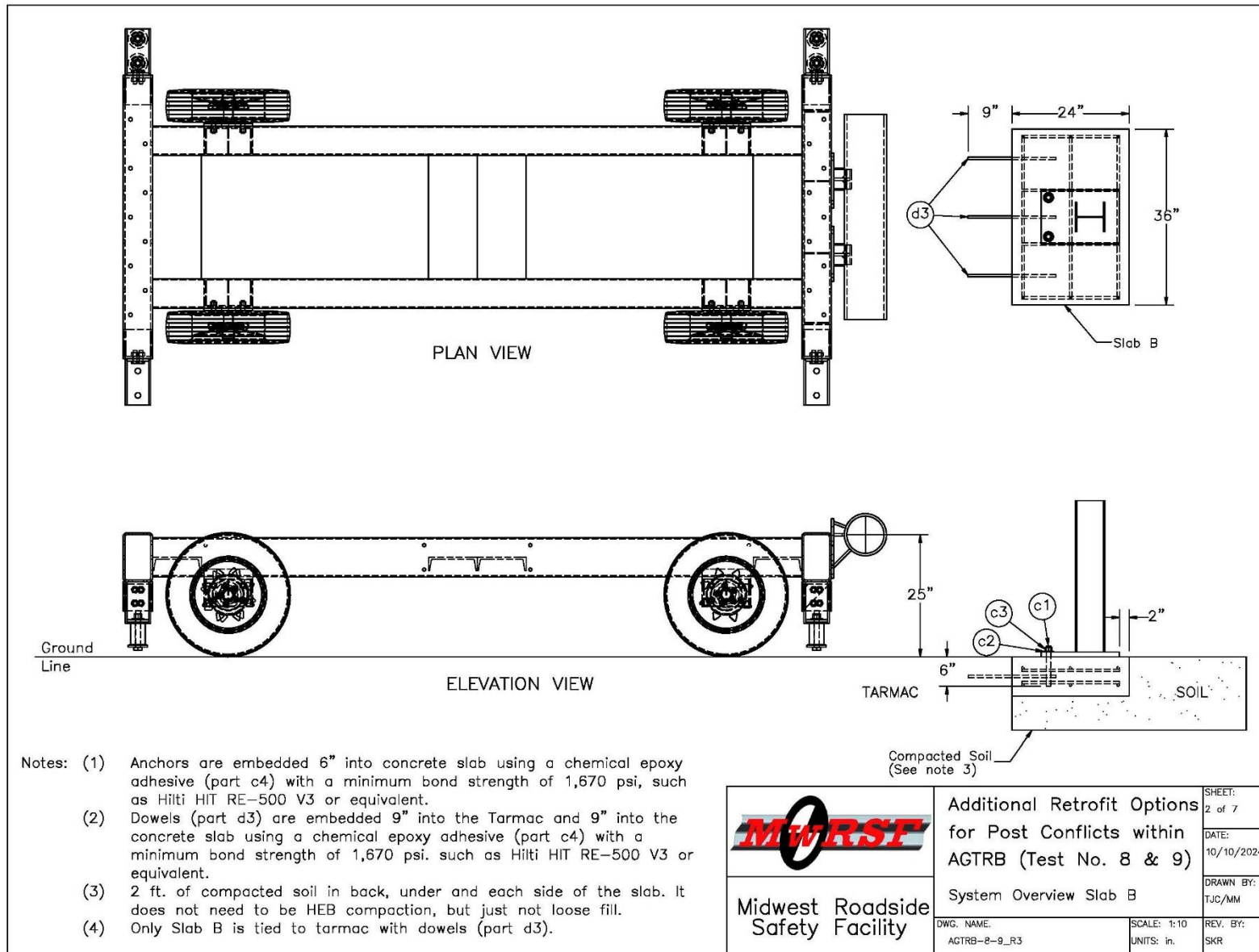


Figure 54. Dynamic Component Testing Setup – Test No. AGTRB-8

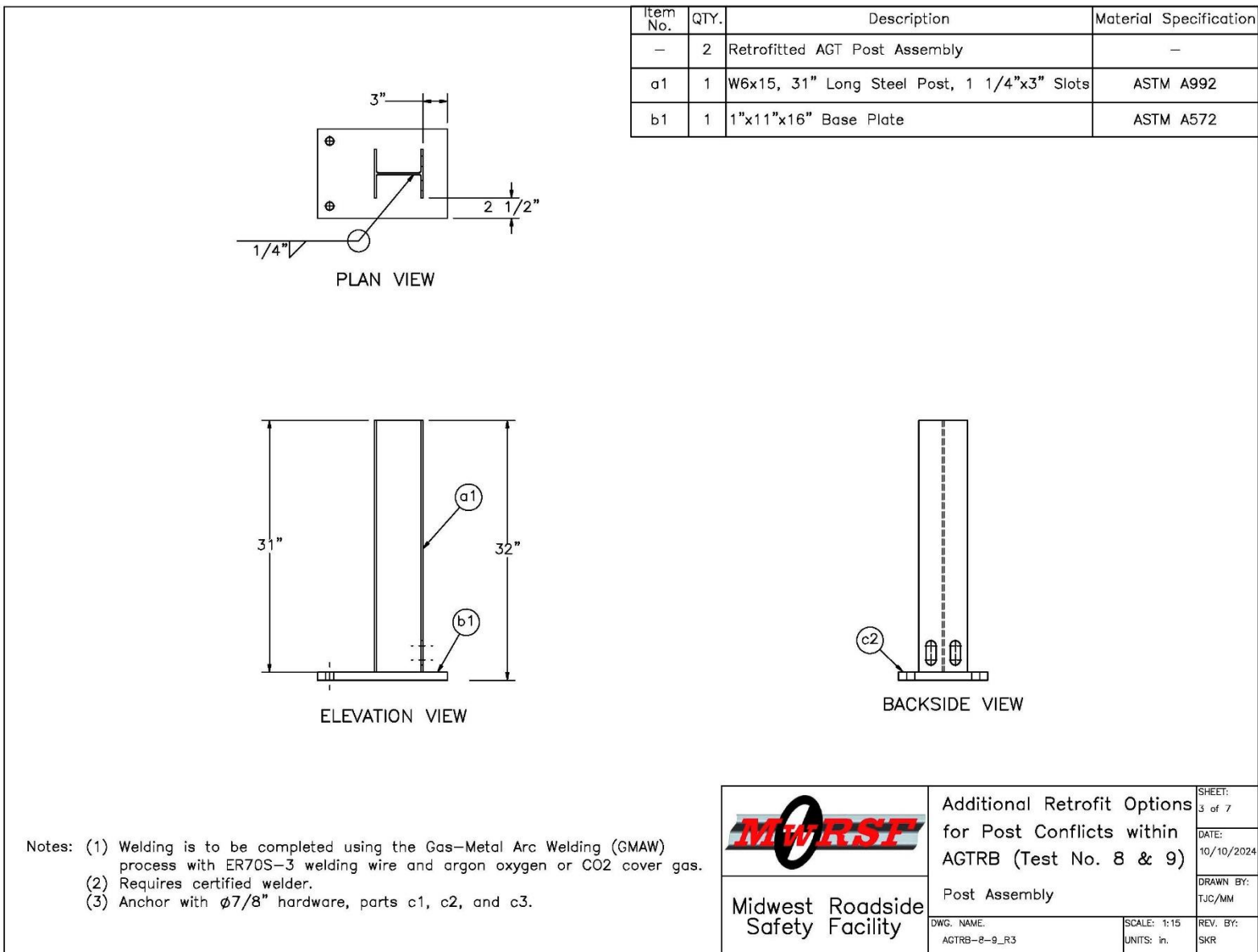


Figure 55. Test Article Details, Round 3 – Post Assembly

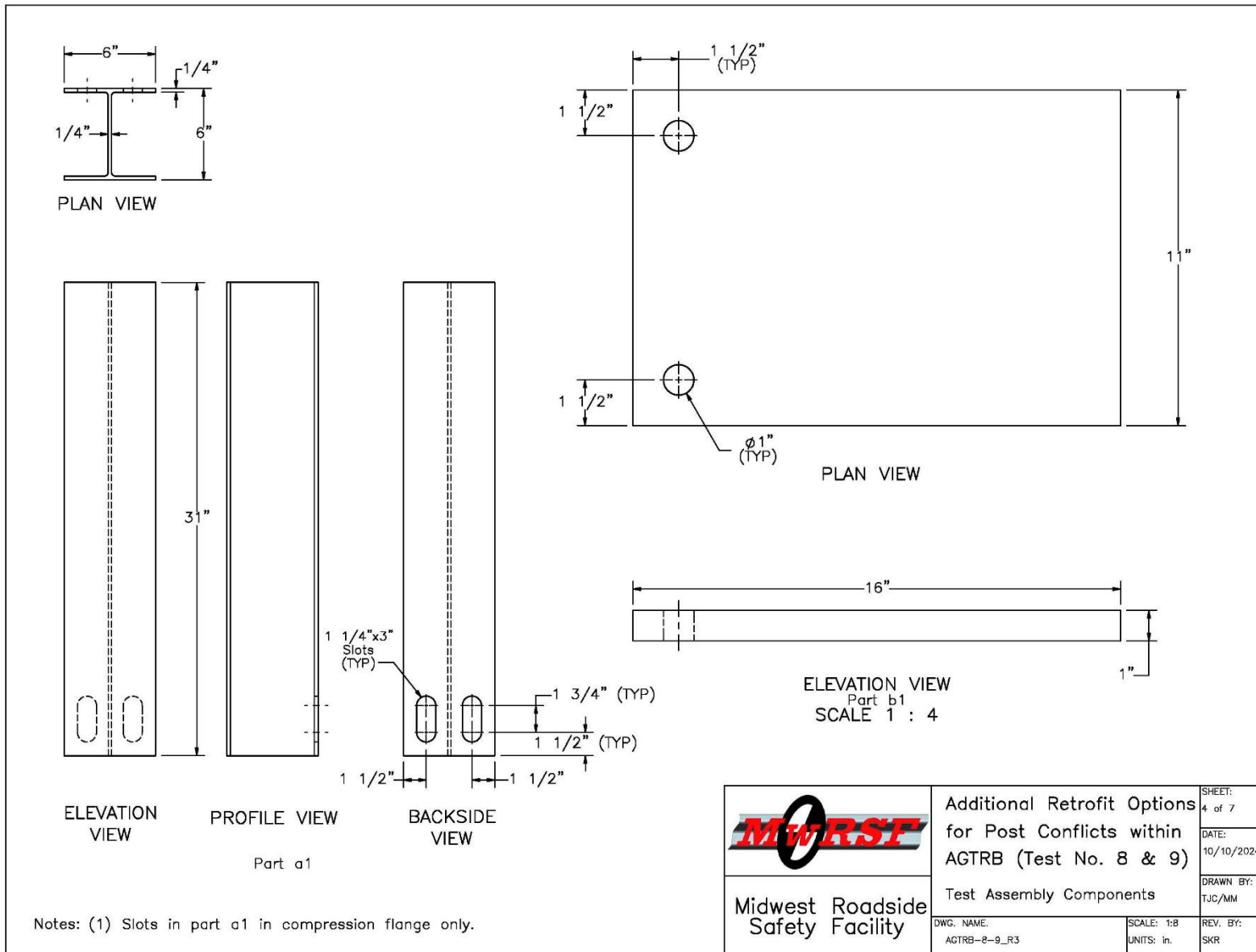


Figure 56. Test Article Details, Round 3 – Post and Base plate

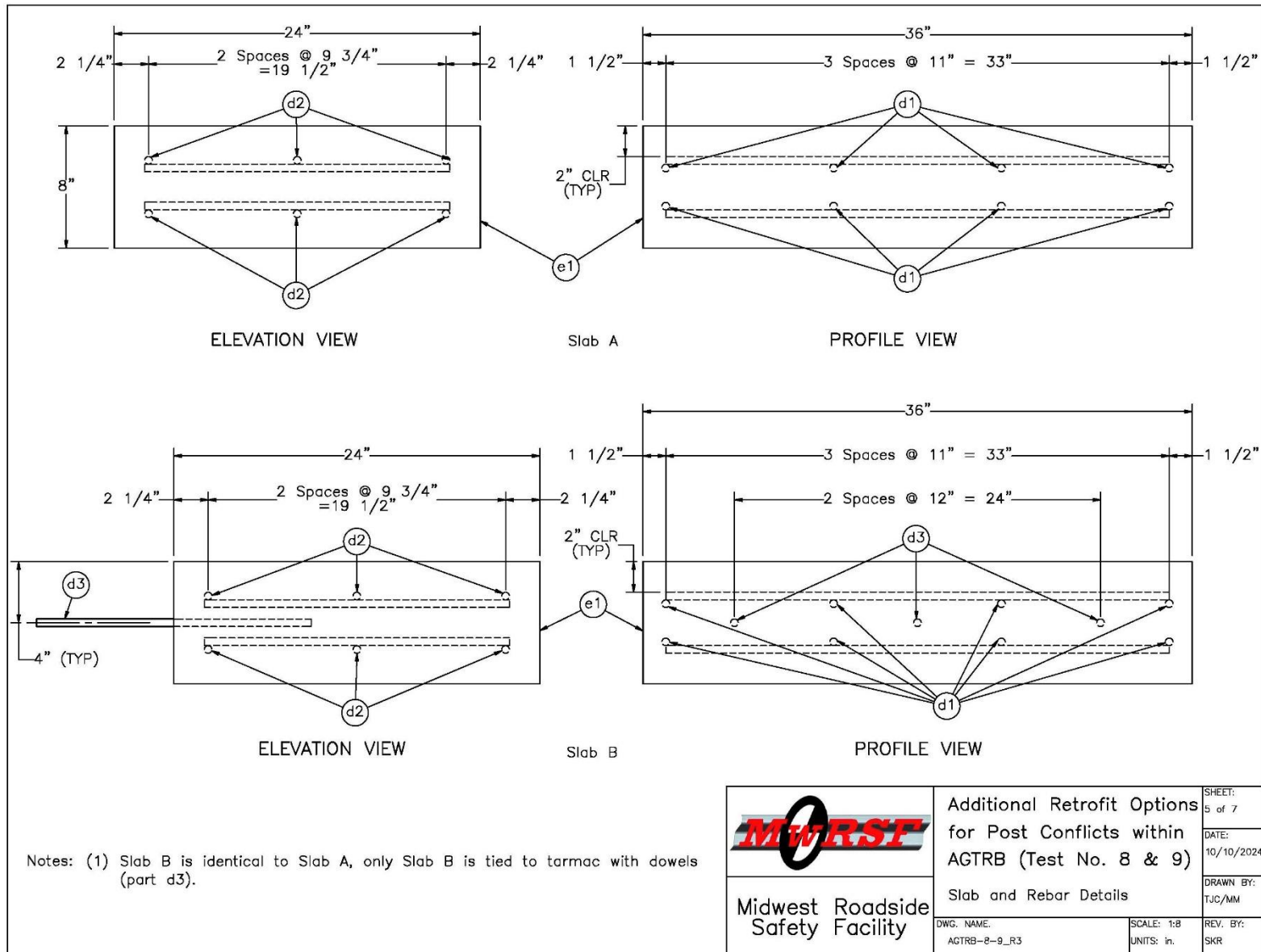


Figure 57. Test Article Details, Round 3 – Concrete Slabs

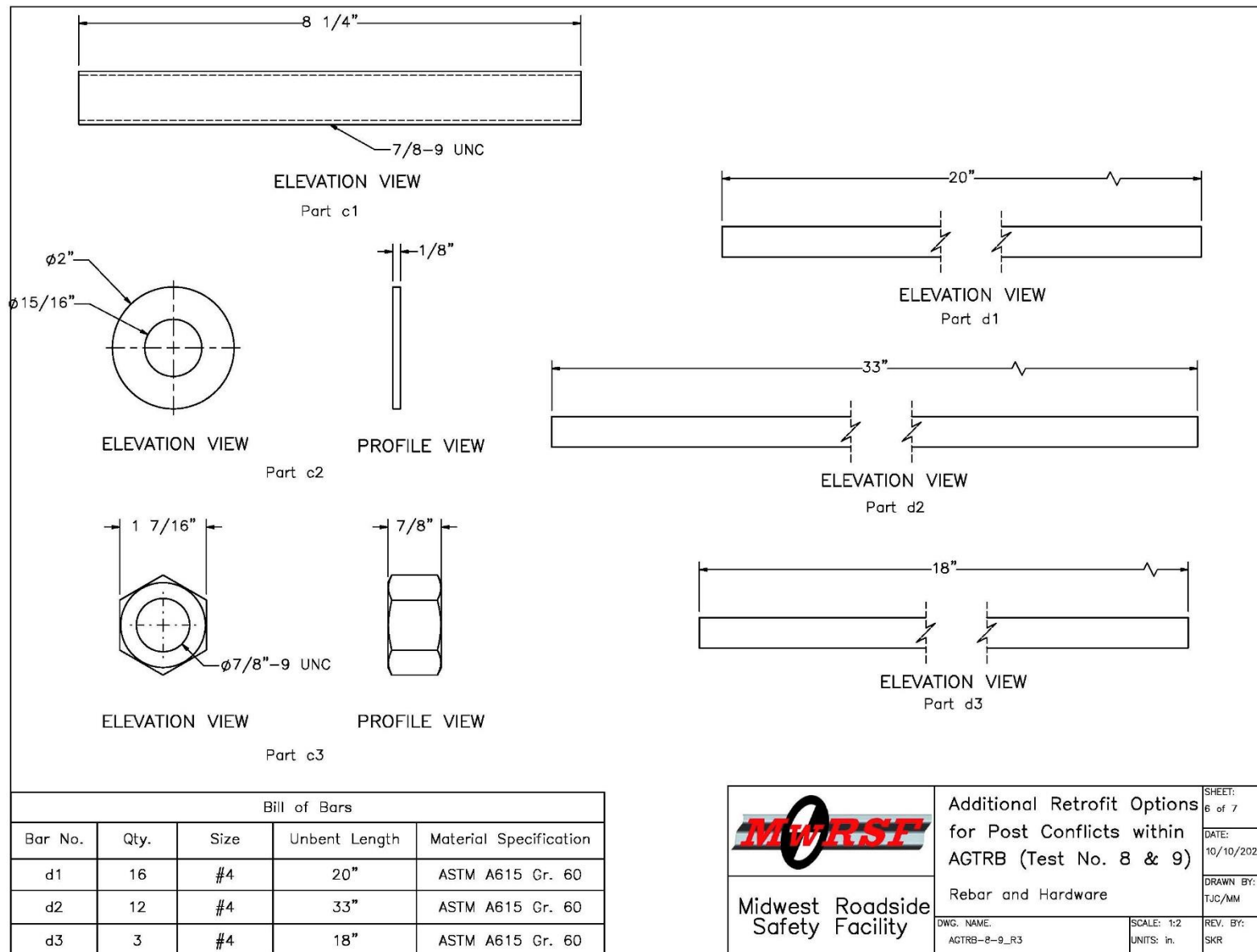


Figure 58. Test Article Details, Round 3 – Anchorage Hardware

Item No.	QTY.	Description	Material Specification	Treatment Specification	Hardware Guide
a1	2	W6x15, 31" Long Steel Post, 1 1/4"x3" Slots	ASTM A992	ASTM A123	–
b1	2	1"x11"x16" Base Plate	ASTM A572	ASTM A123	–
c1	4	7/8"-9 UNC, 8 1/4" Long Threaded Rod	ASTM A193 Grade B7	–	FRR22c
c2	4	7/8" Dia., Plain Round Washer	ASTM F844	ASTM A123 or A153 or F2329	FWC24a
c3	4	7/8"-9 UNC Heavy Hex Nut	ASTM A194 Grade 2H or Equivalent	ASTM A153 or B695 Class 55	–
c4	–	Chemical Epoxy	Hiti HIT RE-500 V3	–	–
d1	16	#4 Rebar, 20" Long	ASTM A615 Gr.60	Epoxy Coated (ASTM A775 or A934)	–
d2	12	#4 Rebar, 33" Long	ASTM A615 Gr. 60	Epoxy Coated (ASTM A775 or A934)	–
d3	3	#4 Dowel, 18" Long	ASTM A615 Gr. 60	Epoxy Coated (ASTM A775 or A934)	–
e1	–	Concrete	min f'c = 4,000 psi	–	–
–	–	Soil	–	–	–

66

 <b>Midwest Roadside Safety Facility</b>	<b>Additional Retrofit Options for Post Conflicts within AGTRB (Test No. 8 &amp; 9)</b>		<b>SHEET:</b> 7 of 7 <b>DATE:</b> 10/10/2024 <b>DRAWN BY:</b> TJC/MM
	<b>Bill of Materials</b>		
DWG. NAME: AGTRB-8-9_R3	SCALE: None UNITS: in.	REV. BY: SKR	

Figure 59. Test Article Details, Round 3 – Bill of Materials

## 7.2 Results

### 7.2.1 Test No. AGTRB-8

Test no. AGTRB-8 was conducted on Post Assembly M mounted to a 36-in. x 24-in. x 8-in. reinforced concrete slab, which was tied to the adjacent tarmac using three dowel rods. During test AGTRB-8, the bogie impacted the post assembly at a speed of 19.3 mph. Approximately 0.011 sec. after impact, the anchor rods pulled out the concrete slab and the post rotated back freely. The concrete between the anchors and extending to the front edge of the slab also broke away. The post and base plate remained largely undamaged. Time sequential photographs and post-impact photographs are shown in Figure 60.

Force-deflection and energy-deflection curves were created from the accelerometer data and are shown in Figure 61. A peak force of 21.8 kips occurred at a displacement of 2.7 in., right before anchors pulled out of the concrete slab. The resistance force then quickly dropped to zero for the remainder of the impact event.



IMPACT



0.025 sec



0.050 sec



0.075 sec



0.100 sec



0.125 sec



Figure 60. Time-Sequential and Post-Impact Photographs, Test No. AGTRB-8

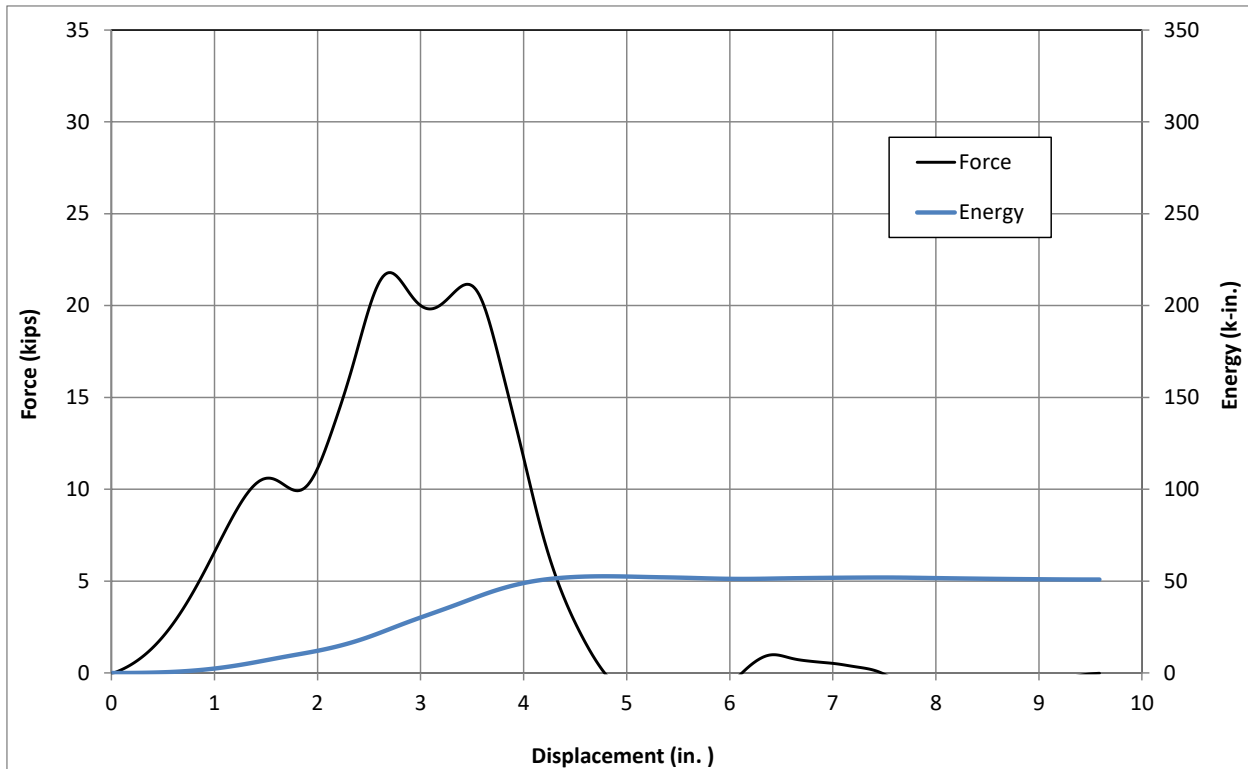


Figure 61. Force vs. Deflection and Energy vs. Deflection, Test No. AGTRB-8

### 7.2.2 Test No. AGTRB-9

Test no. AGTRB-9 was conducted on Post Assembly M mounted to a freestanding 36-in. x 24-in. x 8-in. reinforced concrete slab. During test no. AGTRB-9, the bogie impacted the post assembly at a speed of 19.6 mph. Nearly immediately after impact, the freestanding concrete slab began rotating back about its lower-back edge. The bogie eventually overrode the top of the post at a displacement of 11.7 in. and the post and slab had rotated backward nearly 45 degrees. Upon post-test examination, the post assembly and anchorage were found to be undamaged, but the concrete slab had rotated back with its front edge about 1 ft in air. Time sequential photographs and post-impact photographs are shown in Figure 62.

Force-deflection and energy-deflection curves were created from the accelerometer data and are shown in Figure 63. A peak force of 25.0 kips occurred at a displacement of 2.4 in., and an average force of 14.1 kips occurred through 10 in. of displacement. The resistance force was much lower than previous tests because the force necessary to rotate the concrete slab was less than the force necessary to bend the post.



Figure 62. Time-Sequential and Post-Impact Photographs, Test No. AGTRB-9

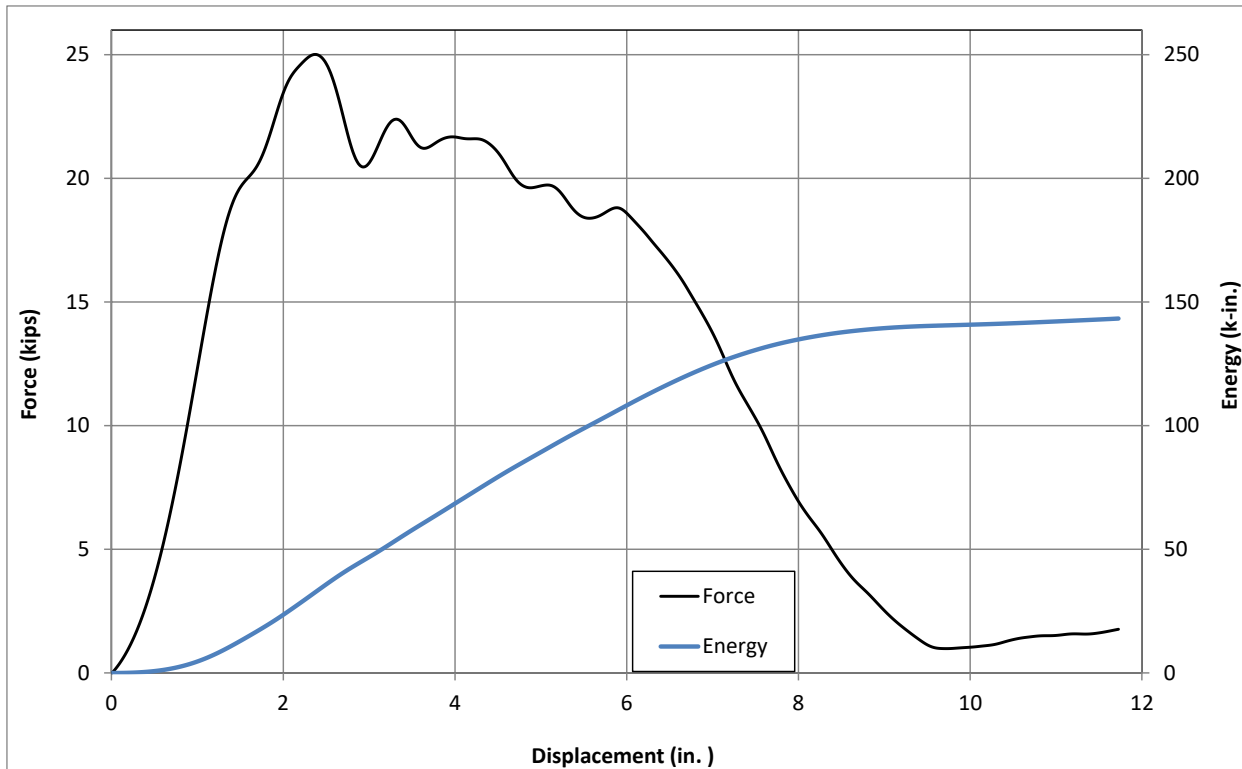


Figure 63. Force vs. Deflection and Energy vs. Deflection, Test No. AGTRB-9

### 7.3 Discussion

Test no. AGTRB-8, which was conducted on the concrete slab tied to the adjacent tarmac with dowel bars, resulted in the anchor rods pulling out of the concrete slab. This behavior was not observed in any of the previous component tests even though the same anchors, embedment depth, and epoxy adhesive were used. After reviewing the test setup, it was determined that the size of the slab was too aggressive and the anchors were located too close to the front edge of the slab.

The anchorage in test no. AGTRB-8 failed due to concrete breakout (i.e., the concrete surrounding the anchors fractured away). As shown in Figure 64, ACI 318 [11] describes the concrete breakout cone as having a diameter of 1.5 times the embedment depth of the anchor,  $h_{ef}$ . For the 6-in. depth used in the retrofit AGT post, the cone size would have a 9-in. diameter. However, in an effort to optimize the size of the supporting concrete slab, the width of the concrete slab was limited to 24 in., and the anchors were placed 7½ in. from the front edge of the slab, as shown in Figure 65. Thus, the concrete breakout strength of the anchors was reduced 17 percent by edge effects. This strength reduction proved critical as it resulted in concrete fracture and the anchors pulling out of the slab. For future installations, a minimum slab width of 30 in. should be used to prevent edge effects from affecting the strength of the anchors and avoid anchor failure.

Test no. AGTRB-9 resulted in the freestanding slab lifting up and rotating without plastic deformations to the post assembly. This behavior was anticipated as the inertia of the slab was not sufficient to prevent slab movement under impact loading. This test illustrates the importance of having the concrete slab tied to adjacent roadway slabs or subsurface concrete structures like wing walls to prevent slab movement.

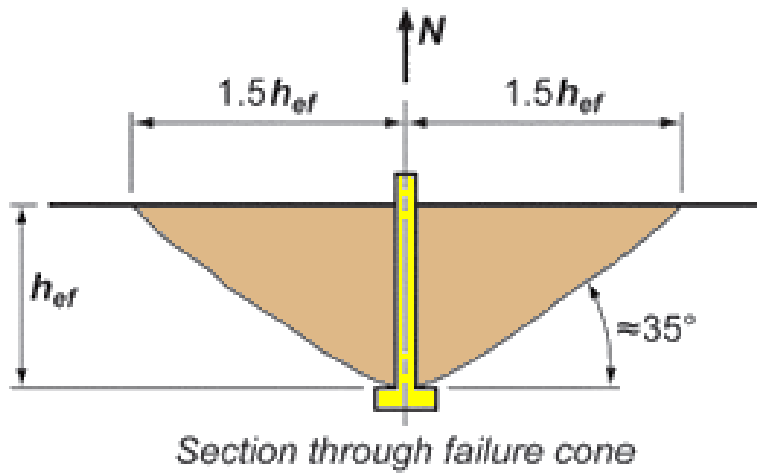


Figure 64. Concrete Breakout Cone Shape [11]

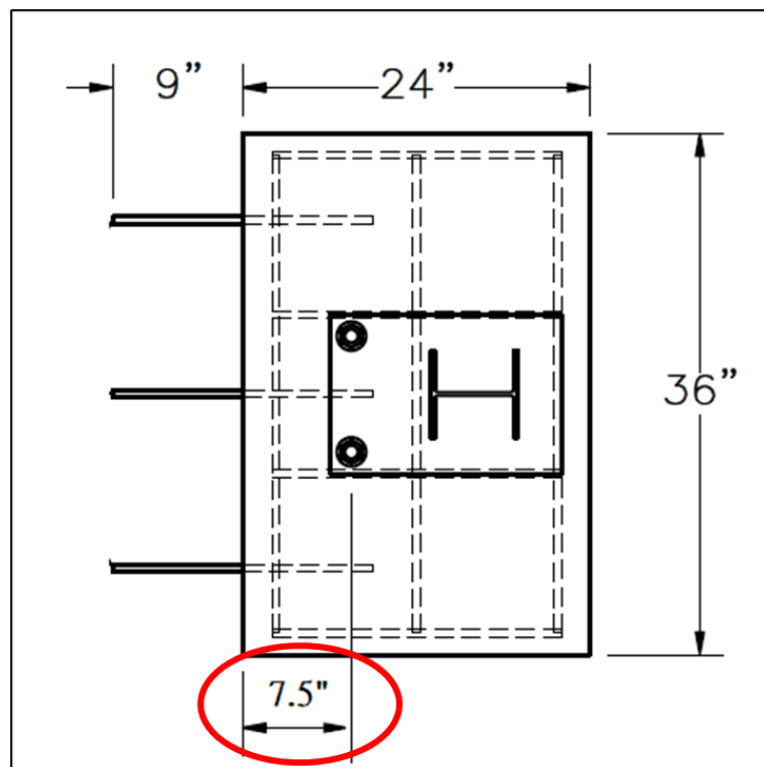


Figure 65. Anchor Location for Test No. AGTRB-8

## 8 SUMMARY AND CONCLUSIONS

The objective of this project was to develop retrofit options for AGTs where obstructions prevent the proper installation of the guardrail posts. The project began with a survey of sponsoring state DOTs to better understand the ground obstructions and site issues preventing posts from being properly installed. From this survey, it was determined that the best retrofit option would be a surface-mounted post. Thus, the project scope became the development and testing of a surface-mounted W6x15 AGT post.

The retrofit AGT post was to replicate the strength of a typical W6x15 post embedded in strong soil, which was measured as 17 kips through 10 in. of deflection during a previous study. However, a W6x15 post attached to a near rigid base plated and loaded at 25 in. above ground would produce much higher resistance forces than the desired 17 kips. Increased post strength within a guardrail transition can lead to vehicle snag, pocketing, and/or vehicle instability. Therefore, the post or baseplate had to be weakened to achieve the desired strength.

Multiple post and base plate assemblies were configured with varying base plate sizes, base plate thicknesses, anchor rod diameters, post-to-plate weld specifications, weakening holes and cuts in the compression flange of the post. The configurations were evaluated through dynamic component testing. During these physical tests, a rigid-frame bogie vehicle impacted the test articles at a height of 25 in. and a speed of 18 mph. In all, nine component tests were conducted over three rounds of testing. Highlights of the test results are provided below.

- A W6x15 post attached to a near rigid base plate provided a resistance force over 25 kips through 10 in. of displacement, thereby illustrating the need to weaken the post assembly.
- The addition of either  $\varnothing 1\frac{1}{4}$ -in. holes or 1 $\frac{1}{2}$ -in. x 1 $\frac{1}{2}$ -in. chamfers removed from the bottom of the post compression flange reduced the impact load, but not enough as the forces were still above 20 kips.
- A thinner,  $\frac{3}{4}$ -in. base plate allowed the plate to bend and the post to rotate back under a lower load, but the bent plate provided prying action to the anchors and caused the anchor rods to fail – rupturing under combined tensile and bending forces.
- A  $\frac{1}{4}$ -in. fillet weld was sufficient to attach the post to the base plate and develop the full plastic bending moment of the post. The previously used 3-pass weld for W6x9 posts on base plates (top-mounted culvert posts) was not necessary for the retrofit AGT post.
- Placing  $\varnothing 1\frac{1}{4}$ -in. x 3-in. slots in the compression flange resulted in a resistance force of 19 kips through 10 in. of displacement. The slots helped initiate flange buckling and allowed the post to bend and plastically deform in a controlled and predictable manner. Thus, this weakening mechanism was selected as the preferred design, and Post Assembly M was recommended for further evaluation.
- The retrofit post assembly mounted to a freestanding 36-in. x 24-in. x 8-in. reinforced concrete slab resulted in the slab lifting up from the ground and rotating backward. The

inertia of the freestanding concrete slab was not sufficient to resist the impact loads and prevent slab movement.

- To prevent slab movement, three dowel rods were used to tie the 36-in. x 24-in. x 8-in. reinforced concrete slab to the adjacent tarmac. This prevented slab movement, but the anchor rods pulled out of the slab via concrete breakout failure. The anchors were placed too close to the front edge of the slab (7.5 in.), which caused edge effects to weaken the concrete breakout strength for the anchors.
- To prevent anchor failure, a minimum slab width of 30 in. was recommended for future testing with the new surface-mounted, retrofit AGT post.

Ultimately, Post Assembly M was selected as the preferred surface-mounted post configuration. Post Assembly M consisted on a W6x15 post with Ø1¼-in. x 3-in. slots in the compression flange and a 1-in. thick base plate. The retrofit post is anchored with two 7/8-in. diameter anchor rods epoxied into the supporting concrete slab with an embedment depth of 6 in. Post Assembly M was detailed previously in Figure 40.

The new retrofit AGT post should be mounted to a concrete slab or structure with a minimum thickness of 8 in. and a minimum width (lateral) of 30 in. so that the anchors are at least 9 in. from the edge of the slab. Since the W6x15 post are spaced at 37½-in. intervals within an AGT, the length of the supporting concrete slab should be at least 36 in. for each retrofit post in the AGT. Additionally, the supporting concrete slab should be tied to the adjacent roadway slab or other large concrete structure to prevent slab movement during an impact event.

There may be installation sites where the support slab cannot be tied to an adjacent roadway slab (e.g., if the roadway slab is thin or if the roadway is asphalt instead of concrete). For these site conditions, the supporting concrete slab would need to be larger (thicker and wider) than the minimum dimensions listed above to provide enough inertial resistance to prevent slab movement and rotation. The required size for a freestanding slab is currently unknown, but could be investigated with further physical testing in later phases of the project.

Testing of the surface-mounted, retrofit post (Post Assembly M) showed promising results that were similar to the strength of a regular W6x15 AGT post embedded in strong soil. However, further evaluation in the form of MASH crash testing should be conducted prior to the use of the retrofit post in real-world installations.

## 9 REFERENCES

1. Jowza, E.R., Faller, R.K., Rosenbaugh, S.K., Sicking, D.L., and Reid, J.D., *Safety Investigation and Guidance for Retrofitting Existing Approach Guardrail Transitions*, Report No. TRP-03-266-12, Midwest Roadside Safety Facility, University of Nebraska-Lincoln, Lincoln, NE, August 21, 2012.
2. *Manual for Assessing Safety Hardware, Second Edition*, American Association of State Highway and Transportation Officials (AASHTO), Washington, D.C., 2016.
3. Dey, G., Faller, R.K., Hascall, J.A., Bielenberg, R.W., Polivka, K.A., and Molacek, K., *Dynamic Impact Testing of W152x13.4 (W6x9) Steel Posts on a 2:1 Slope*, Report No. TRP-165-07, Midwest Roadside Safety Facility, University of Nebraska-Lincoln, Lincoln, Nebraska, March 23, 2007.
4. Wiebelhaus, M.J., Lechtenberg, K.A., Faller, R.K., Sicking, D.L., Bielenberg, R.W., Reid, J.D., Rohde, J.R., and Dey, G., *Development and Evaluation of the Midwest Guardrail System (MGS) Placed Adjacent to a 2:1 Fill Slope*, Report No. TRP-03-185-10, Midwest Roadside Safety Facility, University of Nebraska-Lincoln, Lincoln, Nebraska, February 24, 2010.
5. Haase, A.J., Kohtz, J.E., Lechtenberg, K.A., Bielenberg, R.W., Reid, J.D., and Faller, R.K., *Midwest Guardrail System (MGS) with 6-ft Posts Placed Adjacent to a 1V:2H Fill Slope*, Report No. TRP-03-320-16, Midwest Roadside Safety Facility, University of Nebraska-Lincoln, Lincoln, Nebraska, September 3, 2016.
6. Herr, J.E., Rohde, J.R., Sicking, D.L., Reid, J.D., Faller, R.K., Holloway, J.C., Coon, B.A., and Polivka, K.A., *Development of Standards for Placement of Steel Guardrail Posts in Rock*, Report No. TRP-03-119-03, Midwest Roadside Safety Facility, University of Nebraska Lincoln, May 30, 2003.
7. Bligh, R.P., Seckinger, N.R., Abu-Odeh, A.Y., Roschke, P.N., Menges, W.L., and Haug, R.R., *Dynamic Response of Guardrail Systems Encased in Pavement Mow Strips*, Report No. FHWA/TX-04/0-4162-2, Texas Transportation Institute, Texas A&M University, College Station, TX, January 2004.
8. Sweigard, M.E., Lechtenberg, K.A., Faller, R.K., Reid, J.D., and Urbank, E.L., *MASH 2016 Test No. 3-10 of MGS Installed in an Asphalt Mow Strip with Nearby Curb (Test No. GAA-1)*, Report No. TRP 03-377-17, Midwest Roadside Safety Facility, University of Nebraska-Lincoln, Lincoln, Nebraska, December 14, 2017.
9. Rosenbaugh, S.K., Schrum, K.D., Faller, R.K., Lechtenberg, K.A., Sicking, D.L., and Reid, J.D., *Development of Alternative Wood-Post MGS Approach Guardrail Transition*, Report No. TRP-03-243-11, Midwest Roadside Safety Facility, University of Nebraska-Lincoln, Lincoln, Nebraska, November 28, 2011.

10. Price, C.W., Rosenbaugh, S.K., Faller, R.K., Sicking, D.L., Reid, J.D., and Bielenberg, R.W., *Post Weld and Epoxy Anchorage Variations for W-Beam Guardrail Attached to Low-Fill Culverts*, Report No. TRP 03-278-13, Midwest Roadside Safety Facility, University of Nebraska-Lincoln, Lincoln, Nebraska, August 12, 2013.
11. ACI Committee 318, *Building Code Requirements for Structural Concrete and Commentary (ACI 318-19)*, American Concrete Institute, (2019).
12. Society of Automotive Engineers (SAE), *Instrumentation for Impact Test – Part 1 – Electronic Instrumentation*, SAE J211/1 MAR95, New York City, New York, July 2007.

## **10 APPENDICES**

## **Appendix A. State DOT Survey**

The survey/questionnaire used to gather information from State DOTs on AGT post obstructions and current practices is provided in this appendix.

## Year 30 AGT Retrofit

### Overview

#### Page description:

MwRSF has begun work on the Year 30 Pooled Fund project related to retrofits for MASH approach guardrail transition (AGT) installations. The objective of this project is to develop retrofit options for AGTs where site conditions and/or obstructions prevent the proper installation of guardrail posts.

In an effort to identify common site conditions and post obstructions, MwRSF has created a survey to solicit feedback regarding AGT installation issues. With a better understanding of the issues preventing proper post placement, MwRSF can develop retrofit options to address as many real-world site conditions as possible. Thus, we are asking that the member DOTs fill out the survey to provide MwRSF with the background materials necessary to address these installation issues.

1. Please enter your name, email, and the name of your state DOT. \*

Name	<input type="text"/>
Email	<input type="text"/>
State DOT	<input type="text"/>

2. Please upload your DOT's current design details for MASH AGTs and connections to buttress/bridge rails.

3. Does your DOT encounter site constraints preventing the installation of one or more AGT posts? \*

- Yes
- No

Please provide additional details.

Reason(s) for post omission(s)

Typical size of obstruction(s)

Maximum size of obstruction(s)

Typical number of posts omitted

Maximum number of posts omitted

Omitted post locations within AGT

Please upload photographs and/or details of AGT(s) with omitted post(s), if available.

[Browse...](#)

4. Does your DOT encounter site constraints that only allow partial embedment of one or more AGT posts? \*

- Yes
- No

Please provide descriptions of the site conditions which limit AGT post embedment.

Please provide additional details.

Typical number of posts affected

Maximum number of posts affected

Approximate loss in embedment depth

Please upload photographs and/or details of AGT(s) with partial AGT post embedment, if available.

[Browse...](#)

5. Does your DOT encounter AGT installation sites with post(s) on or near a slope? \*

- Yes
- No

Please provide a description of both slope rate(s) and offset(s) from posts.

Please upload photographs and/or details of AGT(s) with post(s) on or near slope, if available.

[Browse...](#)

6. Does your DOT encounter installation sites with AGT post(s) embedded in pavement (asphalt or concrete)? \*

- Yes
- No

Please provide a description of the pavement type (concrete/asphalt) and thickness encountered.

What is the reason for the pavement placed under the AGT(s)?

Please upload photographs of AGT(s) with post(s) embedded in pavement, if available.

[Browse...](#)

7. Does your DOT experience other AGT post installation issue(s)? \*

- Yes
- No

Please provide a description of the other post installation issue(s).

Please upload any available photographs and/or details of the other issue(s) described above.

[Browse...](#)

**Current AGT Retrofits**

---

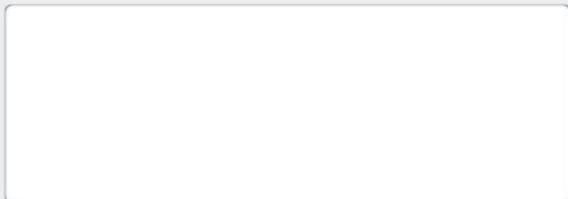
8. Please indicate any installation issues your DOT has had or you foresee having with implementing the retrofits developed as part of the previous Wisconsin DOT study (Report TRP-03-266-12).



9. Does your DOT currently utilize any AGT retrofits apart from those discussed in the Wisconsin DOT study (Report TRP-03-266-12) or within this survey?

- Yes
- No

Please describe the site conditions that cause the retrofit.



Please describe the AGT retrofit.

Please upload photographs and design details of the AGT retrofit currently used in your state, if available.

10. What is your DOT's greatest need in addressing AGT retrofits?

11. Please provide any additional comments or concerns, as it relates to AGT design deviations or retrofits within AGTs.

**Thank You!**

---

## **Appendix B. Bogie Test Results**

The results of the recorded data from each accelerometer used during each dynamic bogie test are provided in the summary sheets found in this appendix. Summary sheets include acceleration, velocity, and deflection vs. time plots as well as force vs. deflection and energy vs. deflection plots.

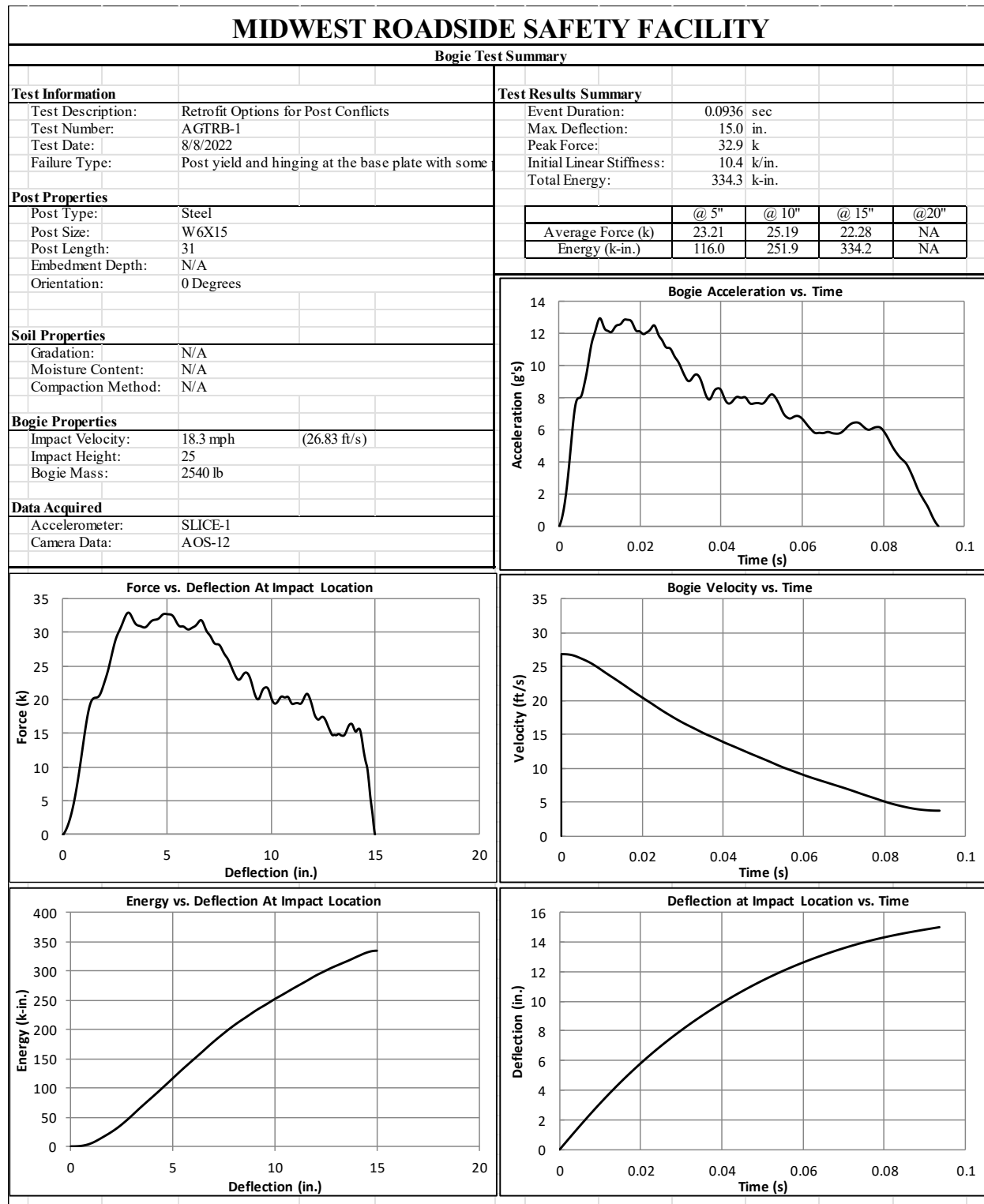


Figure B-1. Test No. AGTRB-1 Results (SLICE-1)

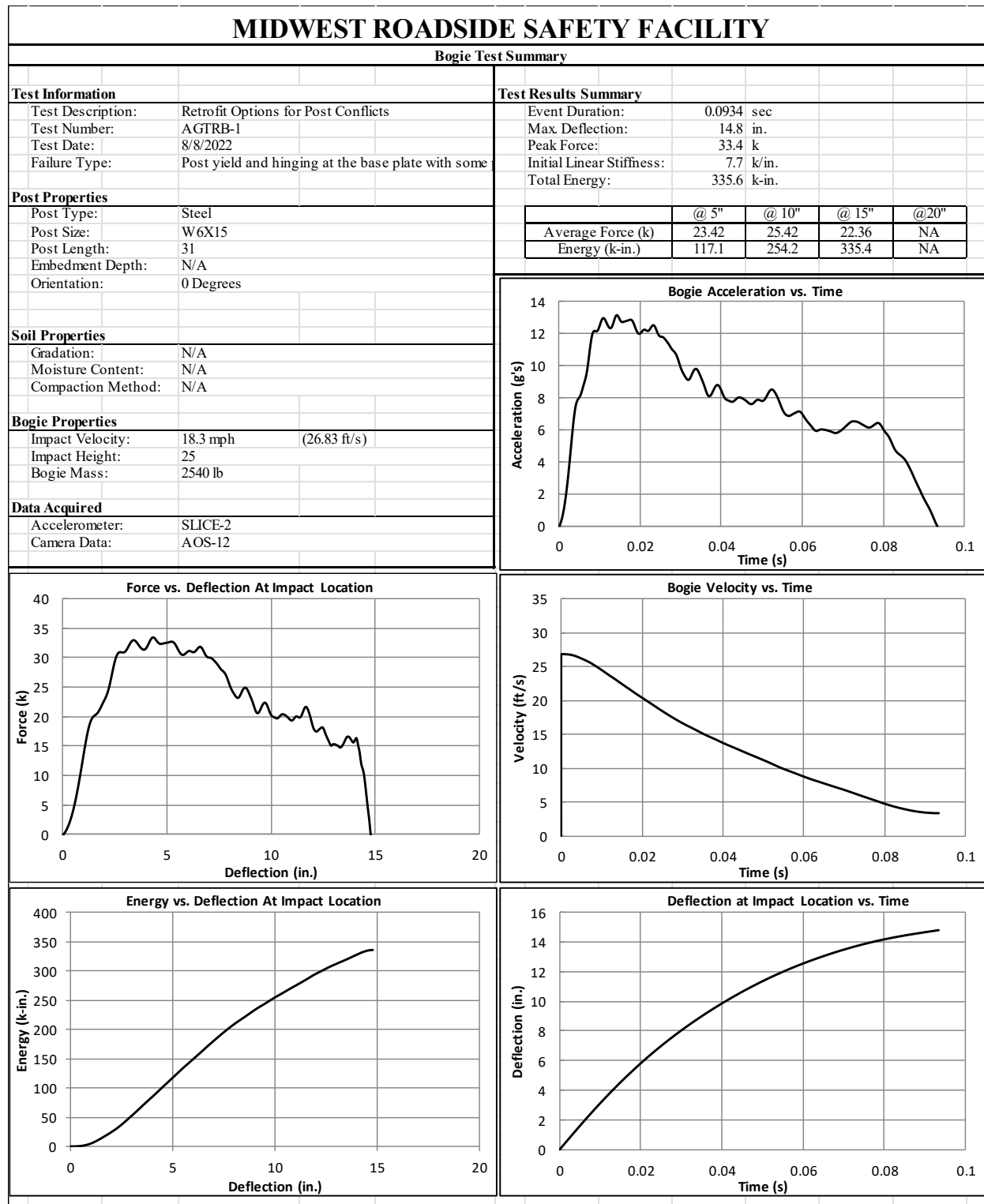


Figure B-2. Test No. AGTRB-1 Results (SLICE-2)

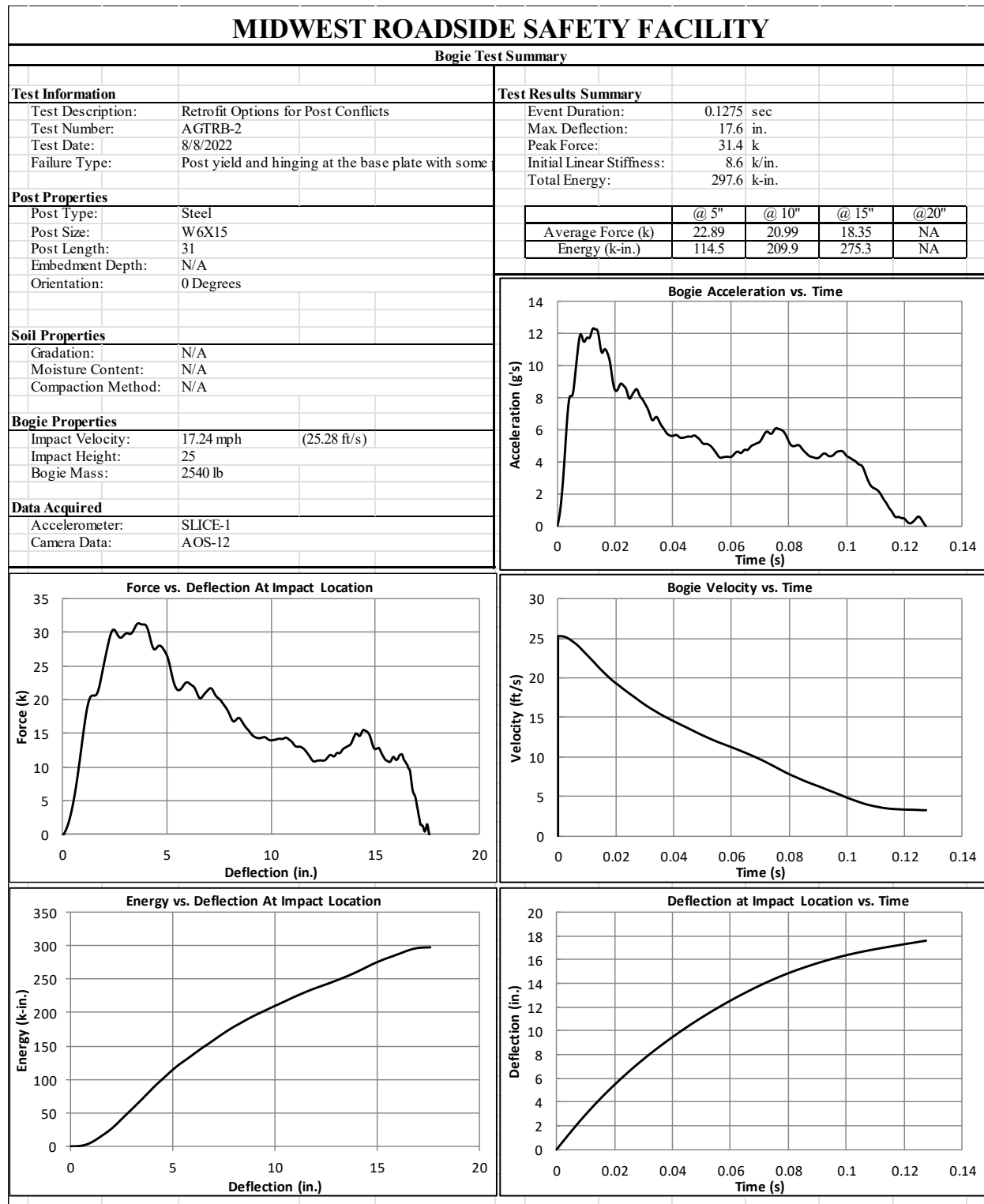


Figure B-3. Test No. AGTRB-2 Results (SLICE-1)

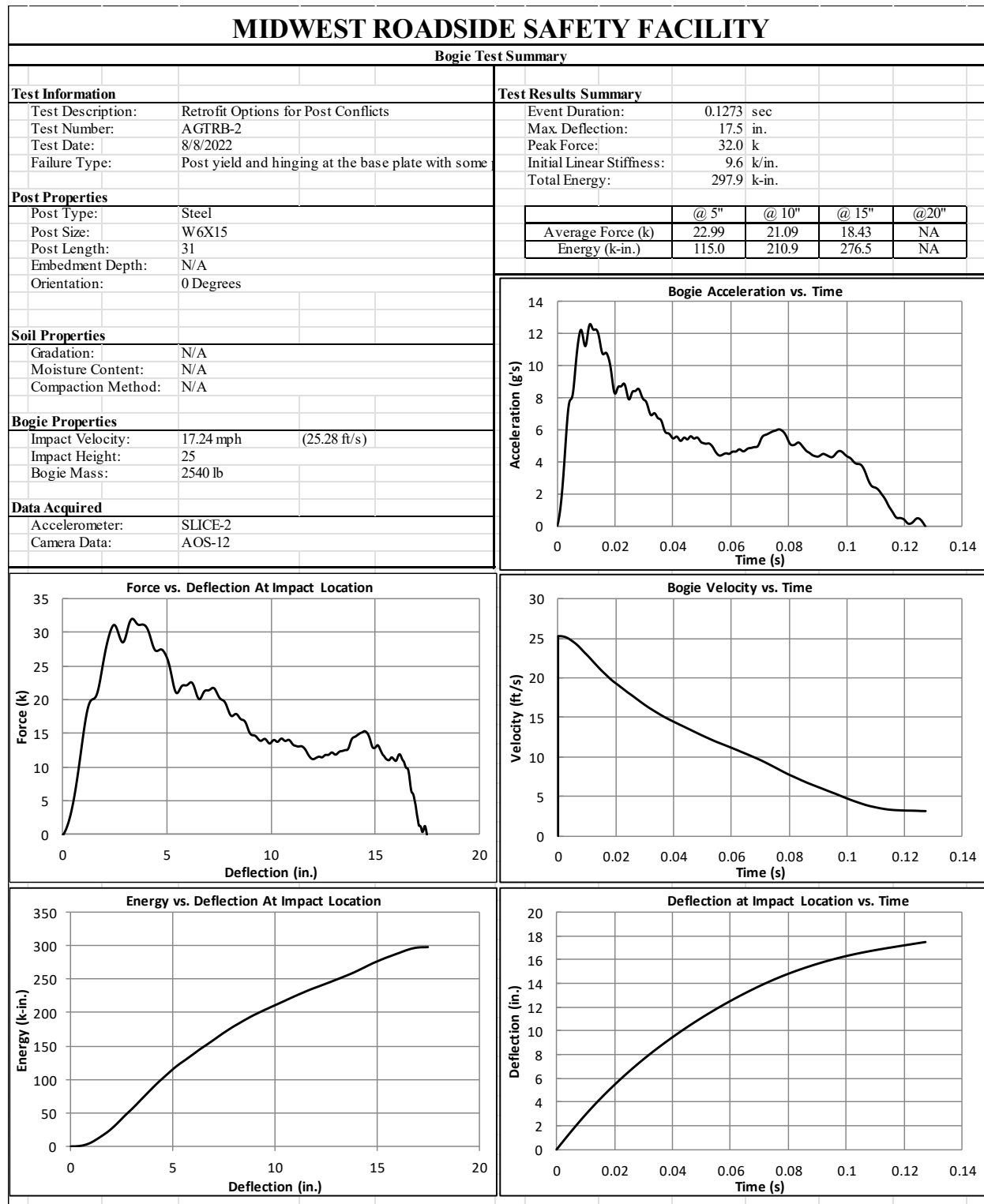


Figure B-4. Test No. AGTRB-2 Results (SLICE-2)

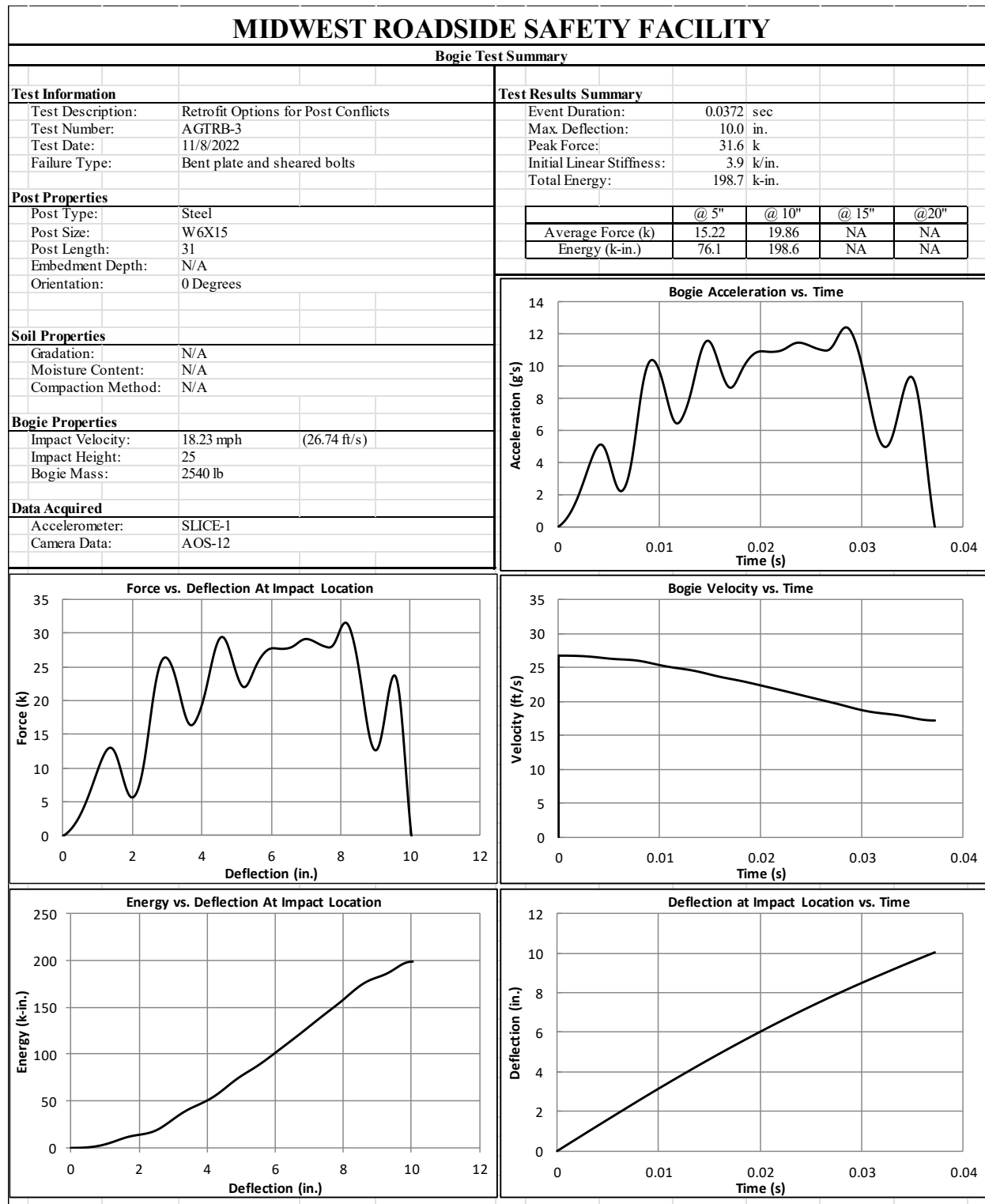


Figure B-5. Test No. AGTRB-3 Results (SLICE-1)

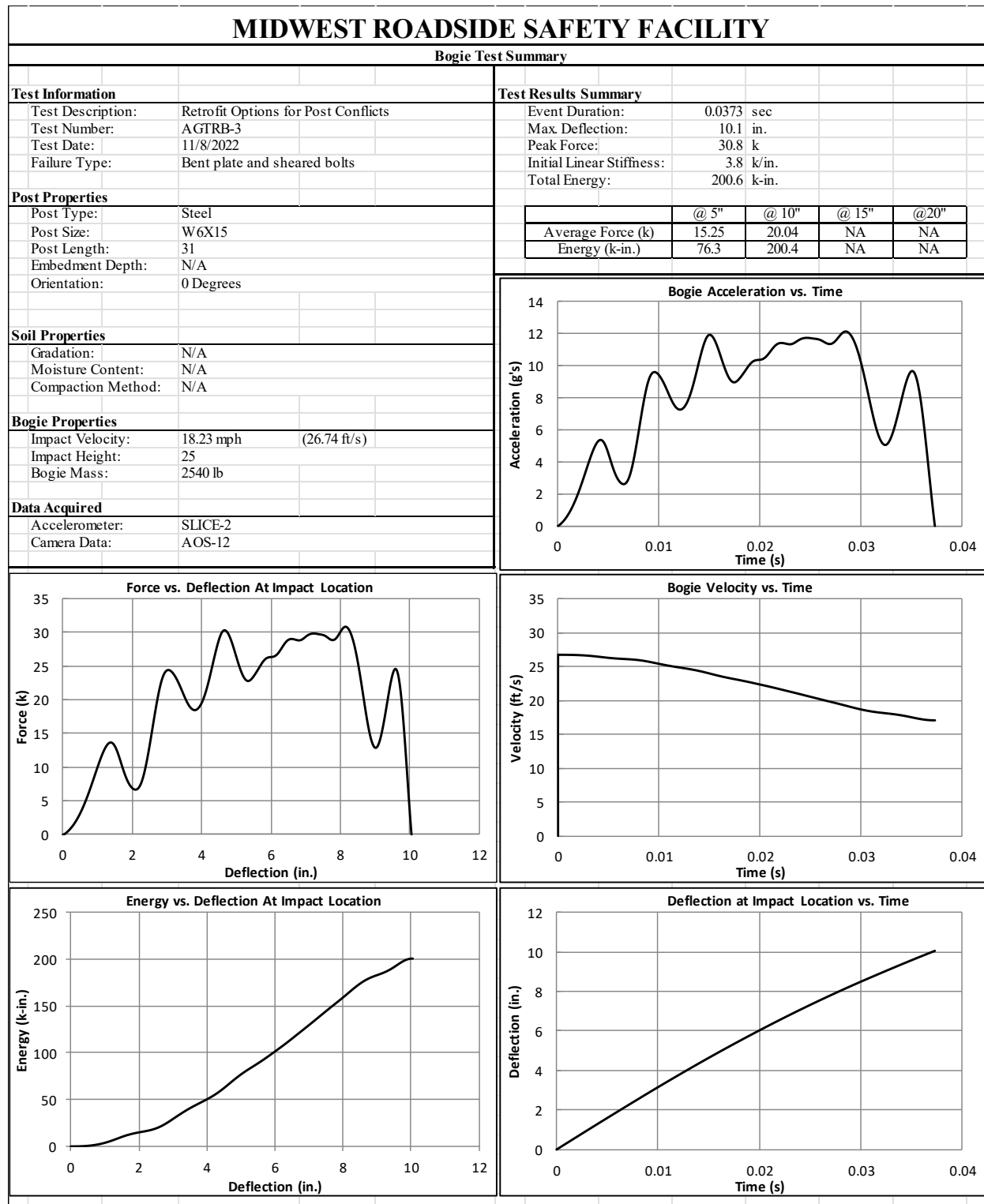


Figure B-6. Test No. AGTRB-3 Results (SLICE-2)

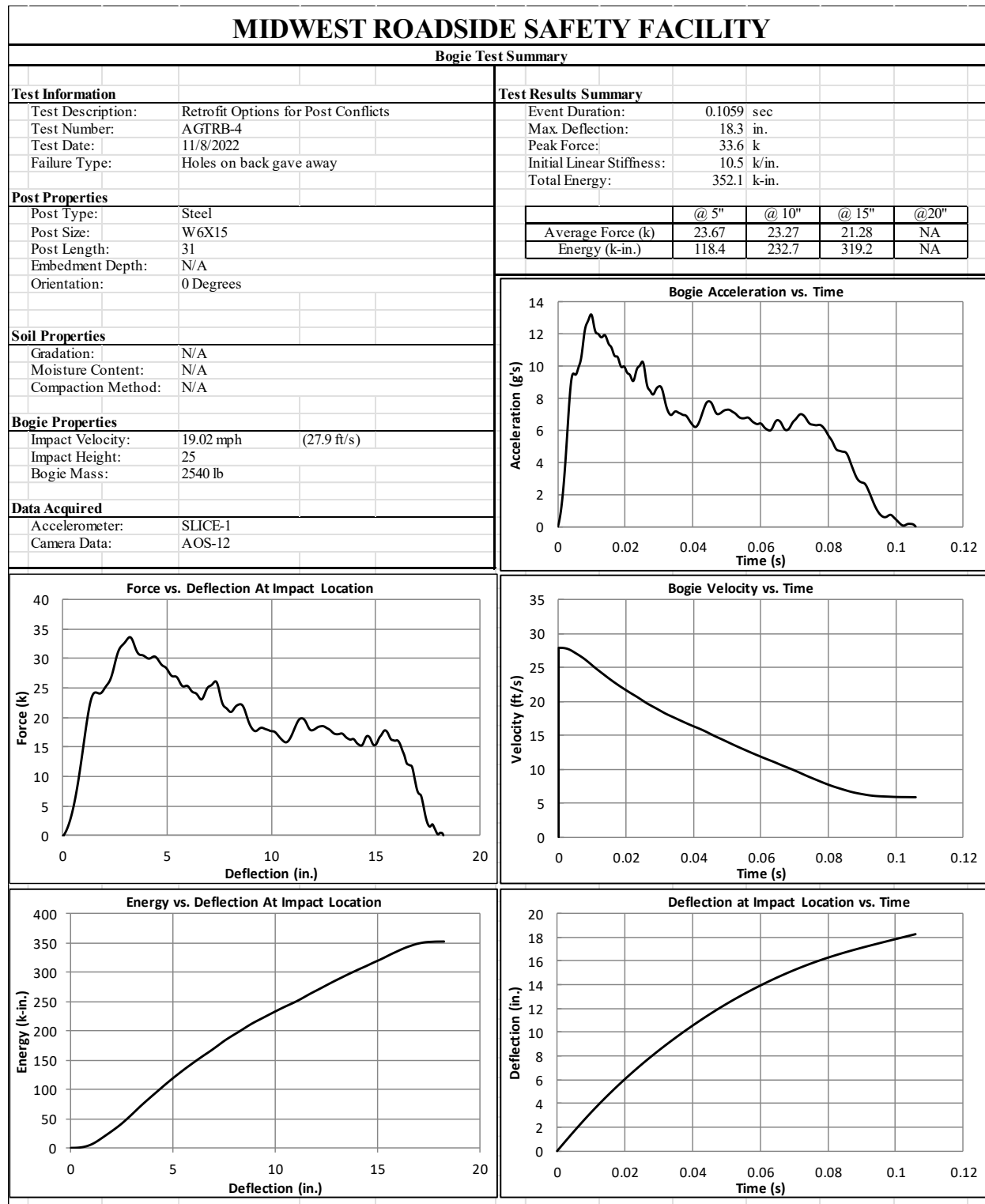


Figure B-7. Test No. AGTRB-4 Results (SLICE-1)

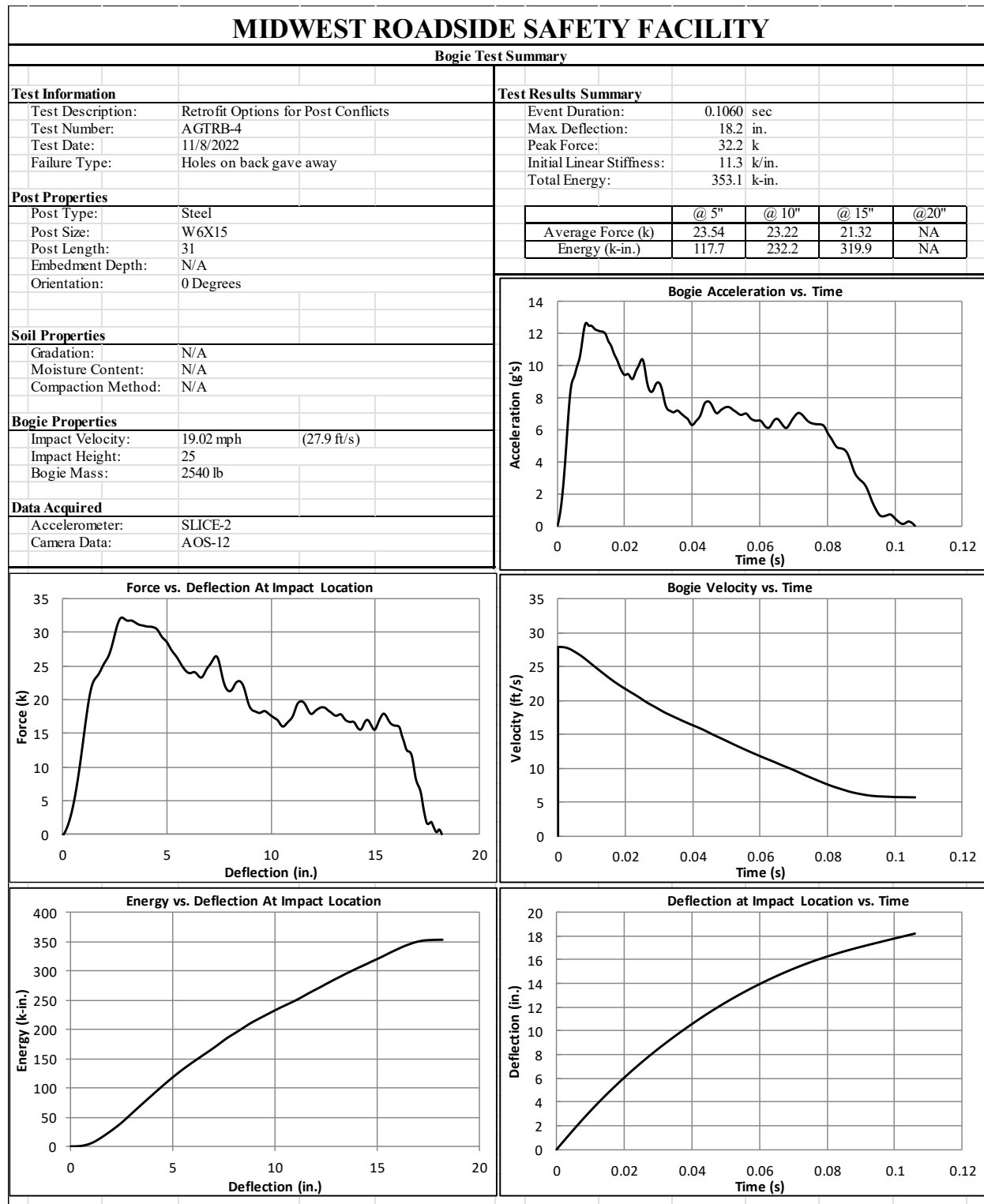


Figure B-8. Test No. AGTRB-4 Results (SLICE-2)

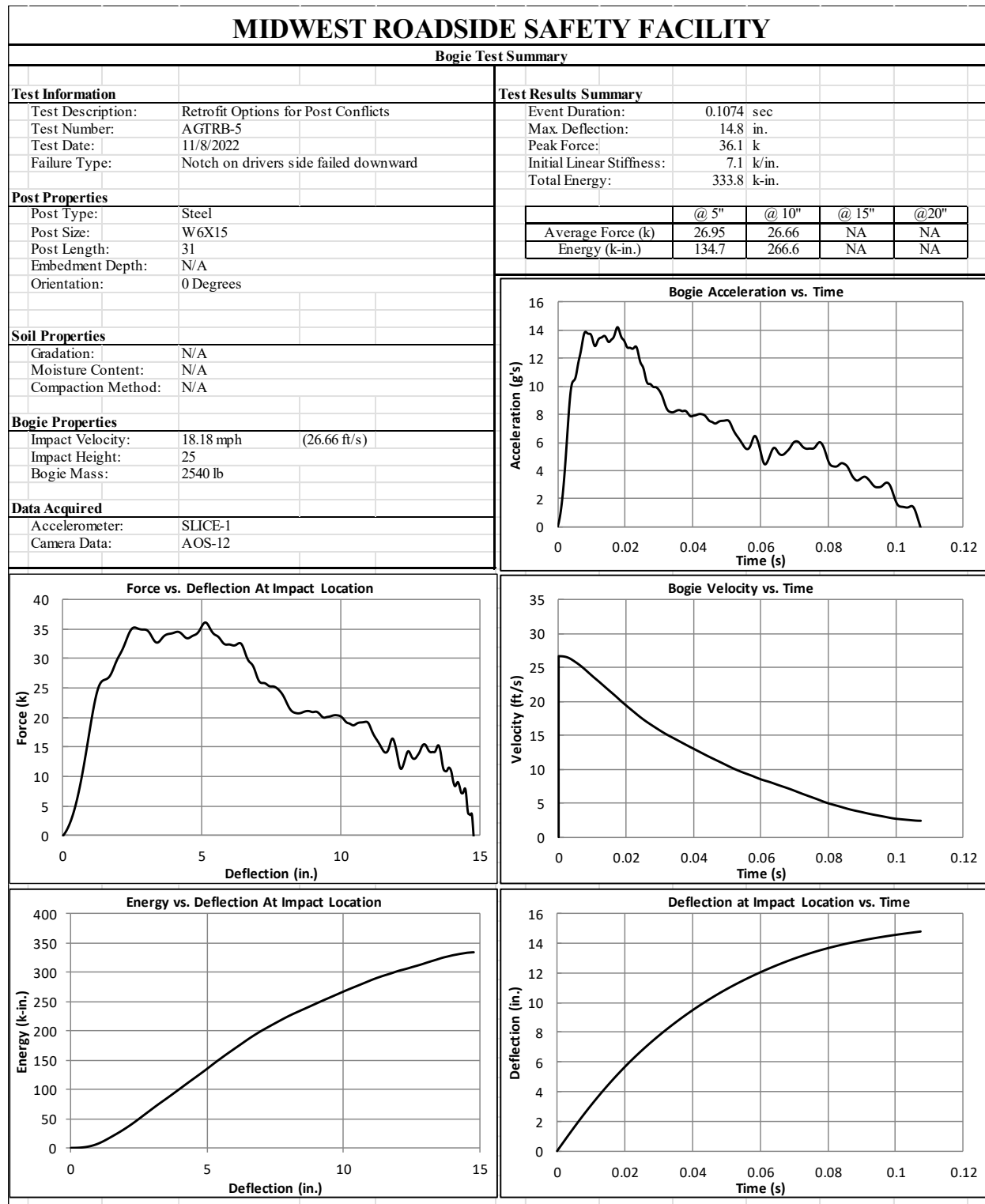


Figure B-9. Test No. AGTRB-5 Results (SLICE-1)

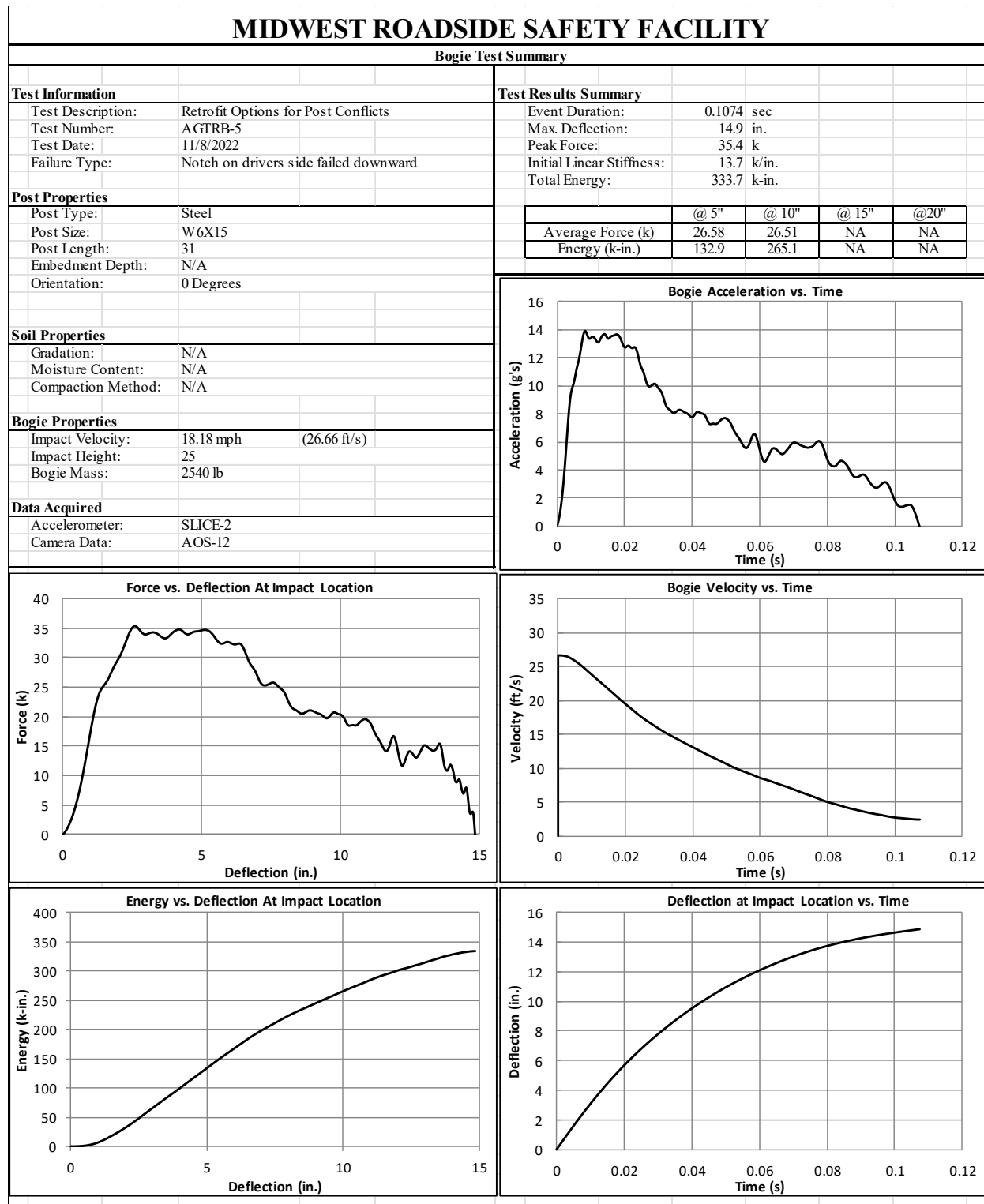


Figure B-10. Test No. AGTRB-5 Results (SLICE-2)

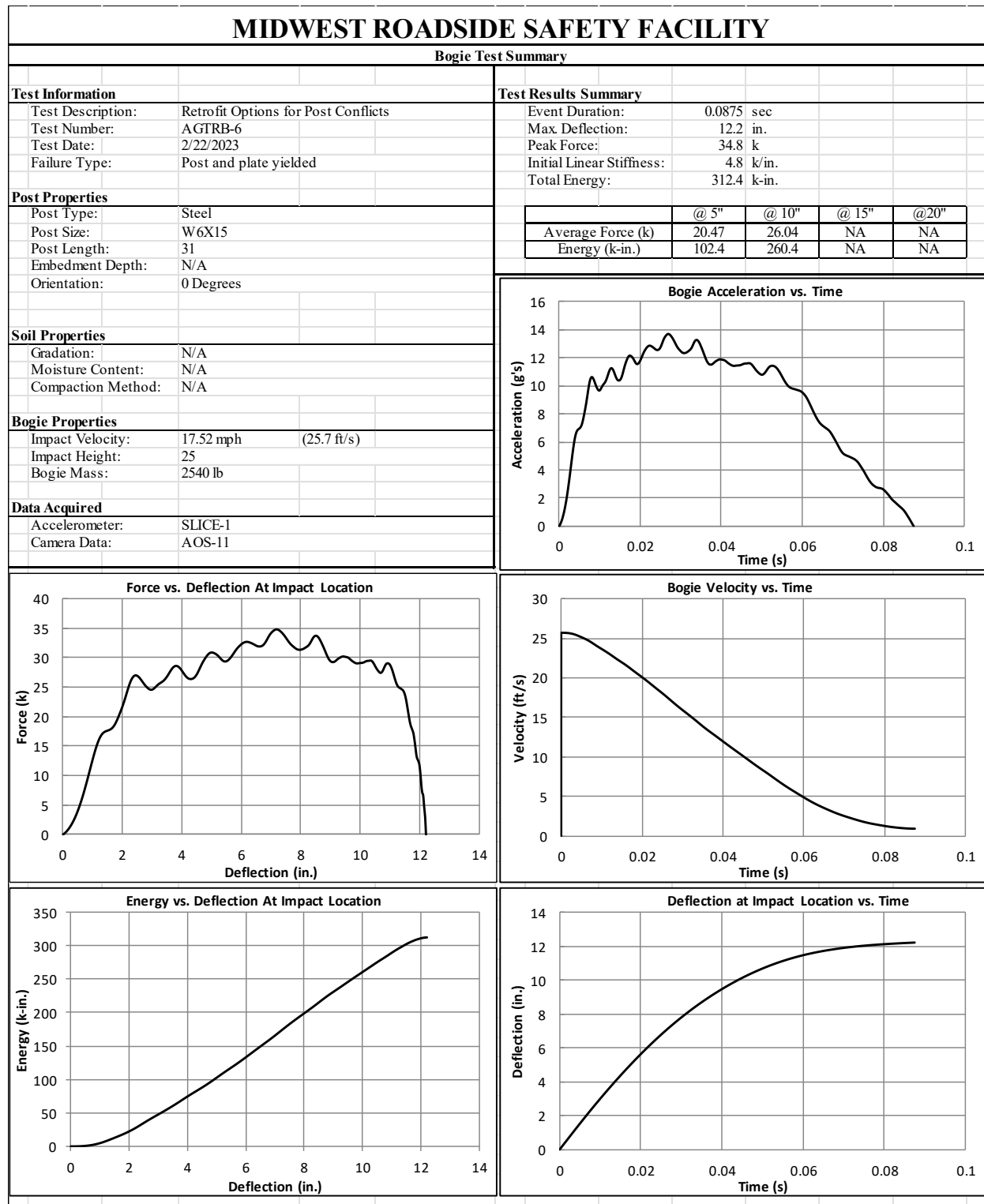


Figure B-11. Test No. AGTRB-6 Results (SLICE-1)

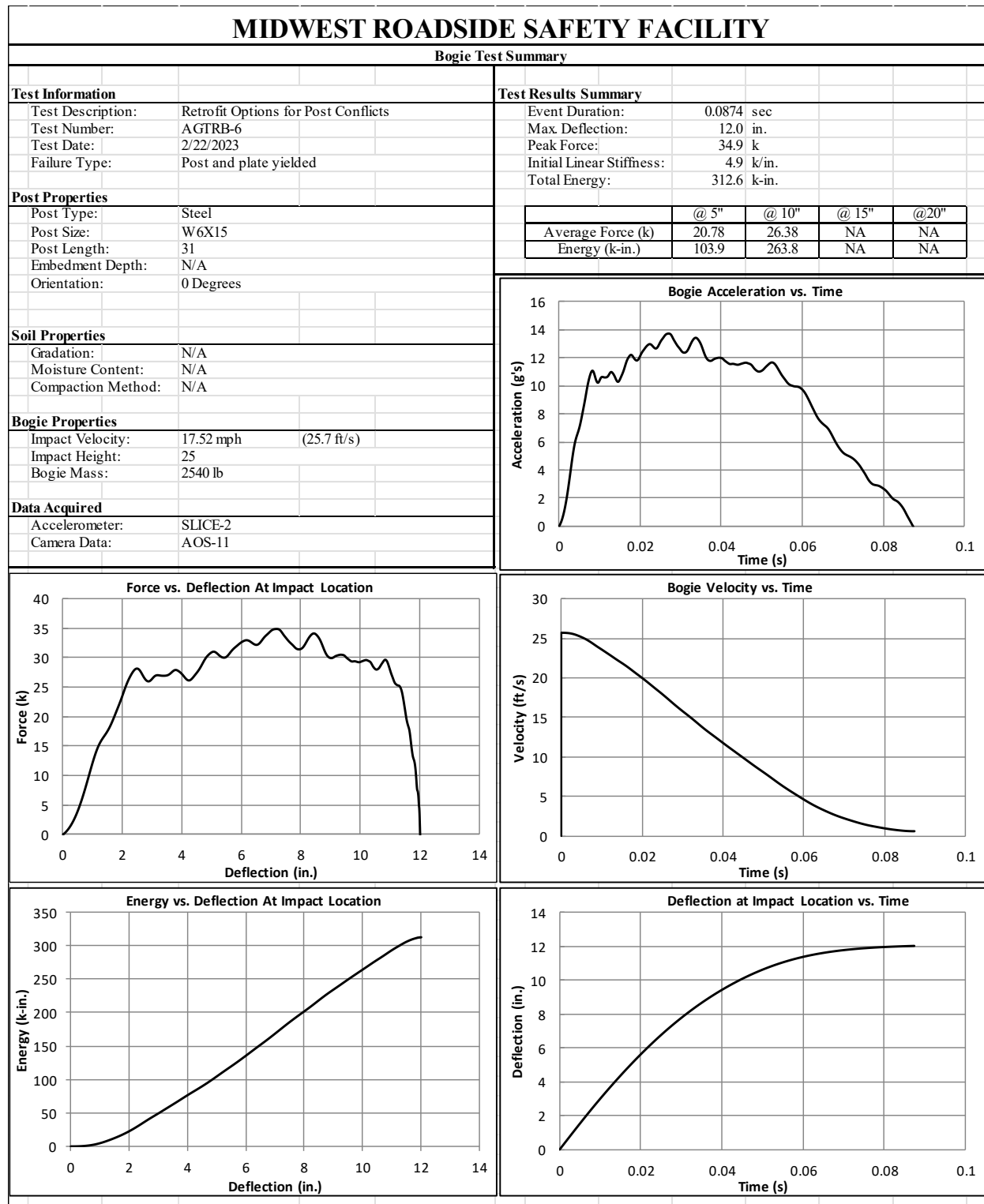


Figure B-12. Test No. AGTRB-6 Results (SLICE-2)

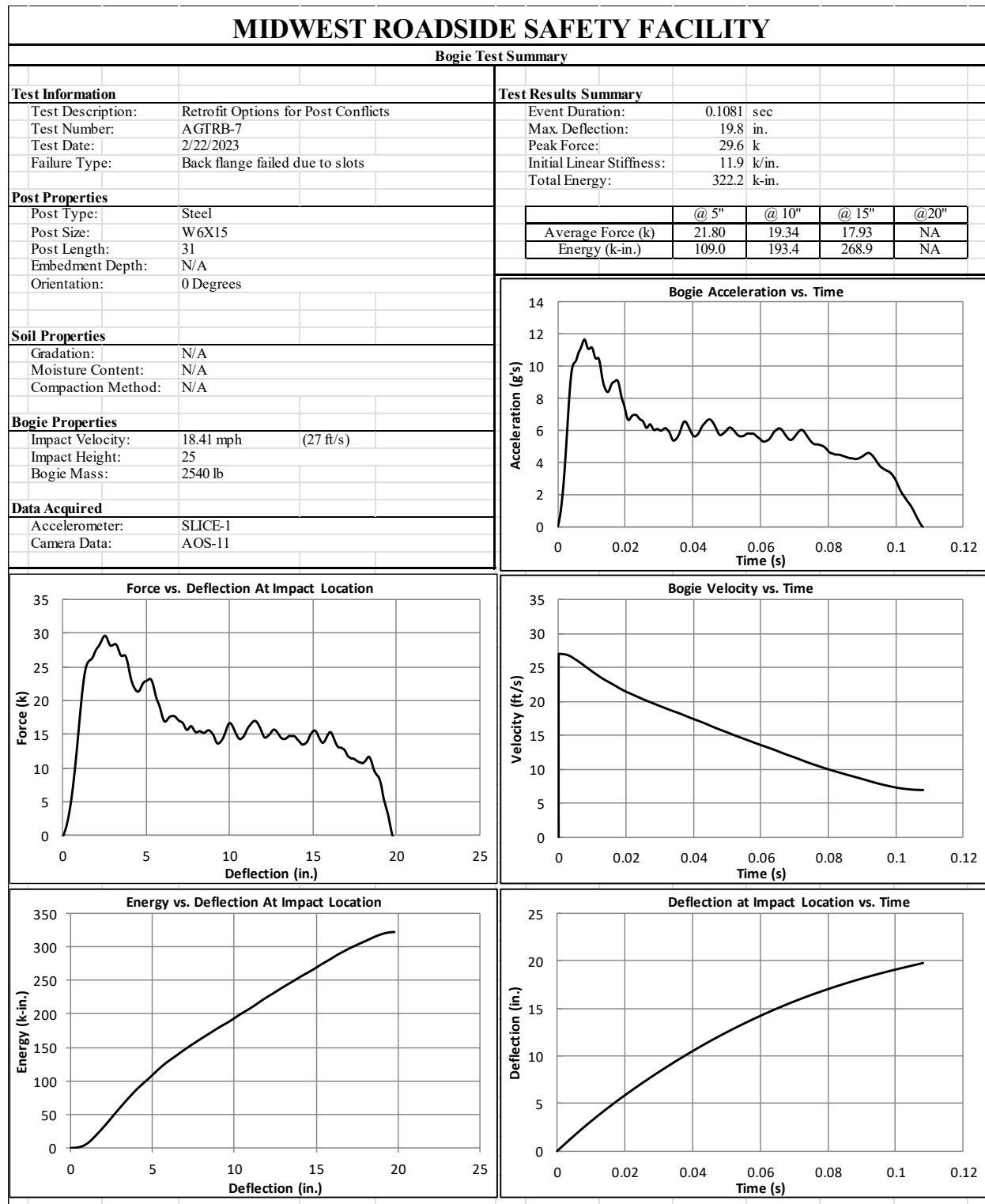


Figure B-13. Test No. AGTRB-7 Results (SLICE-1)

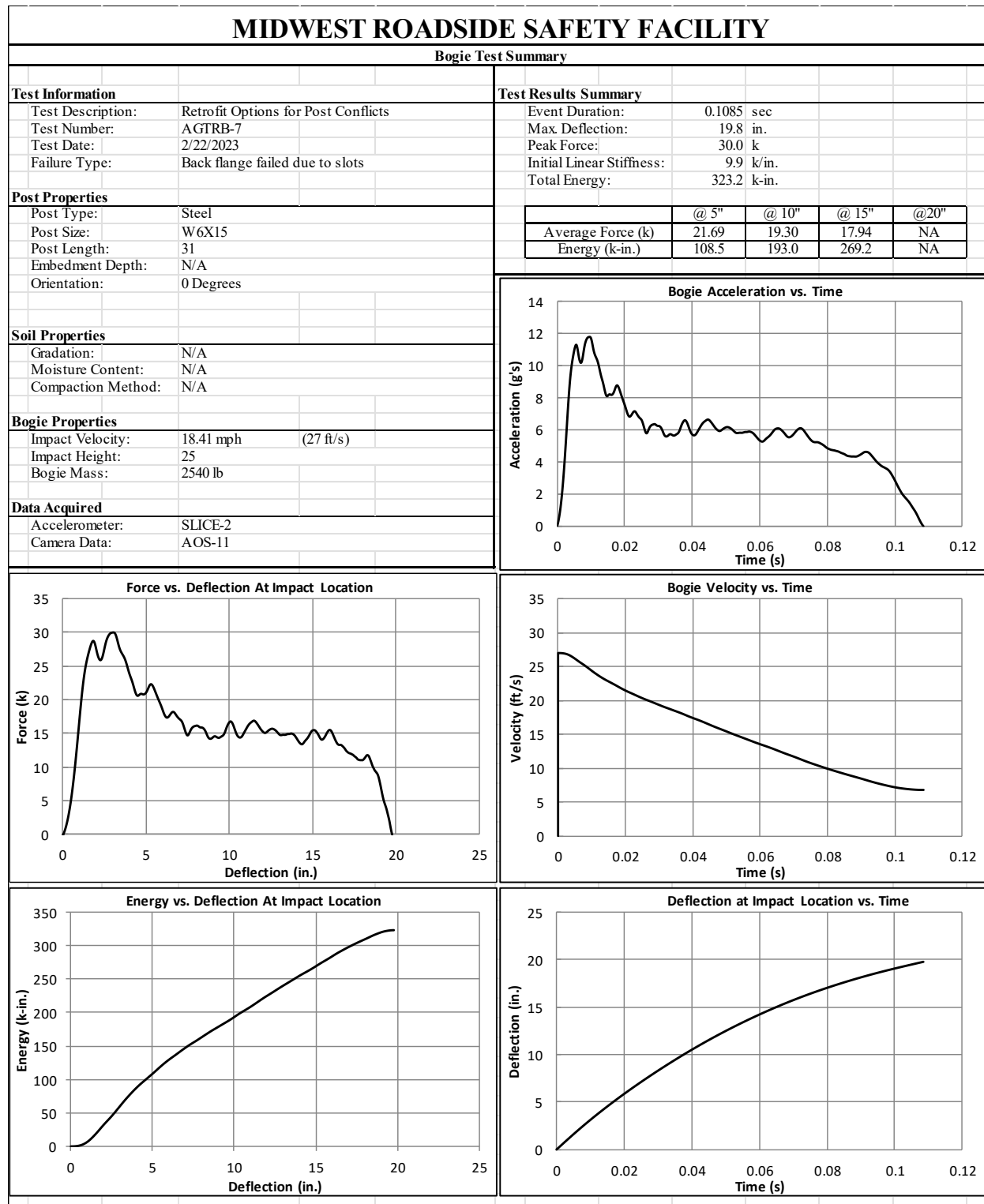


Figure B-14. Test No. AGTRB-7 Results (SLICE-2)

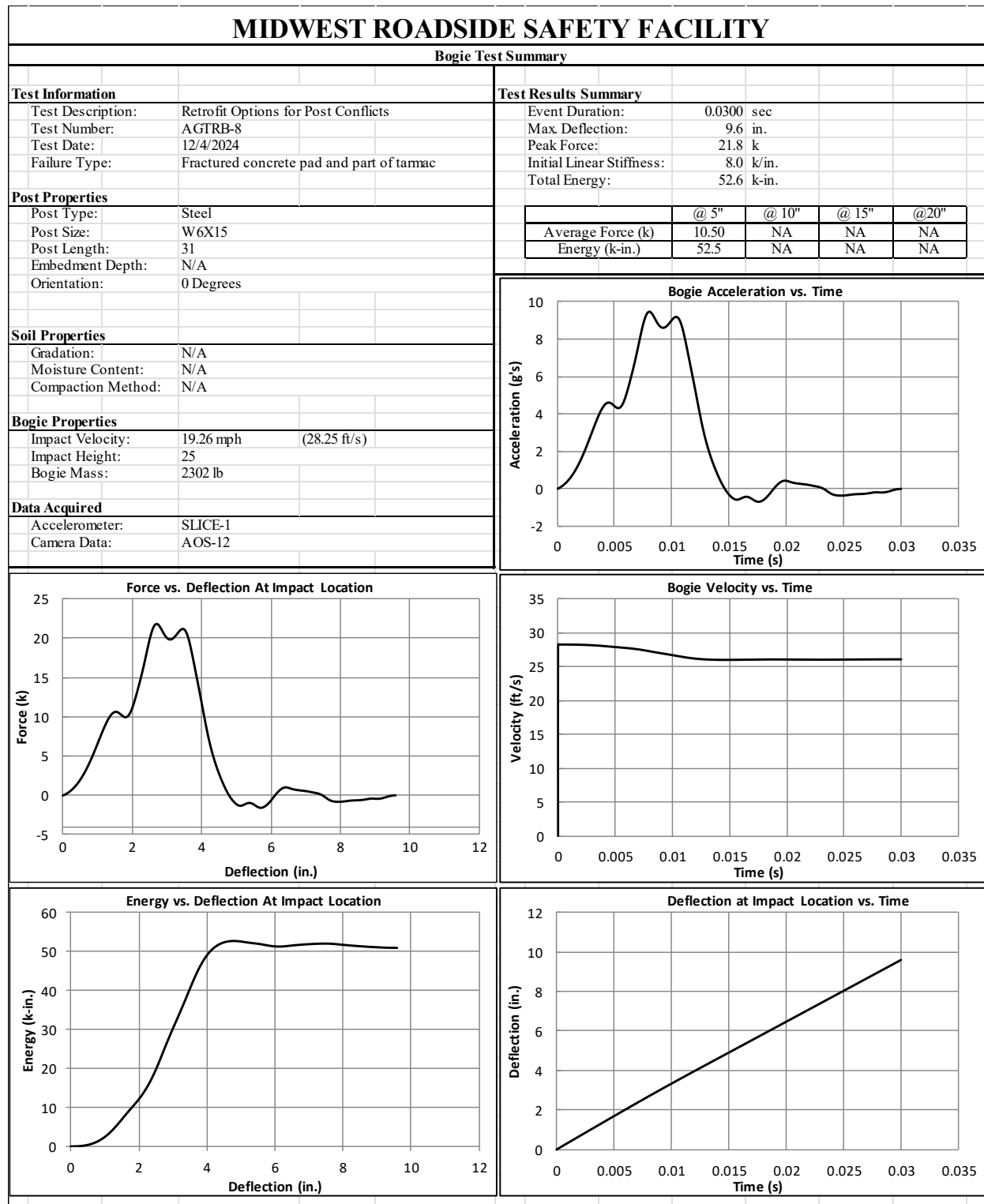


Figure B-15. Test No. AGTRB-8 Results (SLICE-1)

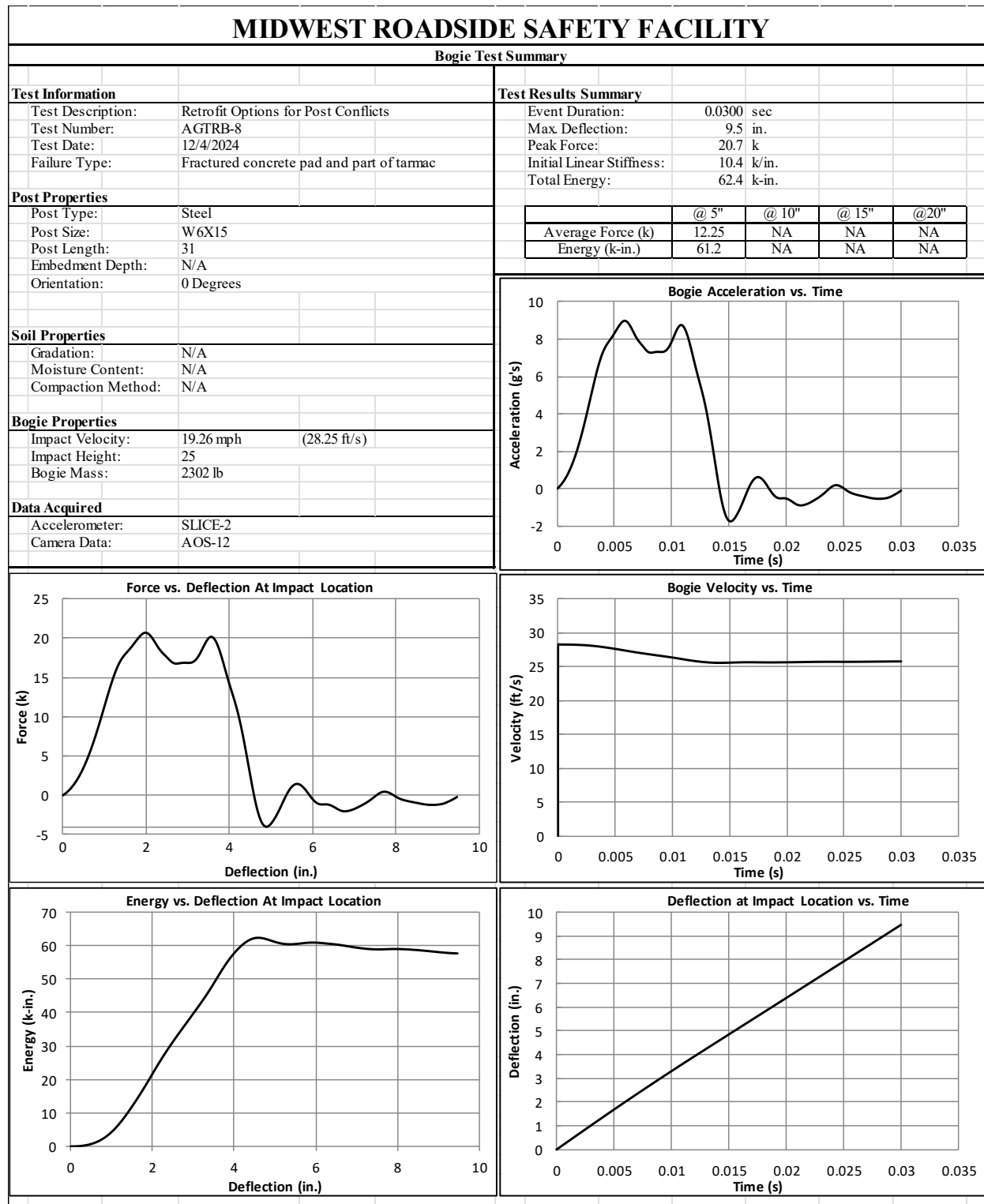


Figure B-16. Test No. AGTRB-8 Results (SLICE-2)

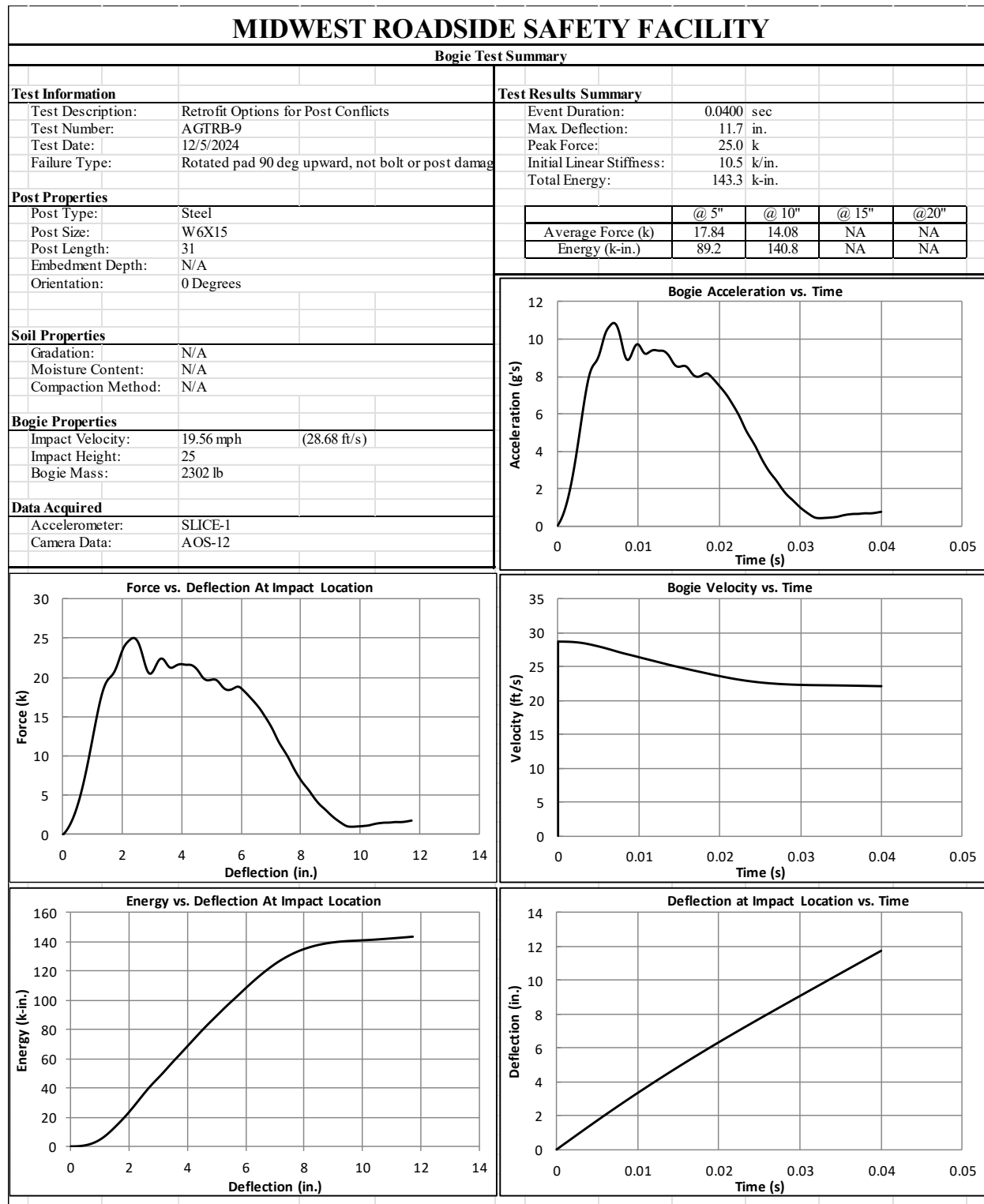


Figure B-17. Test No. AGTRB-9 Results (SLICE-1)

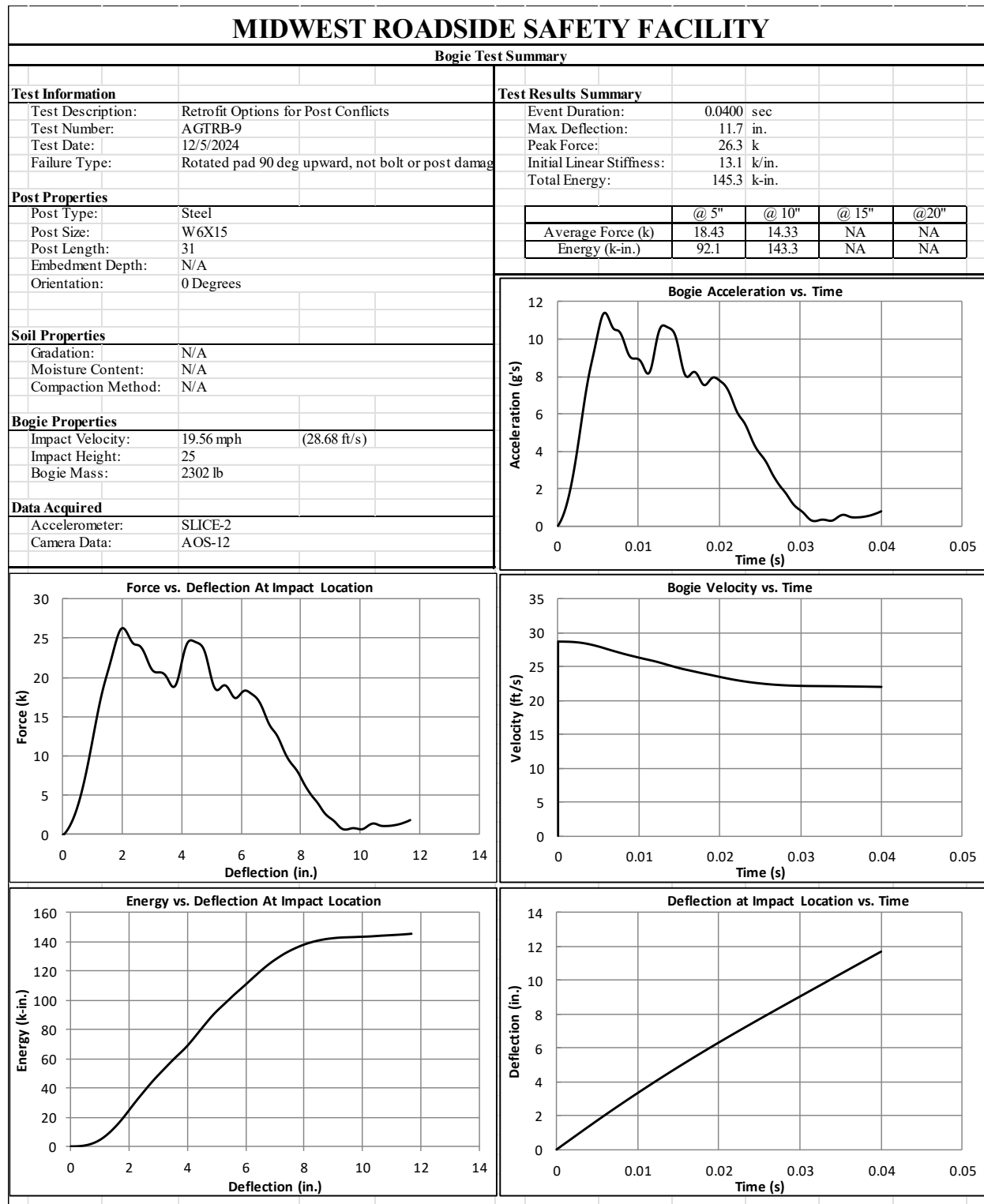


Figure B-18. Test No. AGTRB-9 Results (SLICE-2)

**END OF DOCUMENT**